

CLIMATE CHANGE IMPACT ON A 3D PRINTED CONCRETE BUILDING

A THESIS SUBMITTED TO
THE GRADUATE SCHOOL OF ARCHITECTURE
OF
MIDDLE EAST TECHNICAL UNIVERSITY

BY
FURKAN SİNAN ÜĞÜTMEN

IN PARTIAL FULFILLMENT OF THE REQUIREMENTS
FOR
THE DEGREE OF MASTER OF ARCHITECTURE
IN
ARCHITECTURE

JANUARY 2023

Approval of the thesis:

**CLIMATE CHANGE IMPACT ON A 3D PRINTED CONCRETE
BUILDING**

submitted by **FURKAN SİNAN ÜĞÜTMEN** in partial fulfillment of the requirements for the degree of **Master of Arts in Architecture, Middle East Technical University** by,

Prof. Dr. Halil Kalıpçılar
Dean, Graduate School of **Natural and Applied Sciences**

Prof. Dr. F. Cânâ Bilsel
Head of the Department, **Architecture**

Assoc. Prof. İpek Gürsel Dino
Supervisor, **Architecture, METU**

Assoc. Prof. Çağla Meral Akgül
Co-Supervisor, **Civil Engineering, METU**

Examining Committee Members:

Asst. Prof. Mehmet Koray Pekeriçli
Architecture, METU

Assoc. Prof. İpek Gürsel Dino
Architecture, METU

Assoc. Prof. Çağla Meral Akgül
Civil Engineering, METU

Assoc. Prof. Ulaş Yaman
Mechanical Engineering, METU

Assoc. Prof. Gülsu Ulukavak Harputlugil
Architecture, Çankaya University

Date: 19.01.2023

I hereby declare that all information in this document has been obtained and presented in accordance with academic rules and ethical conduct. I also declare that, as required by these rules and conduct, I have fully cited and referenced all material and results that are not original to this work.

Name Last name : Furkan Sinan Üğütmen

Signature :

ABSTRACT

CLIMATE CHANGE IMPACT ON A 3D PRINTED CONCRETE BUILDING

Üğütmen, Furkan Sinan
Master of Architecture, Architecture
Supervisor : Assoc. Prof. Dr. İpek Gürsel Dino
Co-Supervisor: Assoc. Prof. Dr. Çağla Meral Akgül

January 2023, 108 pages

3D concrete printing has great potential to enhance the development of the construction industry with the benefits of reduced construction waste and decreased labor dependency due to no formwork requirement, ease of construction of complex geometries, and low cost. 3D concrete printing technologies will enable recycled and high-performance materials in printable concrete components, which cannot be used with traditional construction methods. Despite these benefits, it is still not standard in the construction industry because of the lack of fundamental research on the thermal and energy performance of the 3D printed structural elements. There are even less study investigating the energy performance of an actual 3D printed concrete building and the impact of climate change on 3D printed concrete buildings. The effects of energy consumption on the environment and the relationship between energy consumption and the prevailing weather conditions are becoming a significant concern. Due to climate change, the equilibrium between the local climate and the buildings is vulnerable to a substantial shift, which offers a unique threat to buildings. The main objective of this thesis is to examine how climate change will affect 3D concrete printed structures and to compare the energy efficiency of 3D printed structures to conventional buildings. Additionally, it provides a comprehensive analysis based on 3D printing techniques for concrete utilized in the

construction sector by conducting an on-site experiment of the first 3D concrete printed office in Turkey, located in the ISTON Factory.

Keywords: 3D concrete printing, Additive manufacturing, Climate change, Building performance, Building energy simulation

ÖZ

İKLİM DEĞİŞİKLİĞİNİN 3B BETON YAZICILAR İLE ÜRETİLMİŞ YAPILAR ÜZERİNDEKİ ETKİSİ

Üğütmen, Furkan Sinan
Yüksek Lisans, Mimarlık
Tez Danışmanı: Doç. Dr. İpek Gürsel Dino
Ortak Tez Danışmanı: Doç. Dr. Çağla Meral Akgül

Ocak 2023, 108 sayfa

3 boyutlu beton baskı, kalıp gerektirmemesi, karmaşık geometrilerin yapım kolaylığı ve düşük maliyeti yanında, minimize edilen inşaat atıkları ve işgücü gereksinimi sayesinde inşaat endüstrisinin gelişimi için büyük bir potansiyele sahiptir. 3B beton baskı teknolojileri, geleneksel inşaat yöntemlerinde yer alamayan, geri dönüştürülmüş ve yüksek performanslı malzemelerin basılabilir beton bileşenler ile birlikte kullanılmasına da olanak sağlayacaktır. Bu, yaşanmakta olan iklim değişikliğine bağlı tehditlerin önlenmesi açısından pozitif özelliktir. Çünkü yerel iklim ve binaların enerji tüketimi arasındaki denge, binalar için benzersiz bir tehdit oluşturan önemli bir değişime karşı hassastır. Enerji tüketiminin çevre üzerindeki olumsuz etkileri uzun yıllardır bilinmekle beraber yaşanmakta olan iklim değişikliğine bağlı olarak enerji tüketimi ile hüküm süren hava koşulları arasındaki ilişki önemli bir endişe kaynağı haline gelmiştir. Bu yeni teknolojinin var olan faydalarına rağmen, 3B baskılı yapı elemanlarının termal ve enerji performansına ilişkin veriler çok eksik olup henüz inşaat endüstrisinde konuyla ilgili bir standart oluşturulamamıştır. Gerçek bir 3B baskılı beton binanın enerji performansını ve 3D baskılı beton binalarda iklim değişikliğinin etkisini araştıran çok az sayıda çalışma mevcuttur.

Bu tezin temel amacı, iklim deęişiklięinin 3 boyutlu beton baskılı yapıları nasıl etkileyeceęini incelemek ve 3 boyutlu baskılı yapıların enerji verimlilięini geleneksel binalarla karşılaştırmaktır. Ayrıca İSTON Fabrikası'nda bulunan, Türkiye'nin ilk 3B beton baskı ofisinin yerinde incelemesini yaparak, inşaat sektöründe kullanılan betonun 3D baskı tekniklerine dayalı kapsamlı bir analizini sunmaktadır.

Anahtar Kelimeler: 3B beton baskı, Eklemeli imalat, İklim deęişiklięi, Bina enerji performansı

To my family.

ACKNOWLEDGMENTS

First of all, I would like to express my sincere gratitude to my thesis supervisor Assoc. Prof. Dr. İpek Gürsel Dino, for her constant advice, support, motivation, and encouragement throughout the study. In addition, I'd like to thank my co-supervisor, Assoc. Prof. Dr. Çağla Meral Akgül, for all of her guidance and direction throughout the thesis process. Apart from this thesis, I would like to thank them for letting me work as a research assistant in their 3D concrete printing project, which was highly beneficial for pursuing my dreams.

I would also like to thank my jury members, Asst. Prof. Mehmet Koray Pekerçli, Assoc. Prof. Ulaş Yaman, and Assoc. Prof. Gülsu Ulukavak Harputlugil, for their encouragement and trust in my ability to complete the thesis successfully.

I dedicated this thesis to my grandparents, Turan Şenol and İlknur Şenol; they taught me everything I know, and I will always live to make them proud. I would also like to thank my parents and my sister for their unconditional love and motivation, especially my mom for her incredible support and for always being my inspiration throughout my life.

In addition, I would like to give special thanks to Dr. Günsu Merin Abbas, a fantastic teacher, and mentor, for her consistent understanding, motivating debates, and always showing me the light when I get lost. I will never forget her support.

I am grateful to all my colleagues in the 3DPC project for being a family to me and never leaving me alone, and with particular regard, Erman Tunçer made even the most complex tasks possible with his support, and he has been a real brother to me. I am also grateful to Amirali Hashemzadeh; his constant patience and support made me always move on.

I would like to express my gratitude to Assoc. Prof. Dr. Güzden Varinlioğlu for her essential influences and guidance throughout my architecture education. I am very

grateful to her for her continuous support from the first day of my bachelor's degree until my graduation.

I would also like to thank all my friends, Atila Güler and Melodi Canikli, for being with me on my most challenging days, making me feel Ankara was my home, and showing me how always to be strong, and Nur Ulu for her continuous support, and Kaan Etiz, for being with me since we were eight years old, and Monther Khraim, for his emotional support and constant belief in my success.

Lastly, I would like to thank Dr. Sepehr Sayedian for always being with me, even for conducting an experiment during the coldest weather at 4 am, and for all the other most challenging days in my life. His wise advice will always be my guide through my life.

TABLE OF CONTENTS

ABSTRACT	v
ÖZ.....	vii
ACKNOWLEDGMENTS.....	x
TABLE OF CONTENTS	xii
LIST OF TABLES	xv
LIST OF FIGURES.....	xvi
CHAPTERS	
1 INTRODUCTION.....	1
1.1 Motivation and Problem Statement	1
1.2 Aims and Objectives.....	4
1.3 Research Questions.....	5
1.4 Scope of the Thesis	6
1.5 Thesis Structure	7
2 LITERATURE REVIEW.....	9
2.1 3D Concrete Printing Technologies.....	9
2.1.1 Extrusion Based 3D Concrete Printing.....	10
2.1.2 Powder Bed Based 3D Concrete Printing	13
2.2 3D Printable Concrete Properties	15
2.3 Potentials of 3DCP in The Construction Industry	18
2.3.1 Economical Potential of 3D Concrete Printing	19
2.3.2 Environmental Impact of 3D Concrete Printing.....	22
2.4 Thermal Performance of 3D Concrete Printed Structures	24
2.5 Infill Structures of the 3DCP Structures	30

2.6	Analyses of Structural Form and Support Structures.....	32
2.7	Applications of 3D Concrete Printing in the Construction Industry.....	35
2.8	Future of the 3DCP Technology	37
3	MATERIALS AND METHODS.....	41
3.1	Existing Building Data Collection	43
3.1.1	Building Data	43
3.1.2	In-Situ Measurements	44
3.2	Future Weather Data File Generation	45
3.3	Building Condition Assessment Based on Thermal Imaging	45
3.3.1	Measuring Actual R-Values at the Level of Point in 3 Dimention... ..	45
3.4	Developing a Building Energy Simulation	48
3.4.1	Criteria Determination for Evaluating Performance.....	48
3.4.2	Developing a Building Energy Simulation.....	48
4	CASE STUDY	49
4.1	Building Description	49
4.2	Printing Process and Wall Geometries.....	52
4.3	3D Modeling of the Case Building	55
4.3.1	Transforming Printing Paths to 3D Models.....	56
4.3.2	Simulation Model Development.....	58
4.4	Impact of Global Climate Change on a 3D Printed Concrete Building ...	62
4.4.1	Performance Assessment for 3DCP building	63
5	RESULTS AND DISCUSSION.....	65
5.1	Thermal Performance of the Walls	65
5.1.1	Infrared Thermal Imaging.....	65

5.2	Energy Performance of the Building	69
6	CONCLUSION	83
6.1	Limitations and Further Studies.....	85
	REFERENCES	87
	APPENDICES.....	101
A.	CASE BUILDING DETAILS.....	101
B.	EXTERNAL WALLS CONDUCTIVE HEAT TRANSFER GRAPHS ..	106

LIST OF TABLES

TABLES

<i>Table 2.1.</i> Main advantages and difficulties of 3DCP in construction	18
<i>Table 2.2.</i> Thermal transmittance values were determined from E-PLA-filled structures at various mixes with a 20 K temperature difference (Alkhalidi & Hatuqay, 2020).....	29
<i>Table 3.1</i> Properties of Testo 174 T and H dataloggers.....	44
<i>Table 3.2.</i> Technical specifications of infrared camera	44
<i>Table 4.1.</i> Internal load densities (ASHRAE, 2013)	59
<i>Table 4.2.</i> Construction materials for simulations	61
<i>Table 5.1.</i> U-values of the external walls	69
<i>Table 5.2</i> Annual energy demand (kWh) for heating and cooling of the case building examined for the present climate scenario, 2050 and 2080.....	70
<i>Table 5.3.</i> Conductive heat transfer table for each wall and both 3DCP and TS825 scenarios with 2020 weather data in total and average (W)	82

LIST OF FIGURES

FIGURES

<i>Figure 1.1.</i> The structure of the thesis.....	8
<i>Figure 2.1.</i> The process of 3D printing for construction industry (Paul, Tay, et al., 2018).....	9
<i>Figure 2.2.</i> a); 4-axis gantry printer; b) 6-axis robotic printer; c) crane printer (Paul, van Zijl, et al., 2018)	11
<i>Figure 2.3.</i> Contour Crafting Method (Khoshnevis, 2010).....	12
<i>Figure 2.4.</i> Schematic of the 3D printing setup: 0. System command; 1. Robot controller; 2. Printing controller; 3. Robotic arm; 4. Printhead; 5. Accelerating agent; 6. Peristaltic pump for accelerating agent; 7. Peristaltic pump for premix; 8. Premix mixer; 9. 3D printed object (Gosselin et al., 2016).....	12
<i>Figure 2.5.</i> The production and final version of a structure printed on a D-Shape printer (D-Shape, 2015).....	14
<i>Figure 2.6.</i> Parametric forms printed with powder bed based printing technology (Rael, 2018).	15
<i>Figure 2.7.</i> No slump 3D printable concrete printed in ISTON factory	16
<i>Figure 2.8.</i> The column was designed to evaluate constructability with overhanging geometry and the entire system's start/stop behavior, as the column's main part twists and bifurcates twice and twisted entrance column at ISTON office (Li et al., 2020).....	17
<i>Figure 2.9.</i> Cost graph of traditional molded manufacturing and additive manufacturing technologies depending on the number of components (Lim et al., 2012).....	20
<i>Figure 2.10.</i> Cost distribution of traditional molded construction (Jha, 2012).	21
<i>Figure 2.11.</i> The first 3D concrete printed community of houses for low budget construction (Verge, 2018).....	22

<i>Figure 2.12.</i> Environmental benefits of digital fabrication over traditional building due to complexity. The percentage of Global Warming Potential per m ² of the concrete wall represents the environmental impact	24
<i>Figure 2.13.</i> Heat transfer methods of a infill structure node. Case A: conduction inside concrete, Case B: conduction inside concrete and cavity convection, Case D: conduction inside concrete, cavity convection and radiation, Case D cavities filled with foam concrete simulated only conduction (Marais et al., 2021).....	25
<i>Figure 2.14.</i> Methods to 3D printed walls' thermal performance (Pessoa et al., 2021)	26
<i>Figure 2.15.</i> Combination of 3D concrete printed wall with traditional thermal insulation (Kaszynka et al., 2019).....	27
<i>Figure 2.16.</i> Using 3D concrete printed structures as permanent formwork (Furet et al., 2019)	28
<i>Figure 2.17.</i> Printable mixes components percentages (Alkhalidi & Hatuqay, 2020)	29
<i>Figure 2.18.</i> Thermographic image and visible image of the prototype house from different directions (Sun et al., 2021)	30
<i>Figure 2.19.</i> Different infill structures with layer thickness and pattern (Kontovourkis & Tryfonos, 2020)	31
<i>Figure 2.20.</i> Infill structure of the amorphous wall with reinforcement (Lim et al., 2012)	32
<i>Figure 2.21.</i> Support structures to print over gaps used in ISTON	33
<i>Figure 2.22.</i> The cantilever approaches found in commercial 2D slicing software (left) and the tangential continuity method (right) were used to 3D print a schematic cut perpendicular to layers (Gosselin et al., 2016).....	34
<i>Figure 2.23.</i> The 3D printed high-performance concrete multifunctional wall (Gosselin et al., 2016)	35
<i>Figure 2.24.</i> 3DCP applications in the world	37
<i>Figure 3.1.</i> Building energy analysis pipeline	43

Figure 3.2. Reflected temperature measurement: (A) Crumpled Aluminum Foil on the 3DCP wall surface (B) Thermal Image of the Crumpled Aluminum Foil; (C).47

Figure 4.1. Satellite images of the ISTON, Tuzla facility, and building site.....50

Figure 4.2. Aerial photographs of the 3DCP case building's construction and final phases50

Figure 4.3. Site plan of the 3DCP office building in ISTON Tuzla facility51

Figure 4.4. ISTON Building: (a) zone measurements, (b) naming diagram....**Error! Bookmark not defined.**

Figure 4.5. Zone diagram.....52

Figure 4.6. Façade of the case building52

Figure 4.7. Print path and direction of the walls (Red star is both start and the end point of the print).....53

Figure 4.8. a) Printing simulation and slicing process, b) Exterior wall infill structure, c) Interior wall infill structure54

Figure 4.9. (a) Exterior wall infill structures with two window gaps, (b) interior wall infill structure with door gap.54

Figure 4.10. Volumes of the walls55

Figure 4.11. (a) detailed 3D model of 3D printed case building (b) simplified version of the model for simulations56

Figure 4.12. Weekly internal load schedules for the offices (ASHRAE, 2013)60

Figure 5.1. The thermal imaging completed between 2-5 am to minimize the convective heat loss.....66

Figure 5.2. The rooms were heated with both electronic and non-electronic heaters before the thermal imaging66

Figure 5.3. Possible defect areas were identified and examined during thermal imaging.....67

Figure 5.4. Infrared Images of the 3D concrete printed structure envelope67

Figure 5.5. Fixing perspective distortion process67

Figure 5.6. The energy balance graphs for both scenarios are based on the present weather conditions, 2050 and 2080 estimates.71

<i>Figure 5.7.</i> The heating demand for (a) a 3DCP building and (b) a TS825 scenario	74
<i>Figure 5.8.</i> The office building's annual heating demand in baseline and projected future years for both 3DCP (a) and TS825 (b) scenarios.....	75
<i>Figure 5.9.</i> The cooling demand for (a) a 3DCP building and (b) a TS825 scenario	77
<i>Figure 5.10.</i> The office building's annual cooling demand in baseline and projected future years for both 3DCP (a) and TS825 (b) scenarios.....	79
<i>Figure 5.11.</i> Conductive heat transfer graphs for both scenarios (a) wall 3a north-east façade, (b) wall 1 b south east façade, (c) wall 5c south-west façade, (d) wall 3D north-west façade	81

CHAPTER 1

INTRODUCTION

1.1 Motivation and Problem Statement

Since the middle of the 20th century, the relevance of sustainable development for the earth's and humanity's survival has been increasingly acknowledged (Det Udomsap & Hallinger, 2020). The high demand for natural resources has accelerated the destruction of the planet's ecosystems. The exponential rises in global population and consumption endanger the quality of life and the ability of humans to live (del Río Merino et al., 2010). Natural resource depletion has led to global shortages and higher pricing for various materials and commodities (Halliday, 2018). There can be no rational doubt that the world's climate will change over the upcoming decades, but it is still challenging to predict how it will change exactly. These uncertainties could significantly affect the thermal efficiency and, by extension, the long-term viability of all buildings (Andrić et al., 2019). Changes in external peak and average temperatures, for instance, could impair a building's ability to maintain suitable internal comfort levels (Gallego-Schmid et al., 2020). The high levels of material and energy consumption in the built environment and the resulting pollution and waste indicate that the construction sector has a significant role to play in advancing the broader concept of sustainability (Srinivasan et al., 2012).

The built environment's construction and operation have a substantial environmental impact. The construction industry accounts for 36% of global energy consumption and 28% of energy-related CO₂ emissions (UNEP, 2021). As a revolutionary invention, concrete has become an indispensable building material with many features such as low production cost, easy accessibility, formability, durability, and

thermal performance through the historical development of the construction industry (Wu et al., 2016). Even though the usage of concrete continues to rise, various negative environmental consequences of its manufacturing and use in the construction industry have emerged in recent years. Concrete production has a significant carbon footprint, accounting for 4–5% of global CO₂ emissions (Andrew, 2018). The limited reuse rates of molded materials increase the amount of waste in the construction phase and prevent the production of environmentally friendly structures. In addition, the effect of the formwork, which imposes significant restrictions on complex forms, on construction time and the total cost is much more than other components (Marzouk & Azab, 2014). Beyond environmental considerations, the concrete construction industry is a labor- and capital-intensive industry with high material, equipment, and labor expenses (Weng et al., 2020).

The effects of energy consumption on the environment are becoming a significant concern. The Intergovernmental Panel on Climate Change (IPCC) reports increased public awareness of energy use and the implications of climate change and generated a great deal of interest in gaining a more profound knowledge of the relationship between energy consumption and the prevailing weather conditions (CHANGE, 2007). The predicted warming trends are expected to increase daily temperature extremes, increase the frequency and intensity of heat waves, and decrease frost days (Wang et al., 2011). As a result of climate change, the equilibrium between the local climate and the buildings is subject to a significant shift, which poses a particular threat to buildings (Radhi, 2009). Moreover, without the energy given by fossil fuels, modern structures would not be able to function, but the pollutants released by these fuels' present threats to the local and global environment due to the expanding demands of human civilization.

Some effects of climate change on the structures are energy consumption shifts from heating to cooling, as well as a rise in HVAC inefficiency and malfunction rates (Berger et al., 2014). Depending on the future local conditions, these effects could also impact occupant health and thermal comfort, building-related environmental issues, and operational costs. Building energy efficiency has been a research focus

for many years, as existing structures contribute significantly to the building sector's energy use and carbon impact (Shen et al., 2019). For this reason, today, 3D concrete printing technology is the subject of new researches thanks to its potential to reduce the environmental impact of the construction industry.

Three-dimensional concrete printing (3DCP) is a computer-aided process that builds concrete structures by extruding concrete layer by layer through a digitally controlled nozzle. The proper automation of the construction sector using 3DCP has numerous advantages, including reduced costs, time, labor, increased productivity, and improved construction quality. 3D concrete printing removes molds from the manufacturing process by combining digital and material technologies (Lloret et al., 2015). Furthermore, 3DCP eliminates the geometric constraints imposed by traditional concrete construction, allowing for the precise manufacturing of complex, geometric, and hollow structures. In line with the building's form, scale, and material, different types of 3D concrete printers and printing techniques are developed, enabling the elimination of design limitations (Bos et al., 2016).

Technology is still being developed. As a result, 3DCP tools and materials are now more expensive than their corresponding traditional alternatives, especially when printing large-scale structures. With continuing deployment over time, these costs will be anticipated to decline as understanding advances. In understanding the state-of-the-art 3DCP technologies, a few academic reviews based on existing literature have been conducted with the main focus on development.

The materials used in printers, unlike conventional concrete, must have many rheological properties such as pumpability, printability, constructability, and setting time (Paul, Tay, et al., 2018). For this purpose, chemical additives such as viscosity modifiers, retarders, accelerators, and aggregates are being developed to increase the rheological performance of specially developed concrete mixtures (Marchon et al., 2018). There has been ongoing about different printing techniques and the effects of reinforcement and fibers added to the structure during printing to increase the mechanical performance of the printed product (Panda et al., 2017).

In addition to the products' internal structure, structural form, and support elements printed with concrete printers, thermal and acoustic performance analyses are conducted with scientific research. Experimental studies carried out within the scope of these researches are carried out both with prototype production in the laboratory environment and with real-scale construction elements in the site (Xiao et al., 2021). The sharing of test results worldwide, the acceleration of inter-sectoral collaborations, and the establishment of specific standards in material and printing technologies are enabled (Perrot et al., 2019). Soon, 3D concrete printers; it is predicted that it will play a key role in reducing the loss of labor and environmental impacts in the construction sector, increasing job safety and speed of construction (Paul, van Zijl, et al., 2018).

1.2 Aims and Objectives

The main goal of this research is to evaluate the thermal and energy performance of buildings built with 3D concrete printing to those constructed using conventional construction techniques and insulated in accordance with regulations. Additionally, it provides a comprehensive overview of how the various future climatic situations impact the energy and thermal performance of current 3D-printed concrete structures. Moreover, references to current sources in the literature will help to reach additional information on the subject. Within the scope of the thesis, the methodologies used in the production process, printable materials and their properties, interactive performance analyzes of the products, and the multidisciplinary position of technology are examined. Since 3D concrete printing technologies need to meet the expectations in this regard, where sustainability has gained much more importance, the focus has been on the energy analysis of buildings to be printed with a three-dimensional concrete printer. In the conclusion part, comparative analyses were conducted to understand the impact of climate change on 3D concrete printed buildings through the experimental studies on the prototype

production in-situ environment (ISTON) and the thermal and energy performance simulations.

The main aims and objectives of this thesis are;

- To conduct in-situ measurements for building condition assessment and examine the thermal performance of the 3D concrete printed walls with thermal imaging;
- To evaluate the effects of existing and future changing climatic patterns on the energy and thermal performance of the specified 3D-printed concrete building using modeling and simulation;
- To develop the building energy simulation scenarios for comparative analysis of the existing ISTON building and the same model that is insulated according to TS825 standards.
- To understand the potential and limitations of the 3D concrete printing in the architectural design process and conduct a literature review to determine the previous and current trends of 3D concrete printing;

1.3 Research Questions

The main research question and its sub-questions emerged from the research gap described in the introduction section as follows;

Main thesis questions: How well is the thermal and energy performance of buildings produced with 3D concrete printing compared to those built with traditional construction methods and insulated according to standards? How do the varying future climatic conditions affect the energy and thermal performance of existing 3d concrete printed buildings?

Sub Questions: Which in-situ method can be used to calculate the thermal transmittance of 3D concrete printed construction elements? What type of thermal defects can occur on 3D concrete printed walls? How to develop building energy simulation of an existing 3D concrete printed office building? What are the current

implementations of 3D concrete printing in the field of architecture in the literature? What are the benefits and potentials of the 3D concrete printing technology to the architecture and construction sectors? How is the construction sector utilizing 3D concrete printing technology? What is the impact of 3D concrete printing on the construction industry workforce and manufacturing speed?

1.4 Scope of the Thesis

There is a lack of research on the impact of climate change on 3D concrete printed structures though it has an extensive research domain. To ensure the quality and clarity of the research, the thesis must focus on the specific goals and objectives outlined above. The scope of this thesis will be restricted to and exclude the following specific elements:

- Existing 3D concrete printed office building in ISTON is the main focus of this research. Considering that it is the first and only 3D concrete printed structure in Turkey.
- The in-situ non-destructive thermal imaging method is used to calculate the thermal transmittance of 3D concrete printed construction elements. Other methods such as heat flow meter is not used due to its cons versus thermal imaging.
- The scenario created for comparative analysis is insulated according to TS 825 standards.
- Analyses of the climatic conditions were conducted only for Istanbul, Turkey in this research.
- The simulations were conducted for 2020, 2050, and 2080 weather data to investigate the impact of climate change on 3D concrete printed buildings.

1.5 Thesis Structure

This thesis consists of six chapters, shown in Figure 1.1. The first chapter presents a brief introduction, conceptual background, motivation and problem statement, aims and objectives, research questions, and the thesis's main structure. The second chapter covers a comprehensive literature review of the 3D concrete printing technology in accordance with the research's aims and objectives, including application methods, environmental impact, and architectural design solutions as mitigation and adaptation strategies in construction and architecture sectors. The third chapter outlines the thesis' methodology, which takes the research design into account. The fourth chapter investigates the implementation of the proposed method in the selected case study. The findings from the simulation model are described in chapter five. The conclusion, restrictions, and potential future extensions of the thesis are discussed in the last chapter.

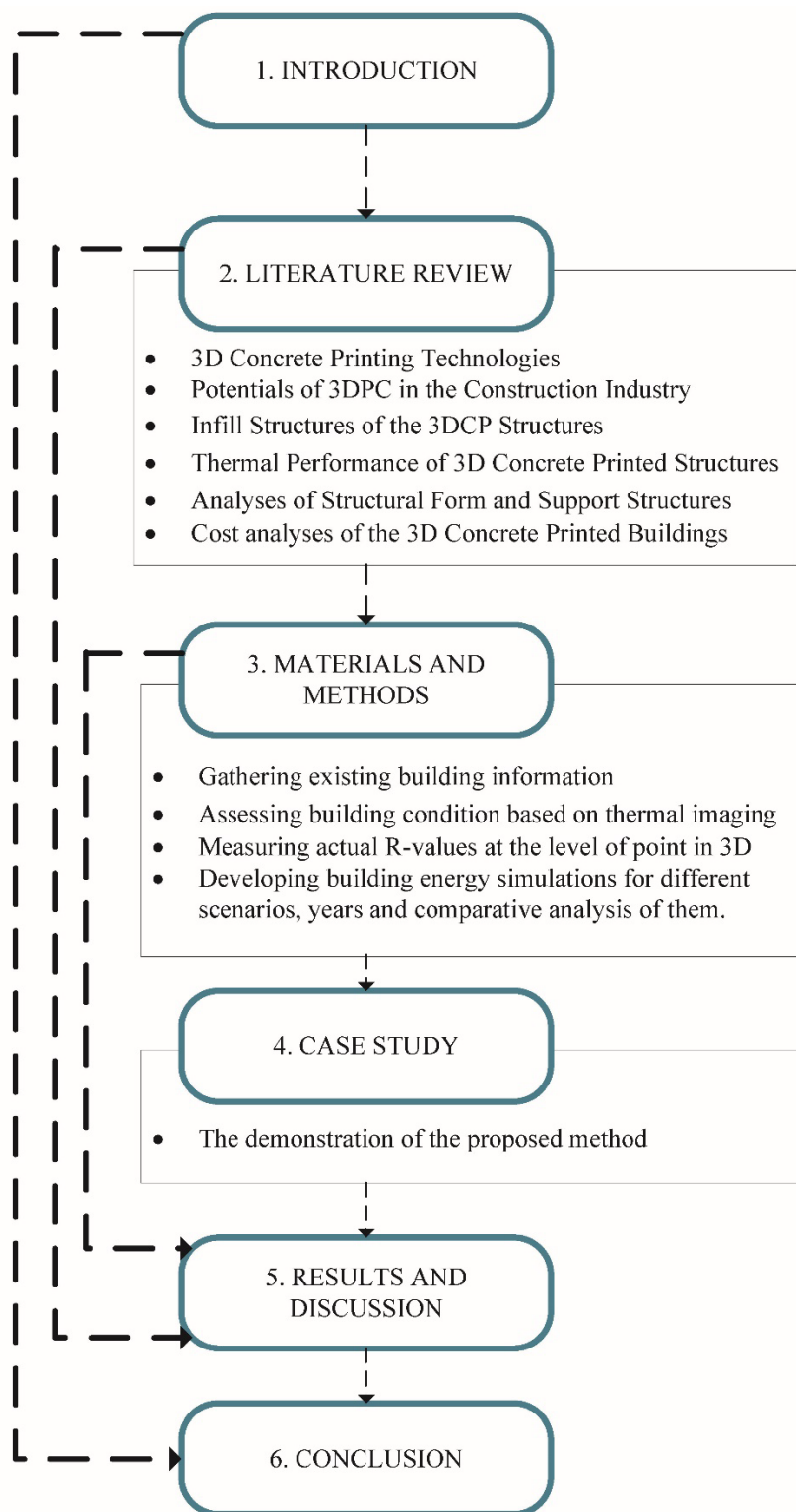


Figure 1.2. The structure of the thesis

CHAPTER 2

LITERATURE REVIEW

2.1 3D Concrete Printing Technologies

3D printers work with the principle of dividing the models in the digital environment into layers using slicing programs and then overlapping these layers by flowing the raw materials in the physical environment. Concrete printers developed for the construction industry have started with a similar principle, and many printer types have been developed to meet their different needs.

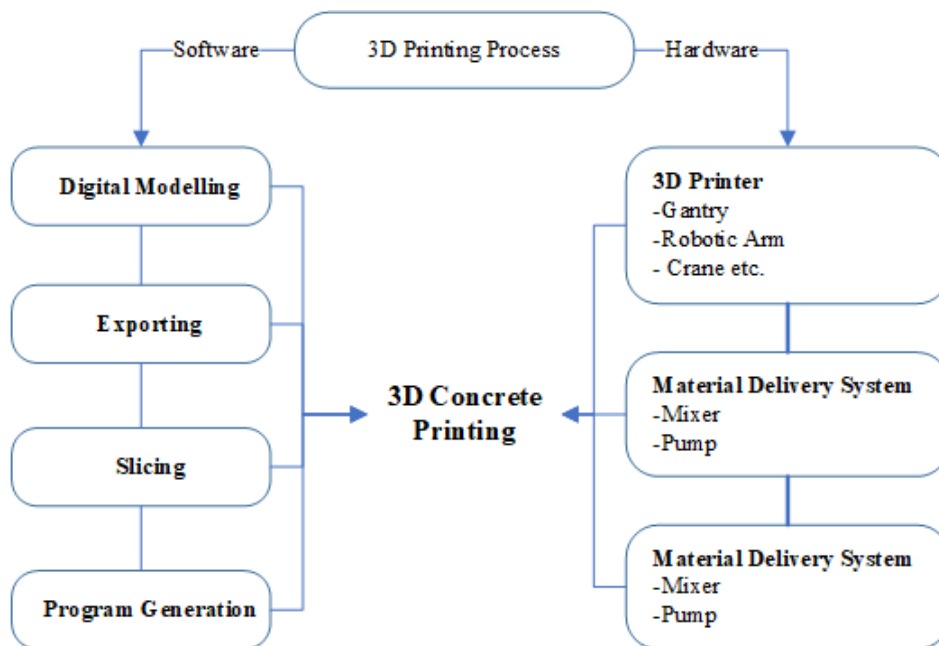


Figure 2.1. The process of 3D printing for construction industry (Paul, Tay, et al., 2018)

Concrete printing, in general, can be defined in two main branches as software and hardware processes. In the software process, after the product designed in 3D

modeling programs is adapted to the printing process, it is transferred to a slicing program to create the G-code file for the printer. G-code is a programming language that allows the printer to read layer thickness, print path, and speed. In the hardware process, printing is carried out with material handling systems and mechanical control elements (Chen et al., 2022). In order to improve the printing quality, it is necessary to ensure the complete harmony of the design, material, and product relationship. Apart from the concrete qualities, it is critical to choose the materials to be utilized correctly based on the complexity of the design and to design the printing parameters by the product to achieve this harmony (Bos et al., 2016). According to the project's requirements, 3D concrete printing can be carried out on-site or prefabricated production in the factory, followed by on-site assembly. With the widespread use of 3D concrete printing technologies, the diversity in building forms has increased, project delays and cost overruns have decreased, and it has been possible to increase resource efficiency, occupational safety, and product quality.

2.1.1 Extrusion Based 3D Concrete Printing

Extrusion-based printers work on the same principle as the fused deposition modeling technique. This kind of 3D concrete printer can be examined in three categories as; 4-axis gantry printer, 6-axis robotic printer, and crane printer (Paul, van Zijl, et al., 2018). Although crane systems are less costly in the manufacture of simple forms and tall structures, robotic arm systems have higher performance in creating complex forms as they have freedom of movement.

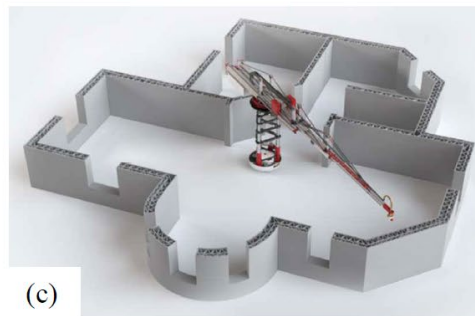
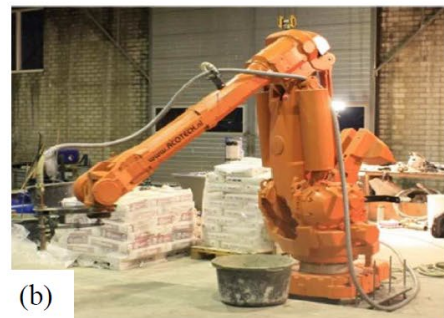


Figure 2.2. a); 4-axis gantry printer; b) 6-axis robotic printer; c) crane printer (Paul, van Zijl, et al., 2018)

One of the first examples developed for large-scale concrete printing technologies, the Contour Crafting method, accelerated the construction industry's research on additive manufacturing technologies (Khoshnevis, 2004). This method, which works with the principle of fused deposition modeling (FDM), provides production by printing the material on each other in layers. Using a cement-like mixture with the help of a rail system and a crane provides an uninterrupted and rapid compression of the entire structure (Figure 2.3). It has an important place in the construction industry as it has excellent potential for the mass production of buildings (Zhu et al., 2019).



Figure 2.3. Contour Crafting Method (Khoshnevis, 2010)

The following example is a large-scale 3D printing process proposed using a 6-axis robotic arm for cementitious materials. In this system, the concrete mix (8) and chemical additives (5) pumped from two separate sources are delivered to the print head with the help of peristaltic pumps (6-7). The pumped materials are extruded in layers by computer-controlled hardware systems (1-2) that control the printing route and the six-axis robot arm (3) to form a 3D printed product (9) (Gosselin et al., 2016).

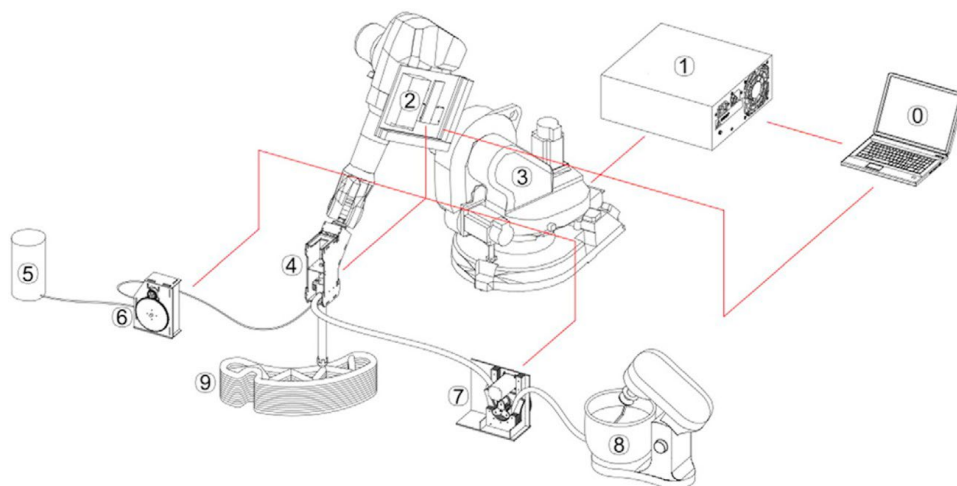


Figure 2.4. Schematic of the 3D printing setup: 0. System command; 1. Robot controller; 2. Printing controller; 3. Robotic arm; 4. Printhead; 5. Accelerating

agent; 6. Peristaltic pump for accelerating agent; 7. Peristaltic pump for premix; 8. Premix mixer; 9. 3D printed object (Gosselin et al., 2016)

The essential factors that play a role in printing the layers at the prescribed thickness in all printing techniques; the yield stress of the material, the cross-section of the nozzle mouth, the correct compression of the poured material by the nozzle, and thus the flowed layers have the strength to carry the following layers to be printed (Mechtcherine et al., 2020). In addition, the fluidity of the material in the pump and its pumpable feature also affect the printing quality (De Schutter & Feys, 2016). For this reason, all scientific studies aim to realize the printing of quality products in all aspects, with the optimization of material-machine interaction.

2.1.2 Powder Bed Based 3D Concrete Printing

In powder bed-based printing technologies, the gantry is spread over the printing area in layers after the system is installed. After each spreading powder layer, chemicals sprayed in layers by the determined structural cross-section with the multi-nozzle print heads mounted horizontally on the crane ensure that the dust particles are bonded to each other (Tibaut et al., 2016).

D-Shape technology, which is one of the most important examples of this printing technique, medium-sized (6m x 6m printing area) and amorphous structures can be created with the help of sandstone powder and binding chemicals. In the system, 300 nozzles placed in rows on the gantry are produced by spraying a binder chemical on the powder material, laid down to a thickness of 1 mm (Cesaretti et al., 2014). Since the raw powder material, which acts as a support element during printing, can be used in other printings when the printing process is finished, material waste can be avoided (Figure 2.5).



Figure 2.5. The production and final version of a structure printed on a D-Shape printer (D-Shape, 2015)

Emerging Objects, which researches serial prototyping of building elements, aims to develop different 3D concrete printing methods to produce durable performance-based building components (*Emerging Objects*, 2013). Their experimental studies have developed mass-produced concrete structural elements by spraying chemical binders on a mixture of small aggregates and fiber-reinforced cement. In addition, by using local geographical materials (sand, limestone) and construction waste added to the cement; Contributions have been made to the researches on the production of structures suitable for regions prone to erosion and desertification (Figure 2.6).



Figure 2.6. Parametric forms printed with powder bed based printing technology (Rael, 2018).

2.2 3D Printable Concrete Properties

The limited material palette in use today is a significant barrier to implementing modern 3D printing in the building industry. Due to fluidity, minimal deformation, and early hardening required from the material during 3D printing, traditional concrete used in molded manufacturing methods, cannot be used in this process (Rael, 2018). Rheology, extrudability, buildability, pumpability, and strength must be considered for printable concrete (Paul, van Zijl, et al., 2018).

Since the printing process necessitates a significant level of continuous material control, high-performance building materials are preferred (Rael, 2018). As indicated in Figure 2.7, in order to ensure minimal or no deformation of the bedding layers, it is necessary to use concrete with a low or zero slump (Ma et al., 2019). Alternately, low-viscosity concrete can be pumped easily but needs a chemical accelerator added at the nozzle for quick hardening after printing (Bhattacharjee et al., 2021).



Figure 2.7. No slump 3D printable concrete printed in ISTON factory

Essential parameters for applying concrete in additive processes are the pumpability and extrusion stability of the wet properties. There are four main properties of the wet process of additive manufacturing (Y. Zhang et al., 2018):

- (a) **Pumpability:** The efficiency and constancy with which material is delivered through a system;
- (b) **Printability:** The efficiency and consistency with which an extrusion device can deposit material;
- (c) **Buildability:** Is a measure of a material's resistance to deforming under load after being deposited, and
- (d) **Open time:** The aforementioned attributes' duration is consistent within acceptable limits.

However, each of these characteristics will differ based on the mix design, the extrusion method, and the deposition tool (C. Zhang et al., 2021). The printing process may also impact the material's hardened qualities (Y. Zhang et al., 2019). Furthermore, the benefit of concrete printing is that the 3D model can be strengthened before production, requiring the least amount of material for the final print, which is not possible with conventional methods of construction manufacture (Wolfs et al., 2019).

Special material compositions have been developed for 3D concrete printers to optimize the printing process (Bhattacharjee et al., 2021; Li et al., 2020; Tey et al.,

2019; Torelli et al., 2020; Wolfs et al., 2019; C. Zhang et al., 2021; Y. Zhang et al., 2018, 2019). In contrast to standard concrete, cement-based composite enables the printing of self-reinforced concrete structures thanks to its high elasticity, thus eliminating the dependence on steel reinforcement (Figure 2.8) (Li et al., 2020).

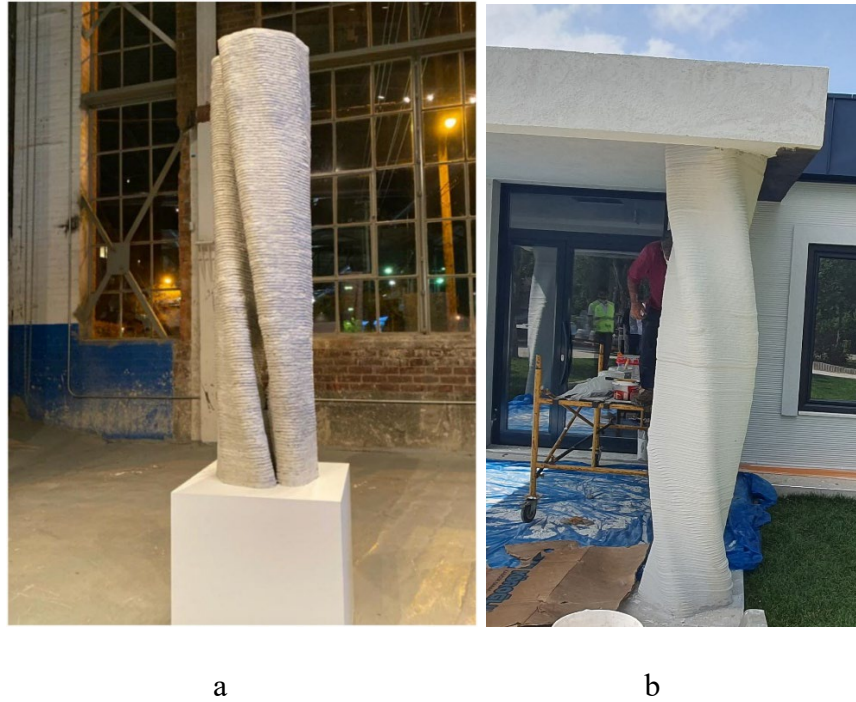


Figure 2.8. (a) Twisted column, University of Michigan (Li et al., 2020), (b) Twisted column, ISTON 3DCP office building entrance.

For the materials developed for 3D concrete printers to strengthen their place in the construction sector, material development and process controls must be optimized and brought to specific standards (Wangler et al., 2016). Established for this purpose by the International Association of Building Materials, Systems, and Structure Laboratories, and Experts (RILEM), "Digital Manufacturing with Cement-Based Materials Commission" examined the existing patented extrusion techniques and application examples in the industry and made the results a resource accessible to all members (Buswell et al., 2020).

2.3 Potentials of 3DCP in The Construction Industry

3DCP has several game-changing advantages over conventional methods for the construction industry, including less material waste, less energy use, in-situ production, increased architectural/design freedom with less resource demand, and related CO₂ emissions throughout the entire product life cycle (Ghaffar et al., 2018). Additionally, it leads to changes in labor structures, safer working conditions, and shifts toward more localized and digitized supply chains. From the perspective of architects, 3DCP can offer a powerful tool for their industry by enabling them to create physical models more quickly, with higher resolution, and capable of capturing the complexity of their designs. Customers can co-design products with 3DCP to create precisely what they want and how they want it (Craveiro et al., 2019).

Additionally, it is unclear if applying 3DCP to the construction sector would result in cost increases or decreases because the sector is still too cost-sensitive in the wake of the most recent economic crisis. In this regard, it will be crucial to examine the life cycle costs of 3DCP in light of the material feedstocks and printing techniques. The key advantages and difficulties of using 3DCP in construction are outlined in

Table 2.1. Main advantages and difficulties of 3DCP in construction

Advantages and Difficulties of 3DCP	Statements
Increased construction speed	In a shorter time, large-scale production of parts and structural components can be built.
Architectural design freedom	Releases the present essential design and technical limitations, providing unrivaled prospects for curved/hollow structures and unique customization, creating functionally lightweight parts while keeping strength (Agkathidis et al., 2019).

Table 2.1 (continued)

Easy to spot errors and defects	Including the digital fabrication process allows for simulating the possible problems before production starts (Muthukrishnan et al., 2021).
Eliminates the formwork	Reduce the cost of materials and labor significantly, and boost site workers' productivity.
Expensive hardware	In addition to continuing maintenance expenditures, expensive hardware is required, though the industrial competition quickly drives prices down.
Lack of standardization	Due to a lack of performance standards, policies and regulations still need to be adjusted to consider this new technology.
Low quality surfaces	Although the final product might not meet current standards, it can constantly be improved or given a human-made finishing touch (Petrovic et al., 2011).

2.3.1 Economical Potential of 3D Concrete Printing

The adaptation of computer technologies in other branches of industrial production has been faster than in the construction sector. Compared to the building industry, other branches of industrial production have adopted computer technologies more quickly. In many stages of the production process, robotic technologies will replace

human labor due to the widespread usage of 3D concrete printers in the building industry. On the other hand, such a decrease in the workforce in the construction sector will increase unemployment. From a more significant viewpoint, new roles will be created for maintenance and repair teams, robot system operators, and other related positions. (Tay et al., 2017).

In conventional mold manufacturing, the cost decreases as the number of components produced with the same mold increases (Figure 2.9). On the other hand, since no formwork is used in additive manufacturing, component diversity does not affect the cost. In molded manufacturing, cost savings are achieved if the element dimensions can be standardized from the design stage. However, the fact that most building elements have unique forms and dimensions in construction increases the variety of formwork and the cost. When a 3D concrete printer is used with BIM software, thanks to the computational design, each building element is provided in a unique shape and size, and it also prevents wastage of formwork, time, and cost (Lim et al., 2012).

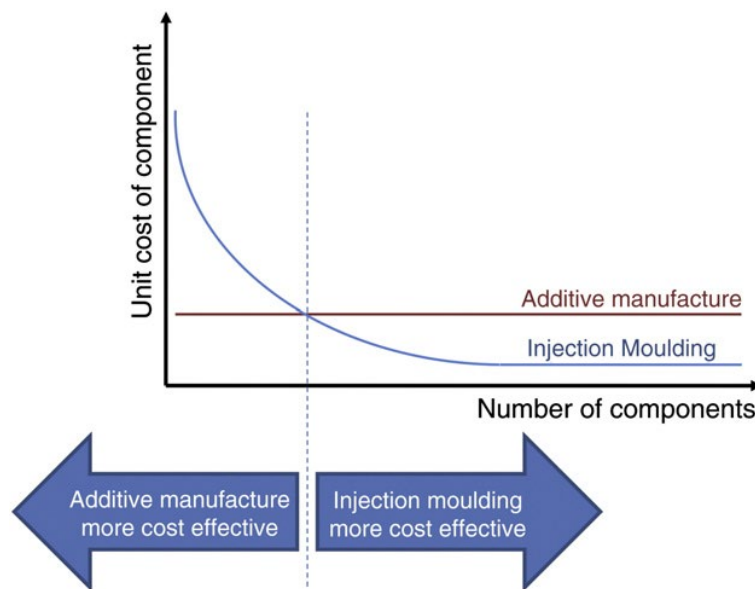


Figure 2.9. Cost graph of traditional molded manufacturing and additive manufacturing technologies depending on the number of components (Lim et al., 2012)

The workforce is used more intensively in the construction sector than in other industries. It causes negativities such as loss of labor, work accidents, inefficient and long-term construction processes due to low-skilled labor. When the costs of mold and concrete production are examined, the labor cost spent is close to 60% (Figure 2.10) (Paul, Tay, et al., 2018). More production is provided in a shorter time with fewer people and 3D concrete printers, lowering construction costs significantly (Delgado Camacho et al., 2018)

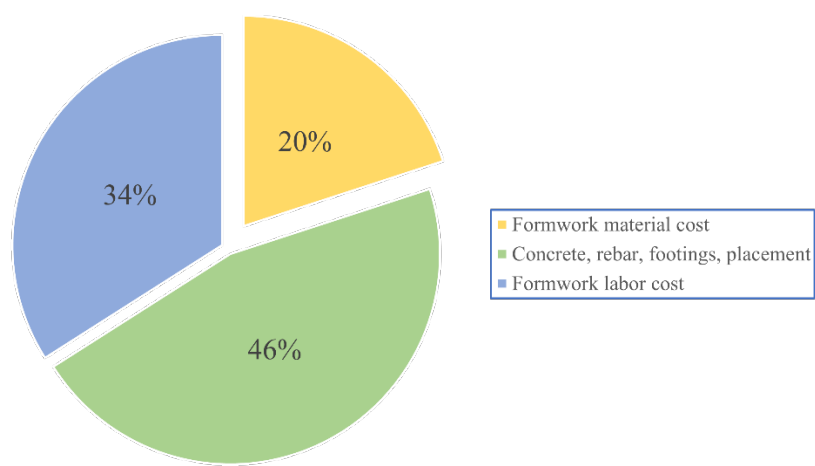


Figure 2.10. Cost distribution of traditional molded construction (Jha, 2012).

Although the cost of the printers used in 3D construction technologies prevents them from becoming widespread, it is predicted that 3D concrete printers will be an answer to the housing problem in the world soon, thanks to work done by companies aiming to produce low-cost structures. One of these companies, ICON, completed each house in the social housing project is developed for the slum areas in Mexico within 24 hours (Figure 2.11). These houses' material and construction costs are approximately \$10,000, and ICON stated that they aim to reduce this cost to \$4,000 (Gregurić, 2021).



Figure 2.11. The first 3D concrete printed community of houses for low budget construction (Verge, 2018)

As a result, with 3D concrete printing technologies, the shelter needs of people in low-income regions of the world will be met quickly, and it will be possible to build green buildings at lower costs.

2.3.2 Environmental Impact of 3D Concrete Printing

Additive manufacturing (AM) technologies have been connected with cost-effective fabrication that reduces energy consumption, resource requirements, and CO₂ emissions over the product's life cycle. In contrast to conventional construction methods, additive construction technologies show a substantial potential for material reduction through topology optimization, the production of complex geometries without supporting structures, and the integration of multi-functionality in building elements. However, life-cycle analyses (LCA) must be carried out to direct the design of 3D-printed structures to create a sustainable construction process. Through a study of relevant scientific papers, this section aims to discuss the environmental benefits of this construction method.

Systems that optimize the total energy consumption in terms of materials and production, defined as "green construction," have become accessible using 3D printing technologies. From the design stage, selecting materials with low carbon

content can provide purposeful projects. The production of 3D concrete printers paved the way for low-carbon cement and recycled aggregates. In addition, production suitable for green construction is supported by adding performance-enhancing materials such as granular blast furnace slag, natural pozzolans, qualified fly ash, and clinker into cement (Cho et al., 2021).

The manufacturing of the robotic arm, the manufacturing and recycling of the lithium batteries required to power the robots, along with the electricity consumed during fabrication all have a negligible impact on the environmental impact of a digitally manufactured wall. Furthermore, the data reinforced the hypothesis that the quantity and kind of building materials utilized have the most significant influence. These findings are not unexpected because previous research on conventional construction has established that the construction period contributes relatively little to the overall life-cycle impact of buildings. Due to mechanical and advanced construction methods, energy consumption in construction has increased. Current research, however, disproves this claim and encourages designers and material scientists to concentrate much more intently on material optimization in the additive building.

With different levels of complexity made using additive robotic fabrication techniques, the environmental performance of reinforced concrete walls was examined, and it was compared to equivalent buildings that would have been built using conventional methods. The environmental assessment findings proved that digital fabrication offers higher environmental benefits than traditional construction for structures with a high degree of shape complexity. As seen in Figure 2.12, the novelty and complexity of the architectural geometry do not increase the environmental impact of the digitally created wall. The potential value of digital fabrication rises proportionally to the complexity of architectural geometry since more complex shapes can be created without incurring more environmental expenses.

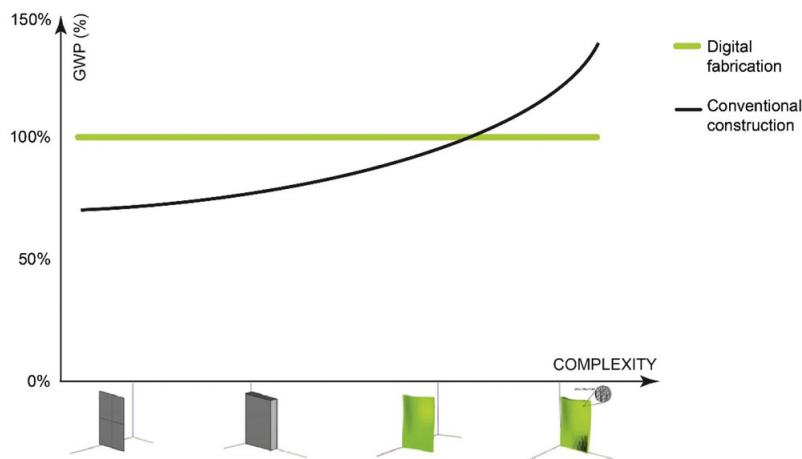


Figure 2.12. Environmental benefits of digital fabrication over traditional building due to complexity. The percentage of Global Warming Potential per m² of the concrete wall represents the environmental impact

However, it is crucial to distinguish between shape complexity utilized as a design technique to save material and shape complexity employed only for aesthetic purposes, which would require more material. The shape complexity made possible by digital manufacturing methods should emerge from an effort to maximize the use of materials in the structure to impact the environment positively.

Some projects worldwide aim to minimize the environmental impact of 3D concrete printed structures by various methods. Project ITACA by Wasp, is an ecosystem that uses the tools required to survive in space to raise standards of living in places with limited access to food, water, and infrastructure. Crane printer is planning to use local organic materials to print the primary framework of the project. The project consists of a 3D-printed home made from materials with no carbon footprint.

2.4 Thermal Performance of 3D Concrete Printed Structures

Building energy efficiency practices aim to keep energy use to a minimum while designing a comfortable space. The purpose of thermal insulation in buildings is to weaken the heat flow fluctuation in the building element to store and release heat

gradually. The use of the material ensures maximum use of solar energy in winter; In summer, it ensures that the temperature inside does not exceed a specific value.

In a study on the thermal performance of building elements produced with 3D concrete printers, a wall with a layer thickness of 15 mm, a width of 200 mm, and a height of 810 mm was printed (Marais et al., 2021). Four different cases were created from this produced wall on a 250 mm x 200 mm section with an internal construction wall thickness of 35 mm. The examination was conducted using the finite element method (FEM) (Figure 2.13). In order: Case A examines only the thermal conductivity in the concrete (conduction), Case B, in addition to the first case examines the heat conduction through the cavity of the wall (cavity radiation), Case C, in addition to the first two cases, also examines the heat radiation in the cavity of the wall (convection). The result of these analyzes is that it is not sufficient to look only at the thermal conductivity of the concrete in the thermal insulation tests performed on the 3D printed walls. It has been proven that convection and cavity radiation are also highly effective in calculating 3D concrete printed structures (Marais et al., 2021).

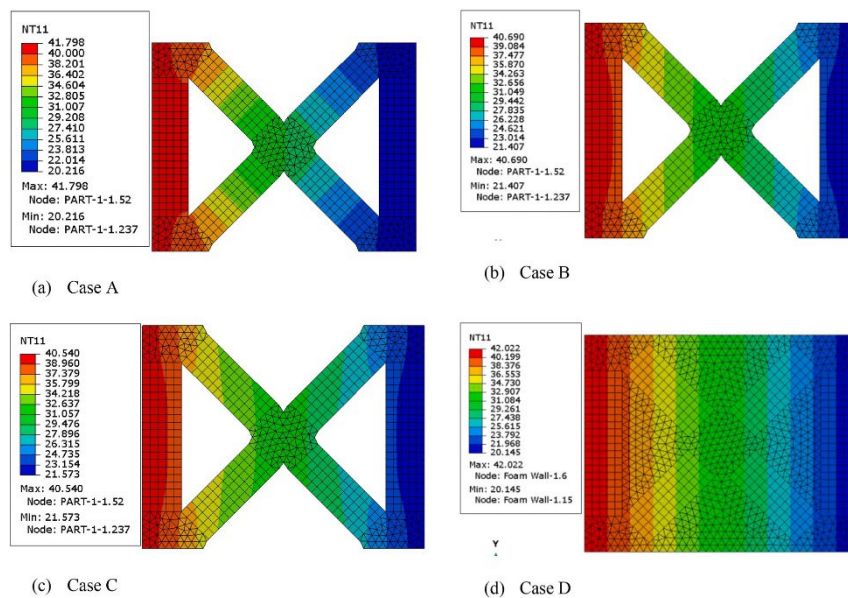


Figure 2.13. Heat transfer methods of a infill structure node. Case A: conduction inside concrete, Case B: conduction inside concrete and cavity convection, Case C:

conduction inside concrete, cavity convection and radiation, Case D cavities filled with foam concrete simulated only conduction (Marais et al., 2021)

Various methods have been developed to strengthen a wall printed with a 3D concrete printer. One of them is to fill the gaps created in the inner wall structure with insulation material. Another method is to build a wall in the vertical section of the wall by using different nozzles (thermal-acoustic insulation, structural strength, etc.), where each section undertakes a different task. Another is to increase the thermal performance with the components added directly into the concrete mix; the point to be considered here is that the added components may adversely affect the load bearing or printability of the wall (Pessoa et al., 2021).

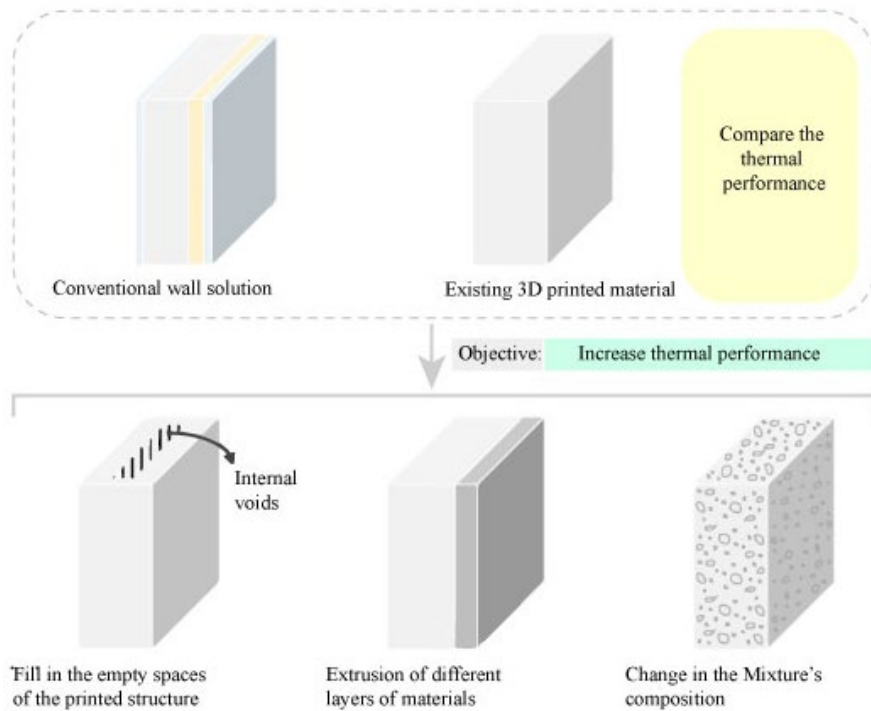


Figure 2.14. Methods to 3D printed walls' thermal performance (Pessoa et al., 2021)

In order to increase the thermal insulation quality of the wall, the gaps in its structure can be filled with certain insulation materials, thus avoiding the necessity of creating a separate insulation layer. Developed for this purpose, expanded polylactic acid (E-

PLA) is a low-density, sustainable, and environmentally friendly insulation filling material (Parker et al., 2011).

A wall was fabricated with mineral wool (5 cm) placed between layers of 3D-printed concrete (3 cm each) and polyurethane foam (14 cm) placed on the outer surface to observe the effect of insulation materials on the wall thickness (Figure 2.15). As a result of the study, it has been seen that although it is the same size as the conventional wall thickness without insulation, it provides the same value as the traditional insulated wall in terms of thermal performance (Kaszynka et al., 2019).



Figure 2.15. Combination of 3D concrete printed wall with traditional thermal insulation (Kaszynka et al., 2019).

In another study, a different technique was used on the house's walls, produced with a usage area of 95m². First of all, 8 cm polyurethane foam was printed on the concrete floor in layers, with the help of an automatic tool and a robot arm, with a gap of 15 cm between them (Subrin et al., 2018) These layers acted as a mold, and this time the concrete mixture was poured between them (Figure 2.16). After printing, plaster and paint were applied to the polyurethane foam, and it was made ready for use. The printed polyurethane foam material was used as a mold while also serving as thermal insulation (Furet et al., 2019).

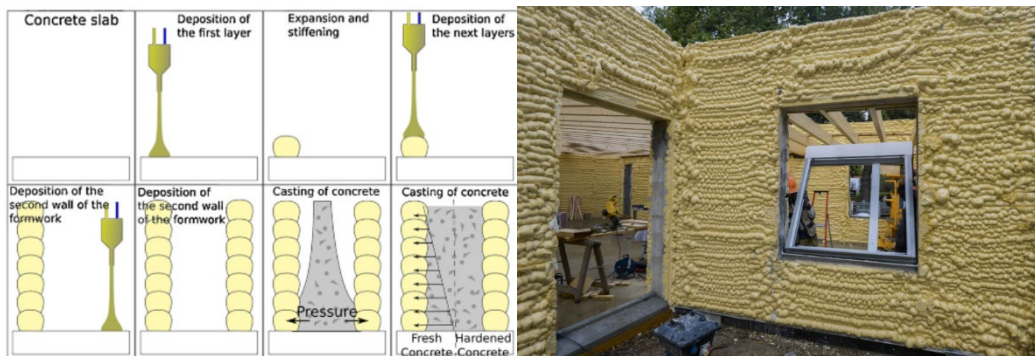


Figure 2.16. Using 3D concrete printed structures as permanent formwork (Furet et al., 2019)

In order to reduce energy consumption in all phases of design, production, and use, it is necessary to estimate how much the building's energy demand can be. ANSYS finite element analysis program is used to determine the structural and thermal behavior of 3D printable concrete. In an experiment comparing conventional concrete, cork reinforced concrete, and expanded clay added concrete with the help of ANSYS, the concrete compared with cork had the best thermal performance (Craveiro et al., 2017).

The diversity of the materials in the printable concrete mixtures creates differences in the thermal performance values of the printed structure, depending on the size and number of the cavities in its internal structure and the type of material filled in these cavities. Figure 2.17 shows three printable concrete mixtures with different proportions of siliceous sand, gravel, sulfur, cement, and polypropylene fibers were used (Alkhalidi & Hatuqay, 2020).

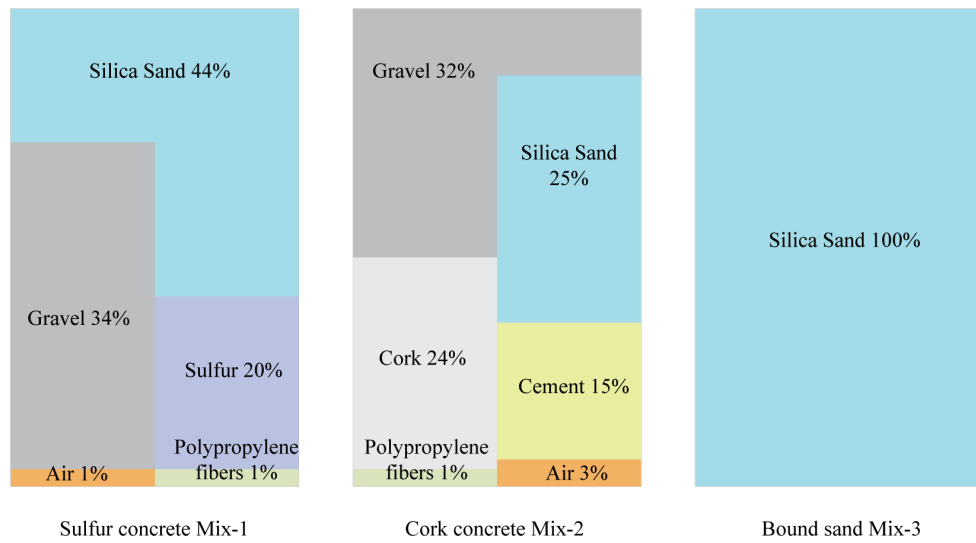


Figure 2.17. Printable mixes components percentages (Alkhalidi & Hatuqay, 2020)

By diversifying the space size, several rows, and filling materials (air, sand, and E-PLA) used in the internal structure of the walls created with these mixtures, it is aimed to reach the thermal performance values determined for different climatic conditions. As a result of the study, E-PLA is the filling material that provides the lowest U-value (Table 2). The increase in the number of rows of the inner structure provides better thermal performance than the increase in the cavity size (Alkhalidi & Hatuqay, 2020).

Table 2.2. Thermal transmittance values were determined from E-PLA-filled structures at various mixes with a 20 K temperature difference (Alkhalidi & Hatuqay, 2020)

Configuration	Mix 1 (Sulfur concrete)	Mix 2 (Cork Concrete)	Mix 3 (Bound Sand)
Single Row10cm	0.55	0.52	0.37
Single Row15cm	0.46	0.44	0.31
Double Row10cm	0.35	0.33	0.23
Double Row15cm	0.23	0.22	0.15
Triple Row 10cm	0.23	0.22	0.15

The thermal performance of the printed structure may also change due to side effects such as the number of layers, pauses during the printing process, and attachment points. In the experiment carried out to analyze these parameters; a 3D-printed house consisting of a single volume (with window and door openings) was started to be

heated 48 hours before the experiment, and temperature measurements were made with thermocouples placed on the inner and outer surfaces of the wall. In addition, heat transfers on the wall surfaces were monitored with an infrared thermography device. When the thermographic analyzes placed on the building image are examined, it is observed that the thermal insulation properties of the tested 3D printed structure are insufficient (Figure 2.18). More research on the subject and improvement of the thermal properties of the components are needed (Sun et al., 2021).

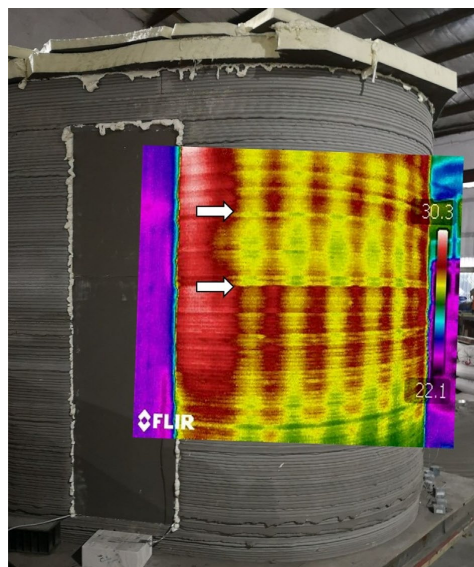


Figure 2.18. Thermographic image and visible image of the prototype house from different directions (Sun et al., 2021)

2.5 Infill Structures of the 3DCP Structures

A 3D printed concrete wall should contain many features such as durability, integrability with upper layers without deformation during the printing process, permeability, and sustainability. For this reason, the optimization of the internal geometry of the building element is of great importance, and the optimization is made possible by using parametric design tools such as Rhinoceros and the add-on Grasshopper. In this way, walls with complex internal structures can be designed, and the performance of the walls can be examined through experimental studies. In

a study carried out with this method, the performance analyzes of the wall made of clay and sand material were made. Experiments can be diversified through wall infill structures (different wall thickness and infill structure design) (Figure 2.19) (Kontovourkis & Tryfonos, 2020).







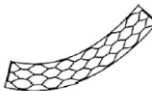


	Nozzle diameter (mm)	4	12	24
1				
	Outside Wall thickness (mm)	4	12	24
	Wall lines count	1	1	1
	Infill (UxV)	no	no	no
2				
	Outside Wall thickness (mm)	40	36	48
	Wall lines count	10	3	2
	Infill (UxV)	no	no	no
3				
	Outside Wall thickness (mm)	4	12	24
	Wall lines count	1	1	1
	Infill (UxV)	5 × 11 Hex	5 × 11 Hex	3 × 5 Hex

Figure 2.19. Different infill structures with layer thickness and pattern (Kontovourkis & Tryfonos, 2020)

Walls with different cross-sections are designed to increase the load-bearing ability of fiber-reinforced concrete. The infill structure designed for use in Contour Crafting technology is shown in Figure 2.20.

In an experiment carried out to increase the load-bearing ability of the products, an amorphous wall with dimensions of 2 m x 0.9 m, height 0.8 m, and 128 layers were printed, then 8 mm diameter reinforcements were placed in the gaps created in the wall (23 pieces) (Figure 2.20). This approach aims to bring the bearing capacity of 3D printed elements to structural elements produced by traditional methods (Lim et al., 2012).



Figure 2.20. Infill structure of the amorphous wall with reinforcement (Lim et al., 2012)

Air gaps or insulating layers are added between building components to control thermal permeability in traditional construction techniques. 3D concrete printed structures have cavities to control the conduction, convection, and radiation heat transfer with different infill designs. Although there is no standardized cavity ratio in such productions, a 1: 2.5 concrete/air cavity ratio is generally used in the studies (Ghaffar et al., 2018).

2.6 Analyses of Structural Form and Support Structures

Analyses of Structural Form and Support In additive manufacturing technologies, the production is carried out by printing the material in layers on each other. For this reason, temporary support elements shown in Figure 2.21 are used to create complex forms and large openings. However, the support elements used in large-scale structures increase the cost and make it difficult to carry out the production at the construction site. For this reason, new technologies are being developed for printing complex geometries without the use of temporary supports.

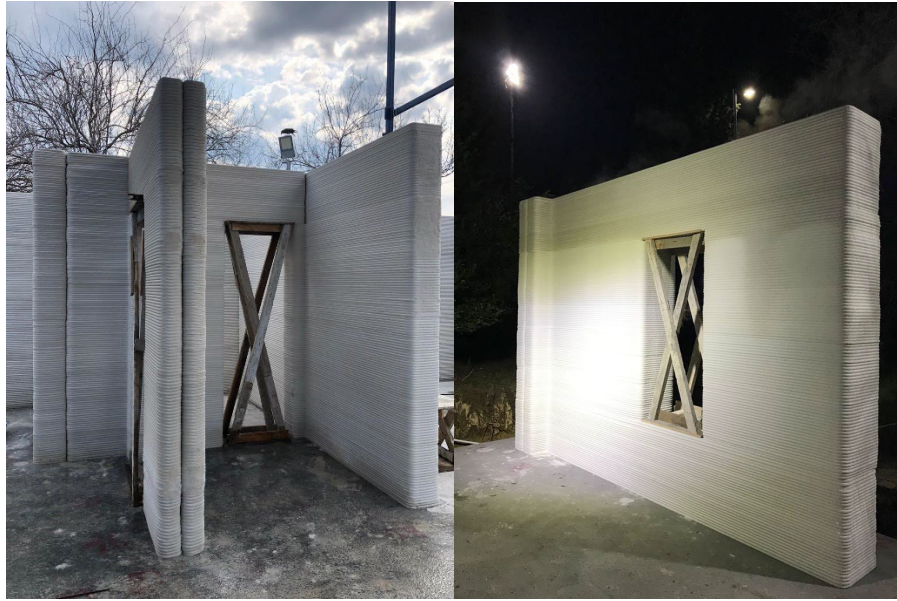


Figure 2.21. Support structures to print over gaps used in ISTON

This technology's most widely used method is to create a printing route by separating the three-dimensional design into two-dimensional layers through a slicing program. The most restrictive factor in this method is that the nozzle works perpendicular to the ground. Although it is suitable for small-scale models, it must be adapted and optimized for complex and large-scale structures because structural elements are three-dimensional. The layers to be printed must be non-planar, of varying thickness.

In order to get rid of these restrictions, the tangential continuity method has been developed. As seen in the left diagram in Figure 2.22 in the traditional method, while the height is constant, the contact surfaces between the layers are variable. In the diagram on the right, the contact surfaces between the layers are maximized, and the layer height is made variable using the tangential continuity method (Gosselin et al., 2016).

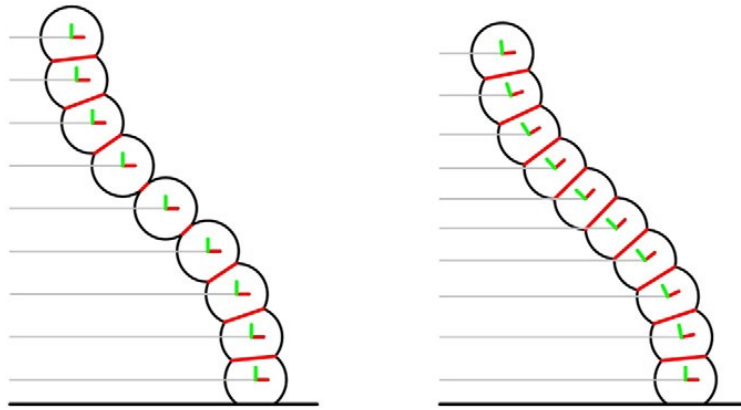


Figure 2.22. The cantilever approaches found in commercial 2D slicing software (left) and the tangential continuity method (right) were used to 3D print a schematic cut perpendicular to layers (Gosselin et al., 2016)

By operating the robot arm in 6 axes in the system, the material extrusion is always perpendicular to the printed layer, thus creating structural elements that are both mechanically stronger and have more geometric freedom. The multi-purpose wall shown in Figure 2.23 was produced with this technique, and it is an indication of the freedom of design and the support of geometry by the function (Gosselin et al., 2016).

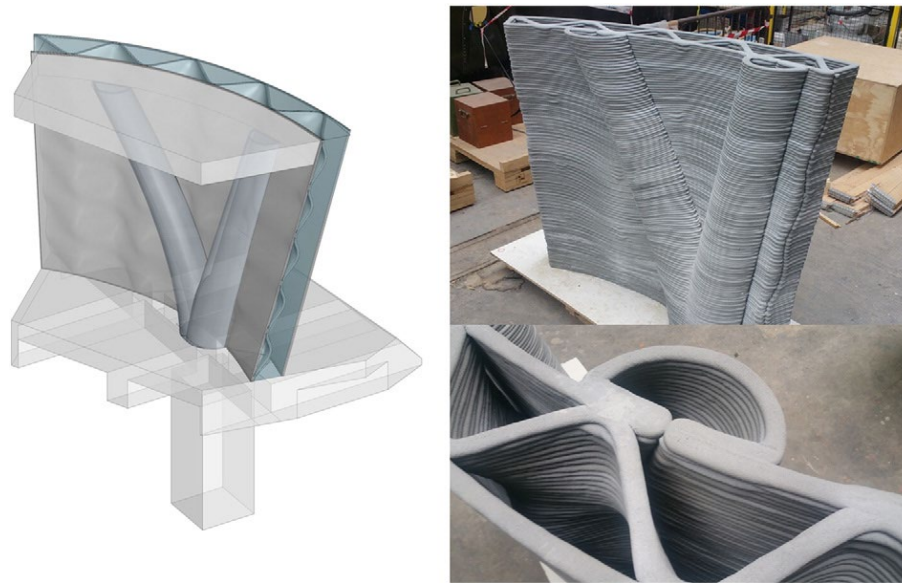


Figure 2.23. The 3D printed high-performance concrete multifunctional wall (Gosselin et al., 2016)

In this process, the collaborative work of the architect and the civil engineer has gained much more importance. It is necessary to optimize the designed elements with experimental feedback. Design freedom can only be achieved through the interdisciplinary study of the computational modeling-experimental feedback and optimization triangle.

2.7 Applications of 3D Concrete Printing in the Construction Industry

Although 3DCP construction is still in its early stages, this technology has already built impressive structures. A full-scale building can be printed on-site in two steps: first, formwork layers are printed using printing mortar on-site, and then reinforcement is added using a different automatic device. A building's produced off-site components may be put together there. Different strategies can be used to print and build a huge structure depending on the printing process that is chosen. The company BAM Infra used a similar approach to print concrete bridge components. The hollow units were printed in a horizontal plan and then joined into structures.

Although printing techniques vary amongst manufacturers, the fundamentals of final structure assembly are the same.



(a) Yhnova House, Nantes University (Furet et al., 2019)



(b) Lotus House, Team WashU (Liam Otten, 2018)



(c) Dentist surgery, České Budějovice (Scoolpt, 2015)



(d) DFAB HOUSE (Dörfler et al., 2019)



(e) Urban Furniture, ISTON



(f) TECLA (Moretti, 2023)



(g) New Story, Mexico (ICON, 2018)



(h) Project Milestone, (Sanjayan & Nematollahi, 2019)

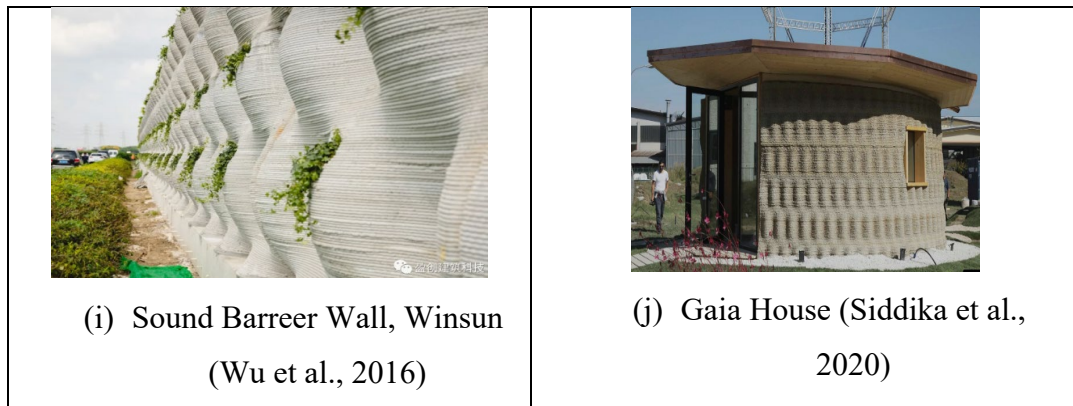


Figure 2.24. 3DCP applications in the world

The government and businesses are paying close attention to the two main civil engineering construction sectors, buildings, and bridges. Manufacturing architectural buildings and bridge components have much promise with 3DCP technology. In order to identify potential difficulties with using 3DCP technology in building and bridge construction, this study evaluated current developments.

2.8 Future of the 3DCP Technology

The definitions of the materials, process systems, operational settings, and applications are all relatively simple (Ma et al., 2022). The difficulty comes from predicting, assessing, and estimating the commercial late-stage development in terms of the degree of automation for digital workflow and process control (He et al., 2020). These variables affect the level of expertise needed by an operator to construct the machine control codes from a CAD model and the operative knowledge and experience concerning materials that enable building oversight to increase manufacturing resilience (Sepasgozar et al., 2020). To appeal to various organizations and market sectors, the degree of investment necessary and the potential advantages are pretty variable.

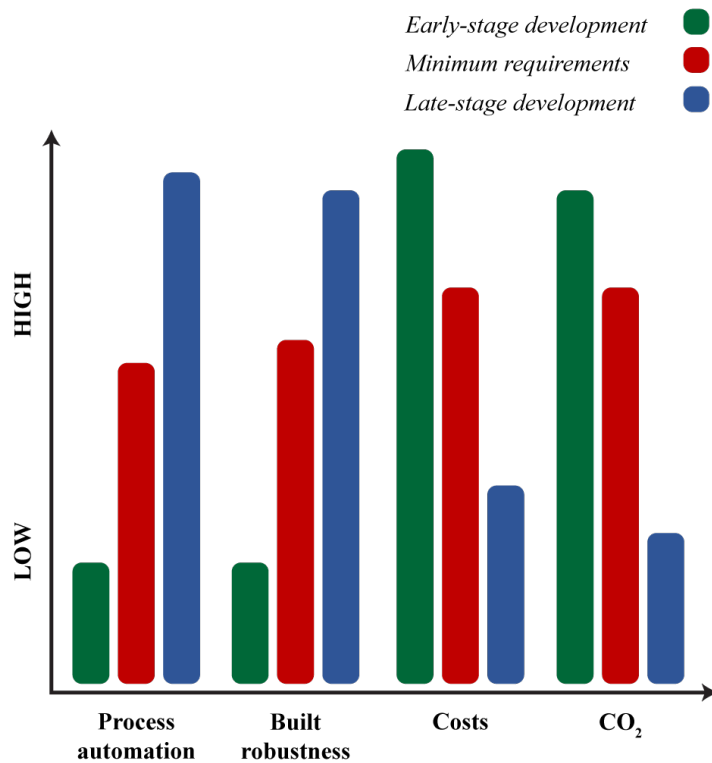


Figure 2.25. Extrusion-based 3DCP evolution is projected graphically with four primary drivers (Ma et al., 2022).

Figure 2.25 displays a graphical representation of the direct cost and sustainability drivers analyzed. For the technology to be commercially viable, it is anticipated that there should be a minimal set of market-oriented requirements (Ma et al., 2022). Additionally, it is anticipated that the sustainability difficulties will be rectified over time through research and development (Bai et al., 2021). As production volume increases, locally produced feedstock becomes more common, and research enhances the overall process robustness through the collected understanding of materials and their relationship to process parameters, material costs are likely to decrease (Marchment & Sanjayan, 2020). As a result, the industry that works in particular market sectors to produce goods and services for applications will decide whether automation is sufficient.

For large-scale practical applications, thorough material design schemes and rheology control procedures must be further developed to assure printability,

economic and ecological viability (Xiao et al., 2021). In order to increase construction efficiency with printing resolution adequate for various practical applications, the equipment and control systems must also be enhanced (Khan et al., 2020). Although various large-scale 3D printing techniques have been demonstrated to be beneficial for practical purposes, there is currently no framework to control these techniques, including design standards, calculation techniques, and manufacturing techniques (Asprone et al., 2018). Lastly, additional research, standardization, and development of the design philosophy and standards for large-scale 3D-printed concrete construction technologies are required.

CHAPTER 3

MATERIALS AND METHODS

In the preceding part, a detailed literature analysis of 3D concrete printing techniques and their potential in the construction sector, the thermal performance of 3D printed concrete structures and structural aspects that affect 3DCP structures, applications of 3DCP in the construction sector, and climate change impact on structures was provided. In addition, the following elements were identified:

- The lack of detailed research on the energy performance of 3DCP structures is observed, especially for the existing buildings.
- The methodologies to analyze the thermal and energy performance of the 3DCP walls should be taken into consideration because there is a knowledge gap about how climate change impacts 3DCP buildings.
- The performance of 3DCP structures is affected by the environment to which they are exposed. The worsening climatic circumstances significantly impact the energy performance of buildings as well as the health and efficiency of their occupants.

The primary objective of this thesis is to investigate the effect of climate change on 3DCP buildings and compare the energy efficiency of 3DCP structures to conventional structures. The thesis methodology is divided into three parts: detailed data collection, developing a building energy performance model, and analyzing the climate change effect on 3D concrete printed structures to compare the energy efficiency of 3D printed structures to conventional buildings. Long-term measurements of indoor and outdoor climatic conditions, along with information on the building's structural features, thermal properties of building materials, and heating/cooling system, are all part of the first phases of Turkey's first 3D concrete printed structure in the ISTON factory. The second phase describes the building's

formal, structural, and occupant aspects. Hourly indoor air temperature data are then used to calibrate the model. Infrared thermography is used to identify potential defects and calculate the U-value of the walls, while on-site monitoring data is used to determine the thermal parameters of the main wall body of the evaluated building. The third phase contains a comparative analysis of the energy performance between 3DCP and conventional buildings. The simulations are repeated for the years 2020, 2050, and 2080 to understand the impact of climate change on the scenarios.

This research evaluates energy performance and prediction of building performance under climate change of a 3D printed concrete office building. The thermal characterization of the walls was performed to determine the U-values of the external walls using semi-empirical and theoretical approaches and numerical analysis. The obtained U-values were used in building energy performance analyses using energy simulations.

Following are some prerequisites for the methodology utilized in structuring the strategies and the analysis processes:

- Information gathering about existing 3DCP building
- Thermal imaging of the external walls of the case building
 - Collecting internal and external air temperature during the thermal imaging process
 - Calculating the reflected apparent temperature of the walls
 - Dividing walls into grids and naming walls for future documentation
 - Fixing perspective distortion of the photos and calculating average pixel color information
- The creation of projected future weather data files
- Evaluation of the building's existing performance
 - Creating 3D model
 - Developing a simulation model
 - Comparative evaluation of performance

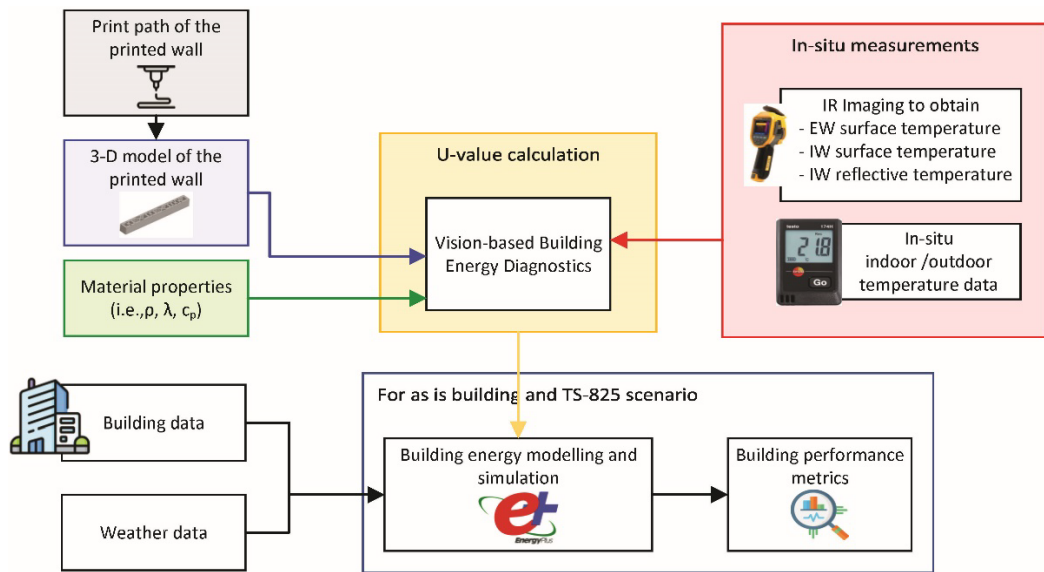


Figure 3.1. Building energy analysis pipeline

3.1 Existing Building Data Collection

Before conducting a climate and performance analysis, it is necessary to collect extensive building information in order to acquire more precise and reliable results. The data collection process includes collecting existing data of the 3DCP building and indoor and outdoor data measurement operations.

3.1.1 Building Data

Existing data was gathered from architectural drawings and robotic arm printing files, photos of the construction process, and included building structural features, thermal attributes of the construction materials, heating and cooling systems, ventilation systems, occupant count, and occupancy duration. Wall thicknesses, thermo-physical properties, and infill structures of the walls were obtained from architectural drawings.

The thermal conductivity (λ) and density of the printed concrete used in this research was taken from an unpublished work by Bayrak et al. (2023) as 0.92 and 1677 kg/m³,

respectively. The specific heat capacity (c_p) of the printed concrete was selected as 1685 J/kgK based on existing literature (Alkhalidi & Hatuqay, 2020).

3.1.2 In-Situ Measurements

Long-term measurements of indoor and outdoor climatic data, temperature, and relative humidity, were conducted by Testo 174 T, and H dataloggers. The properties of data loggers are given in Table 3.1. One of the dataloggers were installed into the office room and the other one is located north façade of the building. Temperature (T) and relative humidity (RH) data were recorded every 10 min between October 13th, 2021 – June 1st, 2022.

Table 3.1 Properties of Testo 174 T and H dataloggers

Temperature - NTC	testo 174T	testo 174H
Measuring range	-30° to + 70°C	-20° to +70°C

Non-destructive in-situ method of infrared thermal imaging technology is used in this study to show the variations of surface temperature to calculate thermal performance of the walls and detect potential thermal defects on walls of the 3DCP building. Thermal images of the prototype house were captured with infrared camera Fluke Ti480. Technical specifications of Fluke Ti480 is listed in Table 3.2.

Table 3.2. Technical specifications of infrared camera

Parameters	Fluke Ti480
Temperature range	≤ -2 °C to +800°C
Accuracy	± 2 °C or 2 %
Spectral range Infrared spectral band	7.5 μm to 14 μm
Image resolution	640 x 480 pixels

Thermal sensitivity	$\leq 0.05^{\circ}\text{C}$ at 30°C target temp
Frame Rate	60 Hz

The Fluke Ti480's calibration parameters, such as emissivity, ambient temperature, relative humidity, and reflected apparent temperature, were measured before the thermographic examination. The ambient temperature and relative humidity were measured with Testo 174 T and H dataloggers (Table 3.1).

3.2 Future Weather Data File Generation

Future climate projections must be created to compare and study the current climatic conditions and estimate how future buildings will perform. The future weather data files for years; 2020, 2050 and 2080 used in this research were taken from work by Tamer et al (Tamer et al., 2022). An existing tool for creating future weather files (CCWorldWeatherGen) was used to create future weather files (Tamer et al., 2022). This tool edits 8760-hour weather data (EPW format) that reflect a typical meteorological year (Energy, 2012).

3.3 Building Condition Assessment Based on Thermal Imaging

3.3.1 Measuring Actual R-Values at the Level of Point in 3 Dimention

The thermal resistance of building assemblies is described by the R-value in the SI unit (m^2/W). The following equation can be used to represent the relationship between thermal resistance (R) and the overall heat transfer rate (dQ/dt) across a building surface with the area of (A) and a temperature difference of (T) between the building's interior and exterior:

$$R = \frac{A \times \Delta T}{dQ/dt} \quad \text{Equation 3.1}$$

There are two main environmental assumptions (Ham, 2015) to conducting the infrared thermal (IRT) process: First, to conduct a thermographic inspection, it is required that the indoor building environment has a quasi-steady-state condition of heat transfer (Fokaides & Kalogirou, 2011) (Dall'O' et al., 2013). This reduces the impact on building envelopes of convective heat loss and surface temperature rise. Secondly, the interior spaces being examined are heated for a few hours before thermographic inspections, which enables energy auditors to record the actual circumstances of heat transfer via building façades throughout the winter (Madding, 2008). Environmental assumptions state that the combination of thermal convection and radiation may adequately characterize the overall heat transfer of building environments (Q). The goal of this study is to determine the actual thermal resistance of 3DCP building envelopes while accounting for potential building occlusions. First, the following equation is used to calculate the amount of heat transfer generated by thermal convection between the interior surface of building environments and the indoor air:

$$Q_{\text{Convective}} = \alpha_{\text{convective}} \times A \times |T_{\text{inside,air}} - T_{\text{inside,wall}}| \quad \text{Equation 3.2}$$

Convective heat transfer coefficients are used in this study based on the methodology described in (Dall'O' et al., 2013) and (Ham & Golparvar-Fard, 2013). The internal and exterior air temperatures, $T_{\text{inside,air}}$ and $T_{\text{inside,wall}}$ are also measured as part of the data collection process using Testo data loggers. Then, using the following equation, the heat transfer generated by thermal radiation between the interior surface of the building environment and the surroundings is calculated:

$$Q_{\text{Radiation}} = \varepsilon \times \sigma \times A \times |T_{\text{inside,wall}}^4 - T_{\text{inside,reflected}}^4| \quad \text{Equation 3.3}$$

The thermal emissivity of building materials is likely to vary depending on the temperature at the measurement time (Barnes et al., 1947). The reflected temperature ($T_{\text{inside,reflected}}$) must also be measured in order to determine the heat transfer resulting from thermal radiation. In accordance with ASTM E1862, the reflected apparent temperature can be measured by using crumpled aluminum foil (*Figure 3.2*). The reflected apparent temperature can be measured accurately from crumpled aluminum foil since it has a high reflectivity and low emissivity (Fluke, 2013). From each pixel that represents the foil surface, the average temperature of the crumpled foil needs to be calculated (Ham & Golparvar-Fard, 2013). To do this, the RGB color values of these thermal image pixels needs to be transformed into the absolute temperature values using a normalized temperature spectrum, and then the corresponding pixels' average values can be calculated *Figure 3.2*.

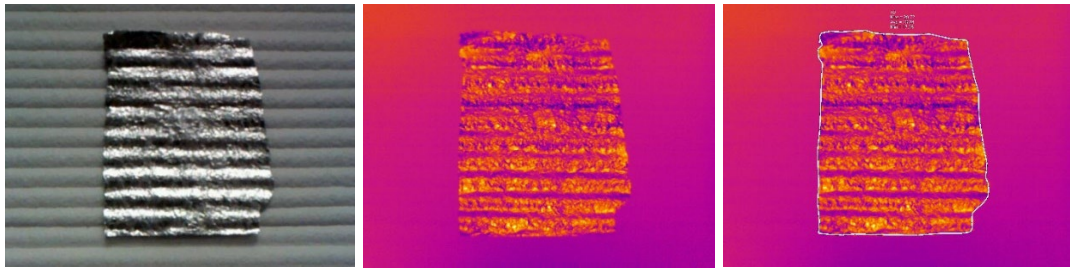


Figure 3.2. (a) Reflected temperature measurement, (b) Crumpled aluminum foil on the 3DCP wall surface, (c) Thermal image of the crumpled aluminum foil

The thermal resistance can finally be described using the following equation, which is the result of combining Equations Equation 3.1, Equation 3.2 and, Equation 3.3.

$$R = \frac{|T_{\text{inside,air}} - T_{\text{outside,air}}|}{\alpha_{\text{con}} \times |T_{\text{inside,air}} - T_{\text{inside,wall}}| + \varepsilon \times \sigma \times |T_{\text{inside,wall}}^4 - T_{\text{inside,reflected}}^4|}$$

Equation 3.4

3.4 Developing a Building Energy Simulation

3.4.1 Criteria Determination for Evaluating Performance

As a first stage, it is vital to determine the performance evaluation criteria because different performance criteria influence the comparative analysis. The study's performance criteria included consideration energy demand of the building and the conductive heat loss of the walls.

3.4.2 Developing a Building Energy Simulation

First, the architectural drawing of the building is transferred to the software by Rhinoceros 7 3D modeling program. Afterward, the two-dimensional file is extruded to a 3D model. A variety of methods can also be used to develop the energy simulation. The necessary details concerning the tool, EnergyPlus, which was used for this research, will be provided in the following chapter. Zone schedules, zone program, zone construction, building load, zone construction, and weather information should all be offered and set. Sub-parameters will also be included in the section on the case study. Then the structure is assigned as rational B spline (Breps) with building materials, infill structures, occupancy schedule, window, and door components. The two different simulations were generated to compare the energy performance of the case 3DCP building versus the conventional building. The only difference between the two settings is the zone constructions to have a valid comparison of the results. The simulations were repeated for 2020, 2050, and 2080 to see the climate change impact on both scenarios. The outcomes are assessed using the given performance standards. Determining the energy consumption and the places with the greatest conductive heat loss is a vital step. To examine and compare the results, the assessment should be performed for both the baseline year and the predicted climate.

CHAPTER 4

CASE STUDY

The approach for determining the effects of the present and future climatic conditions on the performance of an existing 3DCP building was presented in the preceding chapter. The purpose of this chapter is to provide a demonstration of the suggested method through the use of the representative case study, which is Istanbul's first 3D-printed structure.

4.1 Building Description

In order to analyze the performance of existing 3DCP in the present and, future climatic scenario, a one-story office building was chosen as a representative case study since it has the most frequent or typical typology, construction, heating, and cooling properties. The section describes why this building was chosen as a case study:

- The accessibility of the building
- The printing method
- The printable mixture and ease of gathering its thermal characteristics
- The suitability of long-term in-situ measurements
- The construction year

The building is located on the facility of Istanbul Concrete Elements and Ready Mixed Concrete Factories Corporation (ISTON) in Istanbul, Turkey. The site is located at the very south of the ISTON Tuzla facility. On the facility, the 3DCP building, which the Istanbul Metropolitan Municipality owns, is surrounded by other fabrication sites. The construction site is 180 m².



Figure 4.1. Satellite images of the ISTON, Tuzla facility, and building site



Figure 4.2. Aerial photographs of the 3DCP case building's construction and final phases

The building was planned to be an open office for management as a part of ISTON's research and development department. Around the case building there are several exhibition locations, parking lots, security hubs, management buildings and warehouses. Figure 4.3 is a site plan illustration of the case study building.

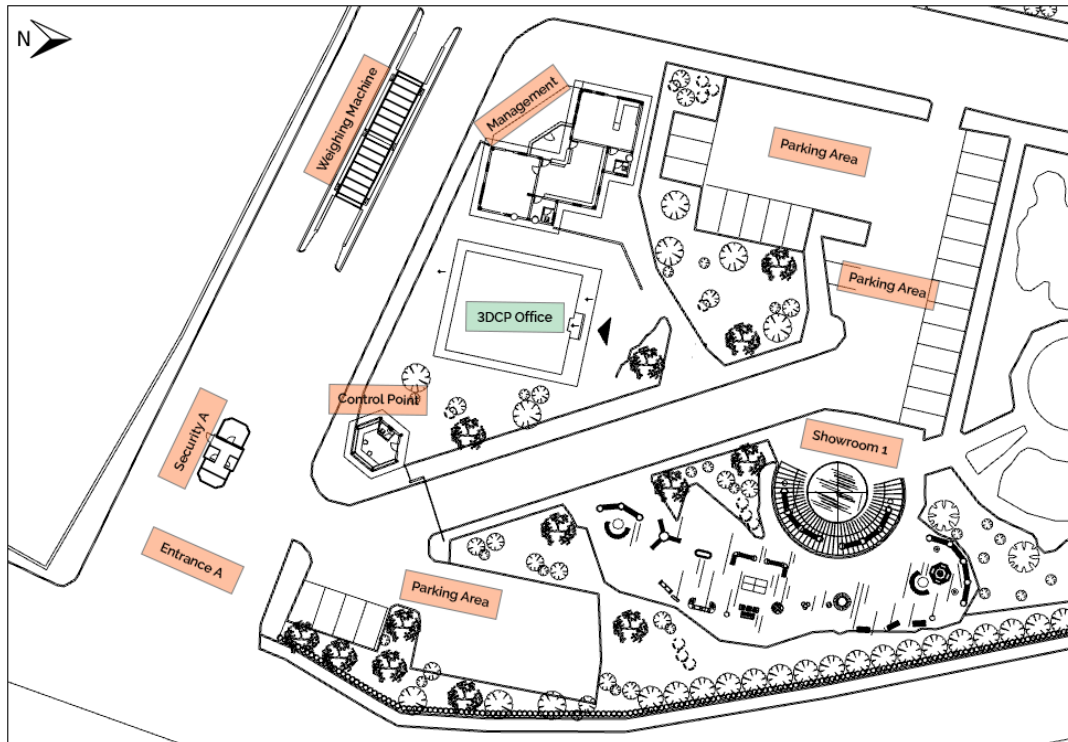


Figure 4.3. Site plan of the 3DCP office building in ISTON Tuzla facility

The construction phase lasted two weeks and was completed in June 2021 (Figure 4.4a). The building is located in Istanbul that belongs to the ‘Csa’ dry-summer subtropical (Mediterranean) climate according to the Köppen-Geiger classification (Peel et al., 2007). The building will be used as an office space and has a total floor area of 150 m² divided into two meeting rooms (MR-1=16.8 m² and MR-2=14.7 m²), a foyer (F=58.7 m²), a conference room (CR=34.8 m²), and a toilet (WC=5.9 m²) (Figure 4.4b). Its ceiling height is 3.0 m. It has a tilted roof with an angle of 4°, under which an unoccupied and unconditioned attic floor is contained.

Table 4.1 ISTON office building zone naming and measurements

Room Name	X Dim. (m)	Y Dim. (m)	Area (m ²)
Foyer (F)	10.8	5.4	58.7
Meeting Room 1 (MR 1)	4.3	4.9	16.8
Meeting Room 2 (MR 2)	4.3	4.9	14.7
Conference Room (CR)	4.3	8.1	34.8
WC	2.6	2.2	5.9

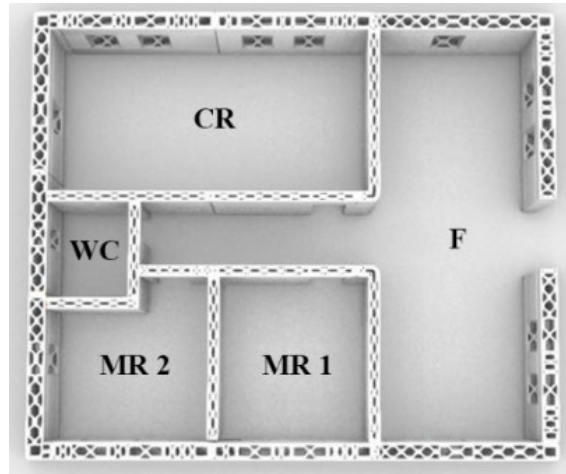


Figure 4.4. Zone diagram

The facade is not coated and it is uninsulated, the printing layers can easily be spotted, and it has the natural texture of a 3D printed surface constructed with additive manufacturing methods. The external and internal walls are printed in 150 layers with 2 cm each. The roof is a pitched roof with a complex shape. Windows are double-glazed with an aluminum frame. The building's orientation in the north direction is determined using Google Maps by drawing a line perpendicular to the north direction and applying it to the model at a 193° angle.



Figure 4.5. Façade of the case building

4.2 Printing Process and Wall Geometries

ISTON have used 6-axis robotic arm to print the building. The 2D drawing of each wall works as a print path for the nozzle. SprutCAM software is used to slice the 3D

model Figure 4.8 (a), the gcode that was used for the robotic arm contains the data of the printing paths (Lim et al., 2012) and the optimized wall parts according to their orientation. In Figure 4.7, the printing path is shown. A red star indicated the printing both start and the ending point. A green star and red arrows were used to represent the first layer's endpoint and printing path, respectively. The nozzle raised 2 cm (the thickness of a single layer) as it reached the endpoint and then started to extrude next layer in same direction, rising an additional 2 cm at the conclusion. Up until the requisite wall height was obtained, this procedure was repeated.

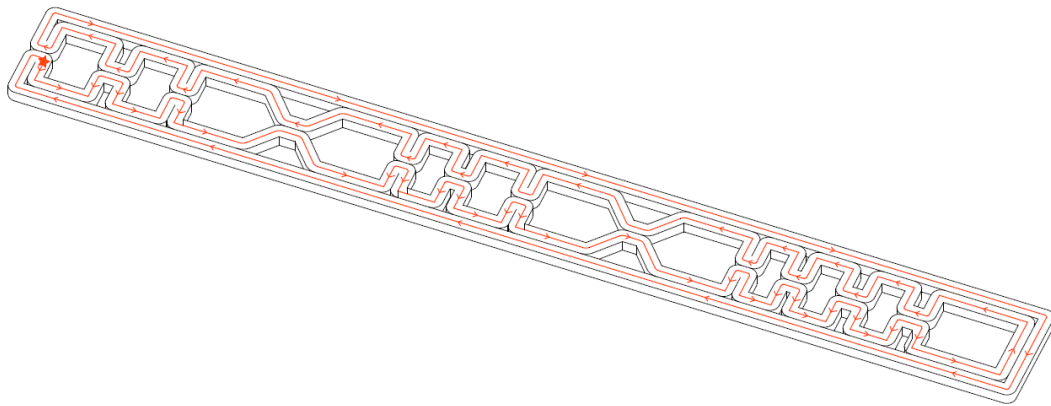


Figure 4.6. Print path and direction of the walls (Red star is both start and the end point of the print)



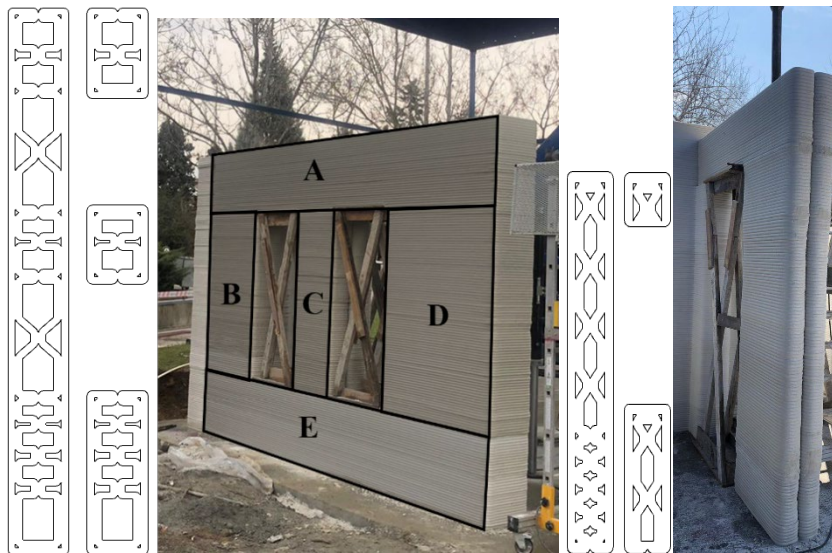
(a)

(b)

(c)

Figure 4.7. a) Printing simulation and slicing process, b) Exterior wall infill structure, c) Interior wall infill structure

There are mainly two types (interior and exterior walls) of infill structures used to print the walls of the building. The walls are printed separately according to their position and the support structures. The exterior walls are designed to be 45.5 cm, and the inner walls are 30 cm . Each layer has a 2 cm height and varies 2-3 cm due to the printing technique.



(a)

(b)

Figure 4.8. (a) Exterior wall infill structures with two window gaps, (b) interior wall infill structure with door gap.

The volume of the walls is calculated from the 3D models in Rhinoceros 3D program. Total volume of the external walls is 35.85 m³, internal walls is 20.17 m³ in total 56.03 m³

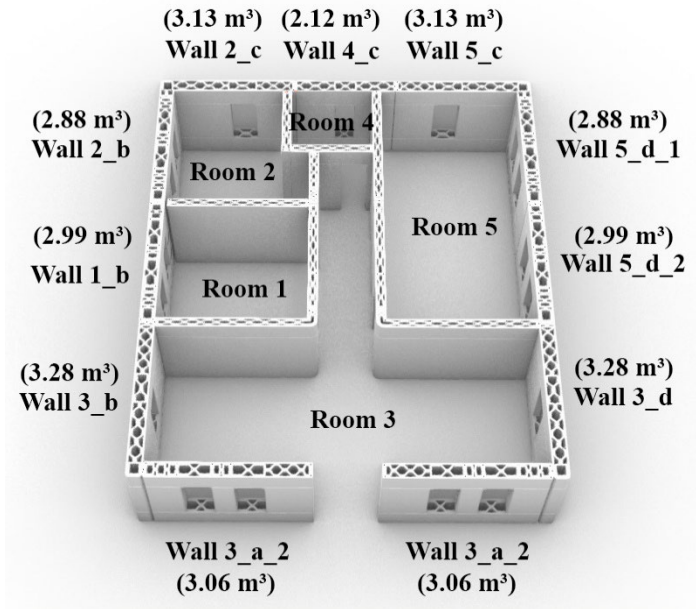


Figure 4.9. Volumes of the walls

4.3 3D Modeling of the Case Building

Therefore, the case building was printed with a robotic arm; the construction process highly depends on the robotic arm reach (maximum radius) of the robot. Even though ISTON developed a unique mechanism to make the robotic arm mobile, the walls should be designed and printed separately and at different times. There is a total of eleven parts external walls and ten parts of internal walls. The building is mirrored in half from the x and y-axis. Each wall art is printed 4 or 5 pieces depending on their window count. Although there were architectural drawings of the building, the printed structure did not match them. The 2d drawings needed to be fixed to start the 3D model of the building.

The Rhinoceros 3D CAD environment was used for the massing 3D model generation operations. Firstly, the 2d printing paths must be redrawn according to

the final design. Each infill pattern was recalculated according to the position of the wall and its type. Then 2d drawings were extruded into masses to calculate the concrete volume afterward (Figure 4.11 a).

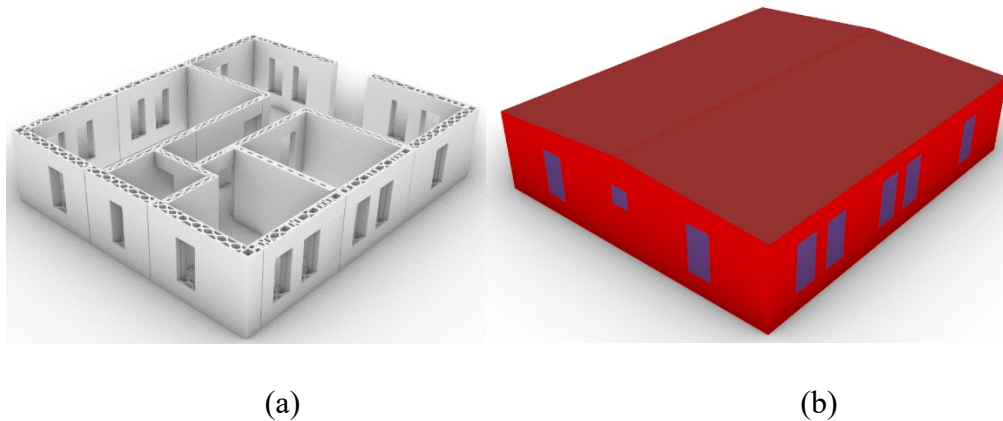


Figure 4.10. (a) detailed 3D model of 3D printed case building (b) simplified version of the model for simulations

The model did not include structural elements, internal divisions within zones, or glazing frames (Figure 4.11 b). Additionally, the elevational layers of the 3D print were disregarded and not modeled for two key reasons, the components needed to be simplified. The simulation program utilized in this study cannot accommodate additional geometric detail, which is the primary justification. Second, the short calculation time of the simple model allows for the testing of more possibilities.

4.3.1 Transforming Printing Paths to 3D Models

There were only simplified architectural drawings (without any infill structure included) and print paths of interior and exterior walls that is why, creating fixed drawings from scratch was necessary for the modeling process. Figure 4.11 shows the drawing stages of the wall 2c (bottom and upper parts. Figure 4.11 a is the drawing that only shows the exterior walls layer thicknesses, and Figure 4.11 b is the print path of the robotic arm; these were the only drawings that ISTON used for the printing process, and none of them included infill pattern or technical drawings of both interior and exterior walls.

The first step was offsetting the print paths according to the layer thickness of the walls. On the other hand, 55 mm layer thickness errors were causing overlapping for the print paths; thus, the print paths were recreated and offset according to fixed ones (Figure 4.11 c). The second step was cleaning unnecessary lines and fixing the wrong corners by fillet according to in situ measurements, as shown in Figure 4.11 d. Lastly, the drawing was simplified to have an extrudable drawing to a 3D model afterward, like in Figure 4.11 e, while the complex drawings were used for diagrams and 2d calculation. The reason that is needed to have a simplified drawing is to pretend to create non-solid meshes, which cases errors during volumetric calculations and Boolean with other solids.

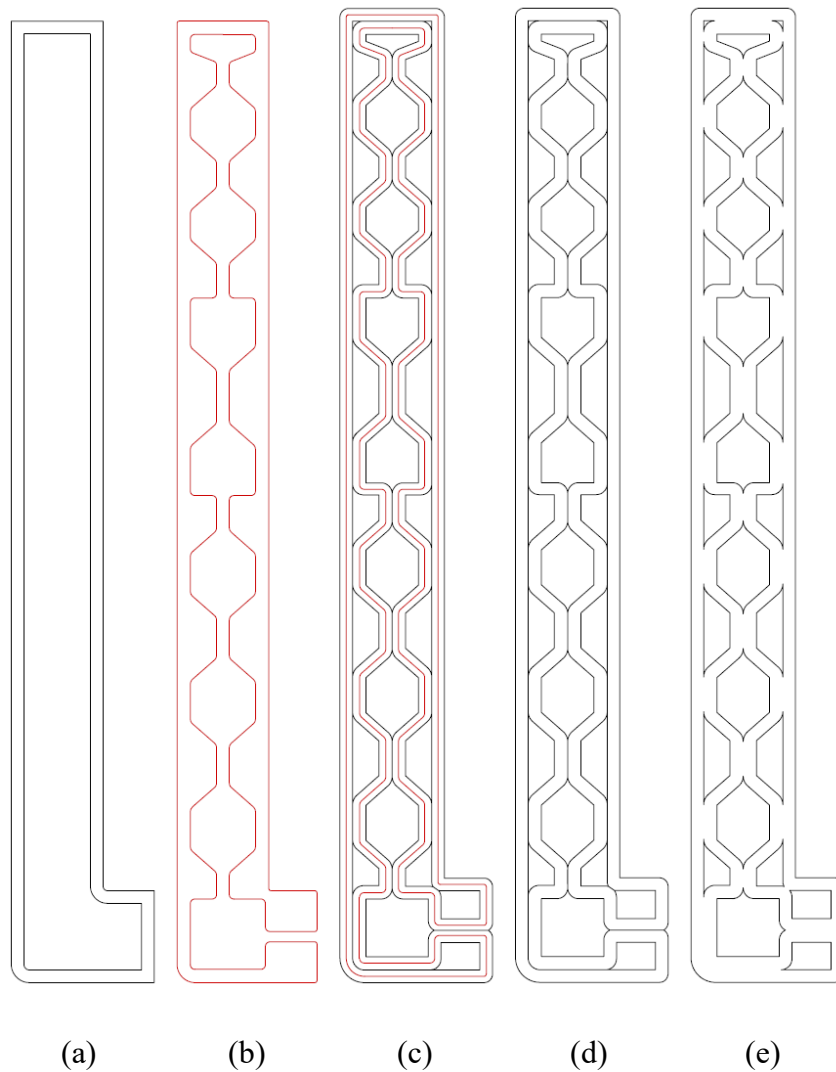


Figure 4.11. (a) Exterior wall thickness, (b) Print path of the wall, (c) Offset process of the print paths, (d) Cleaning unnecessary and error lines, (e) Simplified version for the extrusion process

4.3.2 Simulation Model Development

In this research, Honeybee and EnergyPlus assisted in developing the simulation model. For Grasshopper3D, Honeybee offers free and open-source environmental plugins (Roudsari et al., 2013). Although it examines building masses, it is meant for advanced studies and presents more detailed findings. It can divide the mass into several units, but more importantly, Honeybee can help allocate construction sets, timetables, and internal loads for each area by the program.

EnergyPlus (EP) (v 2.13), an energy analysis and thermal load simulation engine from the U.S. Department of Energy, is used in Honeybee to simulate energy. Honeybee offers a third-party interface for EP because EP itself is not a user interface and accepts data about building location, geometry, building materials, and context geometries as input (Sailor, 2014). The user can also configure intricate schedules and loads for thermostat set points, illumination, plug loads, and occupancy. Honeybee also gives default values for these aspects according to the zone program, whereas EnergyPlus allows overwriting the preset values. After being fully defined, the building simulation model is connected to the weather data file.

For the development of a more accurate model, the following requirements must be met:

Building elements: The 3D model was used to determine the geometry of each zone and the openings.

Zone program: First of all, each zone's program should be defined according to the building program, as Honeybee bases its default internal load and schedules assignments for each zone on this program. Numerous times have been made clear that the study's building program is an open office, and its zone programs are those listed in *Table 4.1* of the previous section.

Building Load: In the simulation tool, interior building loads are described as equipment load, infiltration rate, lighting density, occupancy, ventilation, and recirculated air. The default values provided by Honeybee under the zone programs were utilized for equipment load and infiltration rate, while the existing circumstances in the case building specified values for the number of people and lighting density loads. The internal loads are summarized in *Figure 4.12*.

Zone Schedules: Zone schedules contain occupancy, occupancy activity, heating set point, cooling set point, lighting, equipment, infiltration, and ventilation schedules and offer a new kind of information about the building system.

The internal load densities and schedules were selected according to ASHRAE STANDARD 90.1–2013 OPEN OFFICE, as provided in *Table 4.1* and *Figure 4.12*, respectively (ASHRAE, 2013). Heating setpoint (8am- 8pm) and setback temperatures (8pm- 8am) were set to 21°C and 19°C respectively. Cooling setpoint (8 am- 8pm) temperatures were set to 26°C, respectively.

Table 4.2. Internal load densities (ASHRAE, 2013)

	Office zone
Equipment load (W/m ²)	7.642412
Infiltration rate (m ³ /s-m ²)	0.000227
Lighting density (W/m ²)	11.840357
People density (person/m ²)	0.056511
Ventilation (m ³ /s-m ²)	0.000305

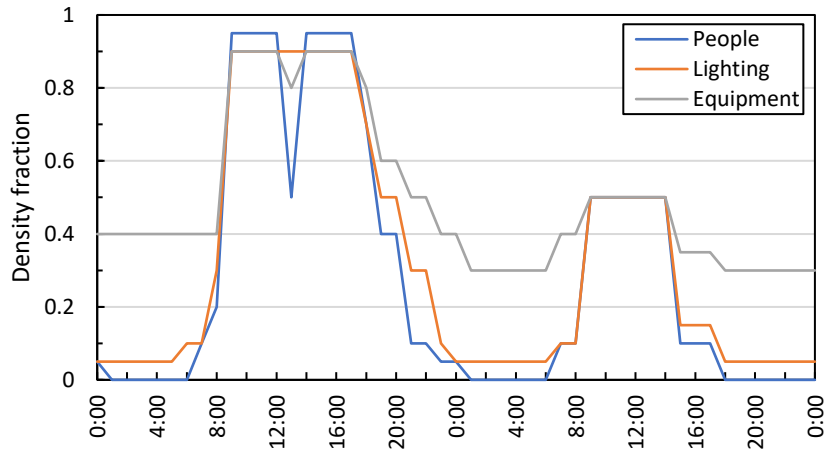


Figure 4.12. Weekly internal load schedules for the offices (ASHRAE, 2013)

Calculating individual energy requirements for space heating and cooling, ventilation, domestic heat water (DHW), power, lighting, and office equipment takes the impact of internal heat loads into account. EnergyPlus is able to take into account all external and internal parameters to perform an accurate simulation of the energy use. A detailed building survey was initially carried out to identify construction materials and schedules. The occupancy schedule for the building was assumed to be between 08:00 and 17:00 from Monday to Saturday. The open office is occupied by 8 staff and it is occupied during the whole year. Split-type air conditioners are used for heating and cooling (19°C heating setpoint, 26°C cooling setpoint). The primary cooling method for the entire building is air conditioner, which is assumed to be active when indoor air temperature is above 26°C and below 19°C.

The simulations were repeated according to the different U-values for the external walls which were obtained with different methods and with the settings of a conventional building to investigate and discuss the results. In all simulations, the annual heating (QH), cooling (QC) and total (QT) energy consumptions for each U-value and year are expressed as kWh per floor area (kWh/m²).

Zone Construction: Since EP has its library of building supplies, users can also create their construction materials. For customized materials, thickness, thermal conductivity, specific heat capacity, and density must be determined. The ability of

a substance to conduct heat is known as thermal conductivity, and its unit is W/m-K. The amount of heat energy needed to raise a substance's temperature per unit of mass is defined as specific heat capacity. It is stated in units of J/kg-K. Several metrics should be attributed to windows, including the U-value, solar heat gain coefficient (SHGC), and visual transmittance (VT). The U-value measures how much heat is lost or gained via windows; the lower the U-value, the higher the window's resistance to heat flow and the better its thermal insulation. The SHGC measures heat transfer from direct sunlight through a window, as stated in the previous section. Low SHGC results in better solar management and is between 0 and 1. The amount of light with a visible wavelength that passes through the glass is known as the VT. The physical characteristics of the building materials for the office are shown in Table 4.2. The internal wall, floor, and ground floor materials remained constant throughout the examination.

Table 4.3. Construction materials for simulations

ISTON 3DCP	Construction Material	Conductivity	Specific Heat Capacity (J/kgK)	Density (kg/m³)	References
External Wall	ISTON 3D printable concrete	0.92	1677	1685	(Alkhalidi & Hatuqay, 2020), Bayrak et al. (2023)
Internal Wall	ISTON 3D printable concrete	0.92	1677	1685	(Alkhalidi & Hatuqay, 2020), Bayrak et al. (2023)
Roof	Metal cladding	60	418	7680	(Gorgolewski, 2007)
	20 mm OSB board	0.13	1552	700	(Igaz et al., 2017)
	80 mm rockwool	0.039	850	150	(Keerthan & Mahendran, 2013)
	0.5 mm galvanized sheet	60	418	7680	(Gorgolewski, 2007)
TS-825 Scenario	Construction Material	Conductivity	Specific Heat Capacity (J/kgK)	Density (kg/m³)	References
External Wall	3mm cement based external coating	1.6	840	2000	(Turkish Standard, 2013)
	35mm EPS	0.035	1500	22	(Turkish Standard, 2013)

	135mm horizontal coring brick	0.33	600	900	(Turkish Standard, 2013)
	2mm plaster based internal coating	0.51	1200	1090	(Turkish Standard, 2013)
Internal Wall	85 mm horizontal coring brick	0.33	600	900	(Turkish Standard, 2013)
Roof	Metal cladding	60	418	7680	(Gorgolewski, 2007)
	20 mm OSB board	0.13	1552	700	(Igaz et al., 2017)
	80 mm rockwool	0.039	850	150	(Keerthan & Mahendran, 2013)
	0.5 mm galvanized sheet	60	418	7680	(Gorgolewski, 2007)

Table 4.4. Thermal properties of the glazing

ISTON 3DCP / TS-825 Scenario	U-Value (W/mK)	Solar Heat Gain Coefficient	Visible Transmittance	References
Windows	2.4	0.85	0.79	(Tamer et al., 2022)

Weather data: As previously mentioned, weather data is a file that includes all hourly weather data for the entire year. In order to compare findings and evaluate the effects of climate change on the building's energy and thermal performance, weather data for the years 2020, 2050, and 2080 were used in this phase.

4.4 Impact of Global Climate Change on a 3D Printed Concrete Building

Climate change is a definite symptom and a direct result of unsustainable development due to rising atmospheric concentrations of human-generated greenhouse gases (such as CO₂, methane, and other gases). Buildings are particularly at risk because the local climate-buildings balance is prone to a significant shift due to climate change (Ruiz-Valero et al., 2021). Some effects of CC on the structures are energy consumption shifts from heating to cooling, as well as a rise in HVAC inefficiency and malfunction rates (Berger et al., 2014). Depending on the future

local conditions, these effects could also impact occupant health and thermal comfort, as well as building-related environmental issues and operational costs.

Typical meteorological year (TMY) weather files can be used by building energy modeling systems to calculate the energy consumption of buildings for the present weather conditions. These files are created by accumulating a year's length of hourly data from representative weeks or months from prior years. To estimate future energy consumption under the effects of climate change, future weather files are developed by changing existing weather data.

4.4.1 Performance Assessment for 3DCP building

The preliminary findings of climate change implications are discussed in this stage concerning energy and thermal performances. Three sets of weather data for 2020, 2050, and 2080 were used to perform the full-year simulation. To calculate and visualize the obtained simulation results, Microsoft Excel was used.

CHAPTER 5

RESULTS AND DISCUSSION

5.1 Thermal Performance of the Walls

5.1.1 Infrared Thermal Imaging

The ASTM 1933 process was followed while applying the reference emissivity material method for emissivity measurement (ASHRAE, 2002). The tested wall's heated surface was covered with a piece of black electrical insulating tape with a known emissivity of 1.00; the emissivity of the white cement concrete was determined to be 0.95 (Sun et al., 2021). Inspections were conducted before sunrise, between 3 and 5 a.m., on a cloudy (*Figure 5.1*), windless day, and building envelopes were not subjected to direct solar radiation and wind loads, as specified by the standard (Ham, 2015). This lowers the impact of convective heat loss and surface temperature rise on building envelopes (Ham & Golparvar-Fard, 2014). By doing so, the potential increase in the surface temperature of a building caused by the daily release of solar radiation can be reduced (Dall'O' et al., 2013).



Figure 5.1. The thermal imaging completed between 2-5 am to minimize the convective heat loss

In addition, prior to thermographic inspections, the interior spaces of the 3DCP walls under inspection are heated for a few hours (*Figure 5.2*), allowing energy auditors to capture the actual heat transfer conditions through the building facades during the winter season (Fokaides & Kalogirou, 2011).



Figure 5.2. The rooms were heated with both electronic and non-electronic heaters before the thermal imaging

Fluke Connect was utilized to process the visual and thermal pictures of 3DCP walls from various angles. Possible defect areas were identified before the thermographic inspection (*Figure 5.3*). On the other hand, these areas were covered with plaster after the printing process, so no defect was left that caused a thermal bridge.

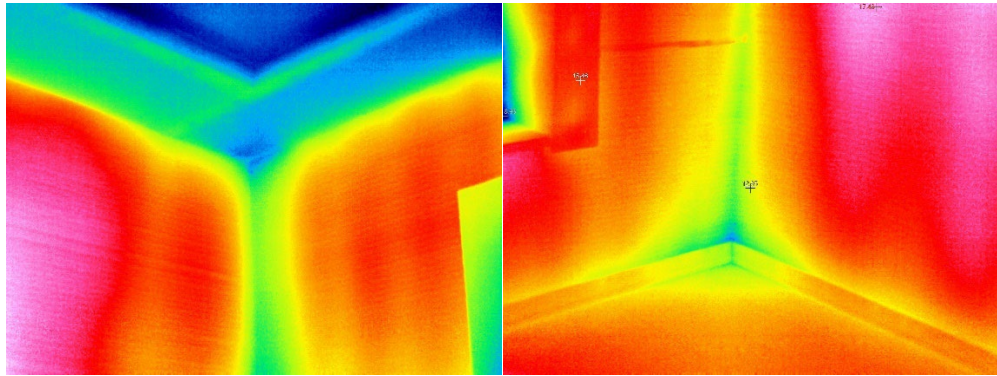


Figure 5.3. Possible defect areas were identified and examined during thermal imaging

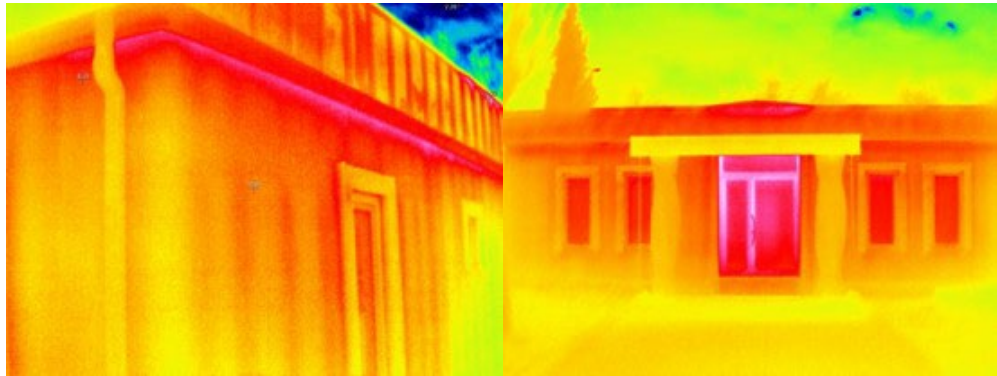


Figure 5.4. Infrared Images of the 3D concrete printed structure envelope

After fixing perspective distortion from each photo, they will be placed in a layout to represent the whole wall next to each other; their average color information was found to calculate the average values of the wall (Dall'O' et al., 2013). Lastly, each value was used to calculate the R-value of each wall by the formula; Equation 3.4.

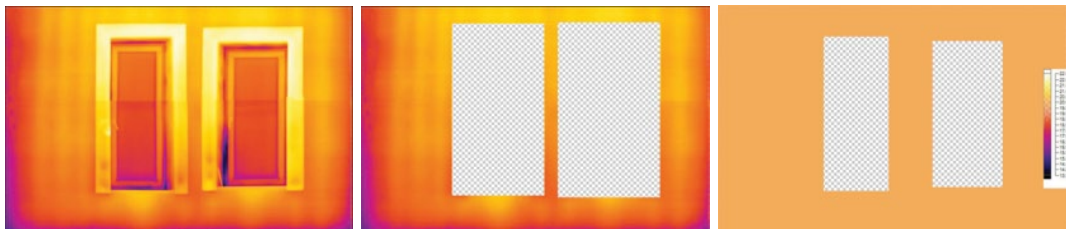


Figure 5.5. Fixing perspective distortion process

The R-value of the walls 1b, 2b and 2c were calculated with in-situ measurements thermal imaging method as mentioned above. There are several reasons that experiments conducted only for specific exterior walls and rooms;

- The office building was not actively used and there was no active heating.
- The limited number of infrared and oil filled heaters were only enough to heat 2 small rooms.
- The rooms were selected according to their infill structures, and those three walls were enough to represent all the other wall structures as they include straight and L-shaped walls.

After these walls' R-values were calculated, the uncalculated walls with different sizes and positions were compared according to their; full-empty ratio, both 2D from their plans and 3D from their models, and the distance of their center of gravity to the edges of the walls. The full-empty ratio represents their solid-cavity ratio, and 3D calculations gave the most correlated results among the three methods. Figure 5.6 shows the correlation of the R-values between the experimented walls according to their 3D solid-void ratio. Finally, with the formula from the trendline of the correlation graph, the R-value of the rest of the walls were calculated.

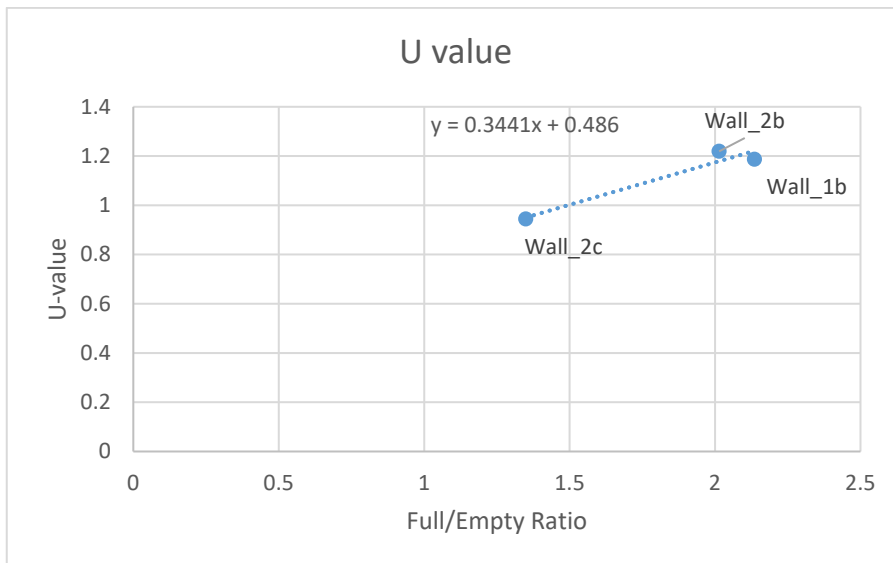


Figure 5.6. U-value correlation graph of the experimented walls

Table 5.1. U-values of the external walls

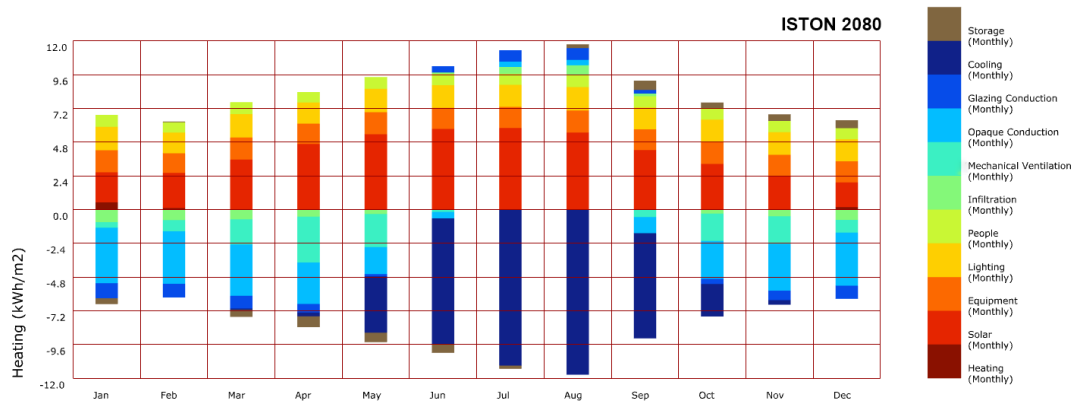
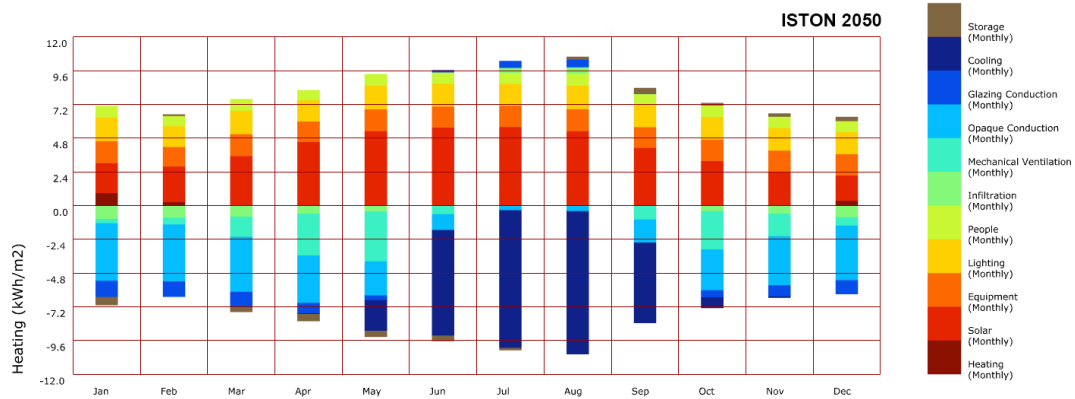
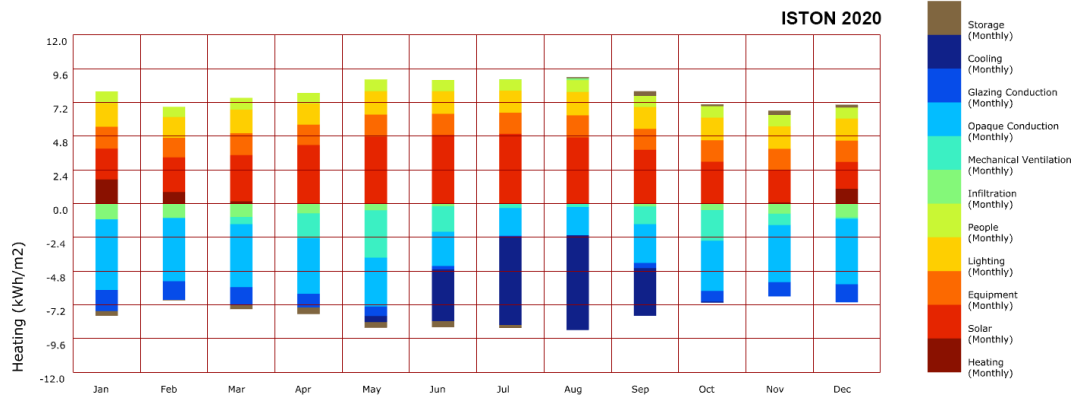
	U-value [W/m ² K]
Walls	Ham (2015)
1b	1.187
2b	1.219
2c	0.944
3a	0.868
3a_2	0.868
3b	1.218
3d	1.218
4c	0.922
5c	0.944
5d_1	1.219
5d_2	1.187

5.2 Energy Performance of the Building

Annual energy demand for heating and cooling is shown in Table 5.2 for the two scenarios for 2020, 2050, and 2080. Future heating requirements (QH) and energy balance (QT) were shown to decrease, while cooling (QC) increased. Figure 5.6 provides an overview of the energy balance for the case building and the TS825 scenario under three different climatic conditions. By 2080, it's expected that the average QC will rise sharply from 41.3 to 93.3 kWh/m² (+77%) for 3DCP building and from 43.9 to 95.9 kWh/m² (+74%) for the TS825 scenario, while the average QH will fall from 7.7 to 1.9 kWh/m² (-121%) for 3DCP buildings and from 5.4 to 1.3 kWh/m² (-122%) for the TS825 scenario.

Table 5.2 Annual energy demand (kWh) for heating and cooling of the case building examined for the present climate scenario, 2050 and 2080.

Wall Type	Current Climate			2050			2080		
	Heating [kWh/m ²]	Cooling [kWh/m ²]	Total [kWh/m ²]	Heating [kWh/m ²]	Cooling [kWh/m ²]	Total [kWh/m ²]	Heating [kWh/m ²]	Cooling [kWh/m ²]	Total [kWh/m ²]
3DCP	7.68	41.32	49.00	2.92	72.79	75.71	1.94	93.33	95.27
TS825	5.38	43.97	49.34	1.94	75.90	77.84	1.31	95.88	97.18



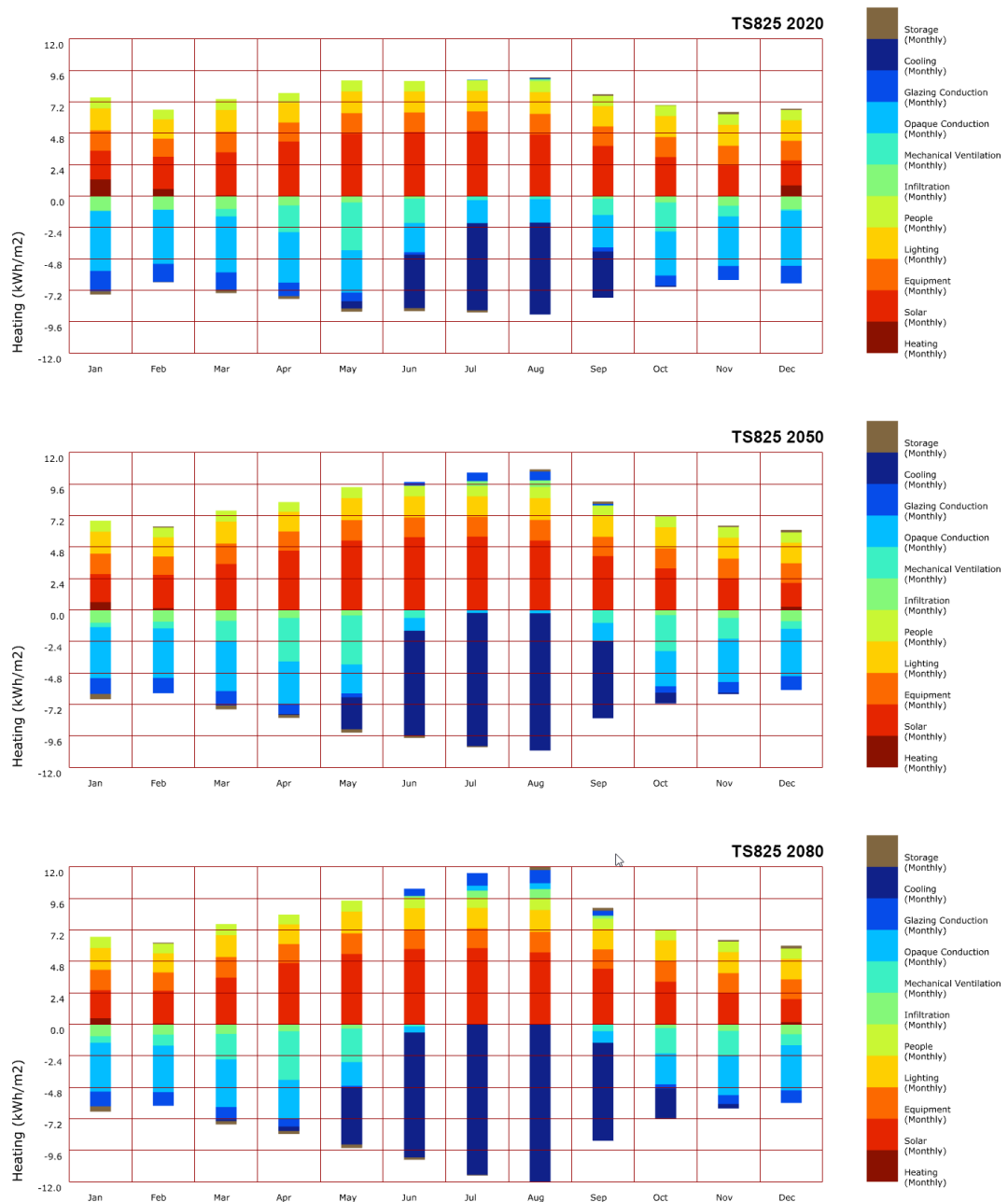
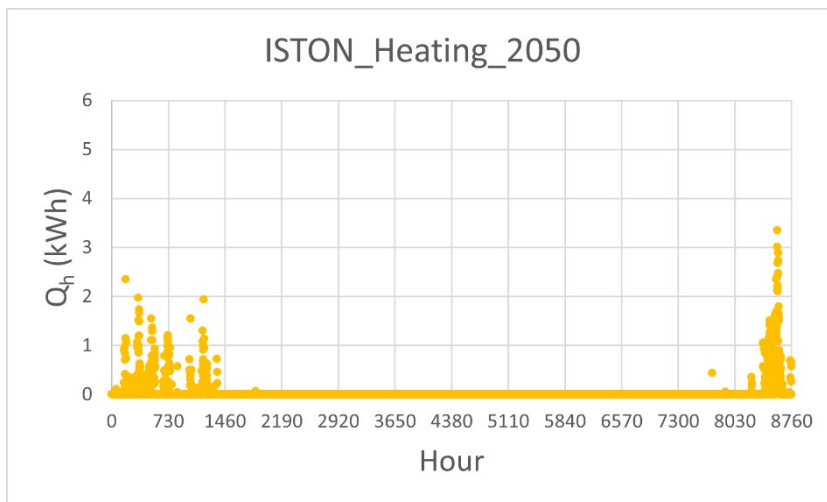
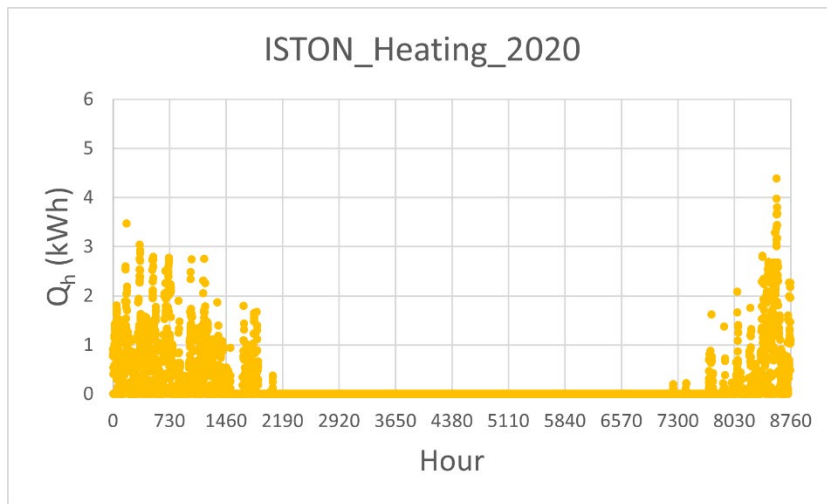
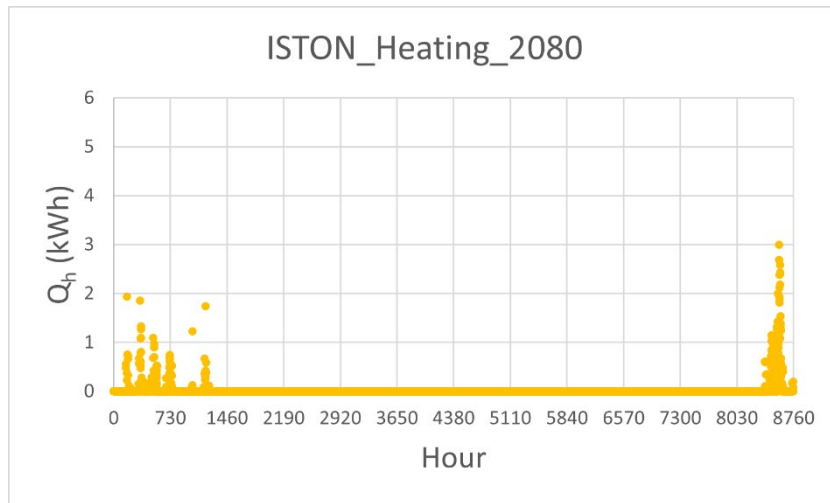


Figure 5.7. The energy balance graphs for both scenarios are based on the present weather conditions, 2050 and 2080 estimates.

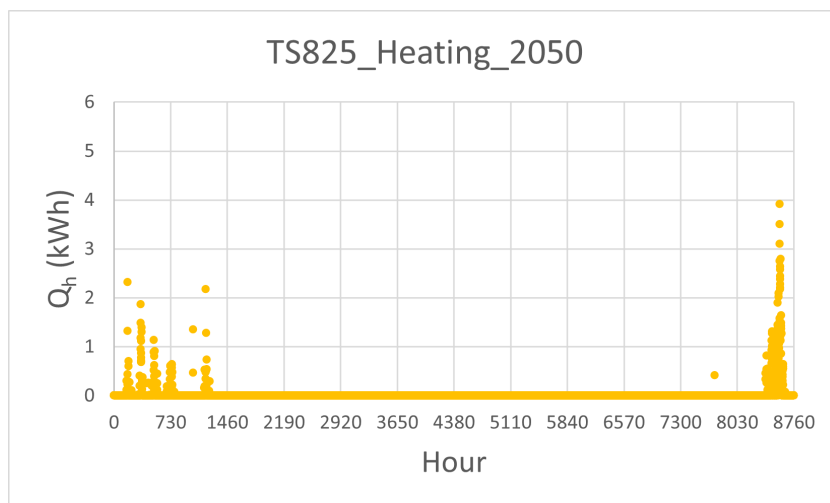
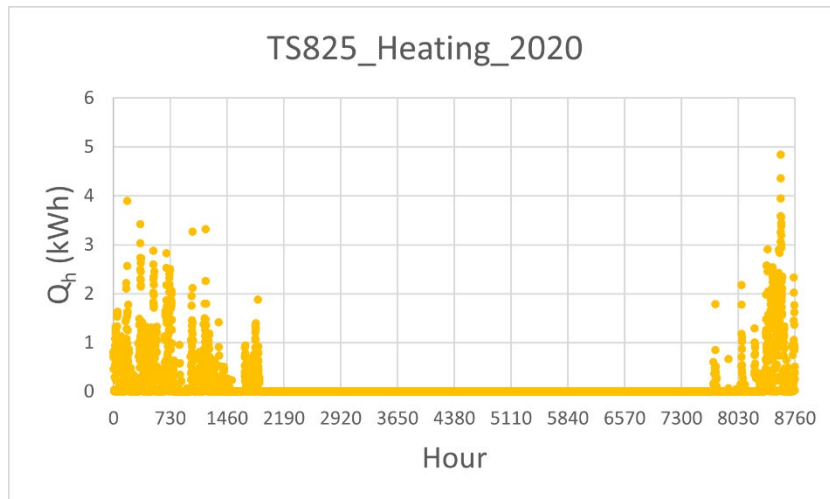
Heating: Open office heating starts in October and continues until April or occasionally May; the heating demand summary (QH) is depicted in Figure 5.7 for both scenarios. From the data in Figure 5.7, it can be seen that the highest demand is for ISTON 2020, followed by the TS825 scenario. The first reason is that different

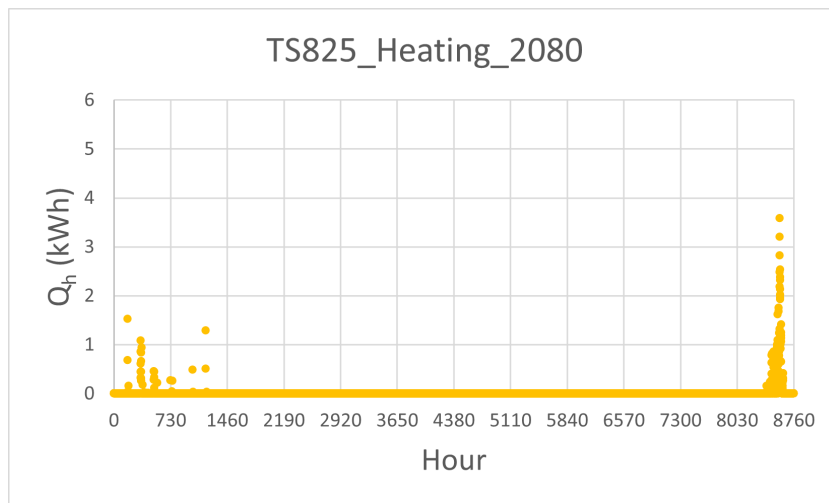
3DCP building has a higher demand for heating; the 3DCP external walls have different infill structures for each room, while the walls for the TS825 scenario all the external walls have the same layers of material. The second reason is that each wall's conductive heat loss rates differ depending on its construction method, infill structure, and orientation. The following section will give a detailed examination of the conductive heat loss of the walls.





(a)

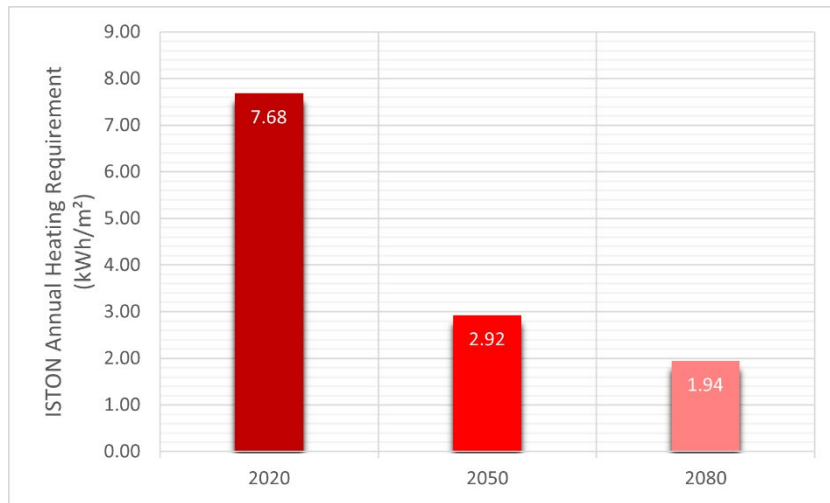




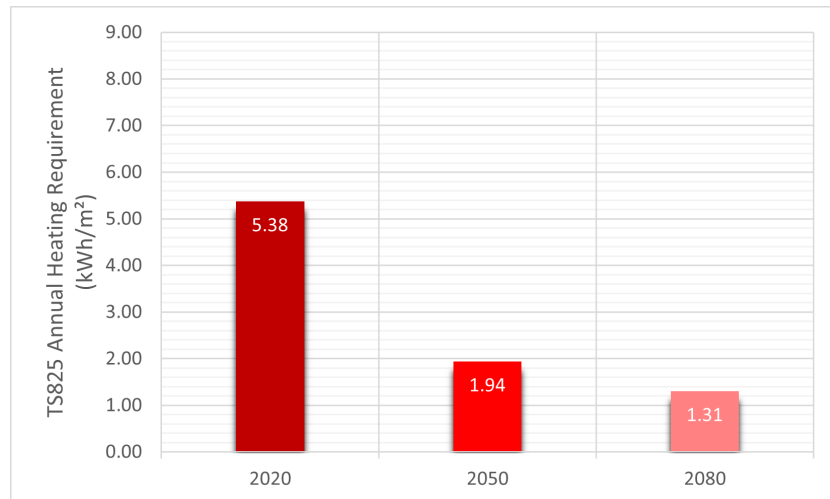
(b)

Figure 5.8. The heating demand for (a) a 3DCP building and (b) a TS825 scenario

The annual heating demand (QH) for the 3DCP scenario decreased by 4.76–5.74 kWh/m² (38.02–25.26%) between the current weather and the 2050–2080 estimates. Figure 5.8 depicts the results, which show that the QH is highest for the weather data for 2020 and lowest for the weather data for 2080. The TS825 scenario's (QH) heating requirement decreased by 3.44–4.08 kWh/m² (36.05–24.34%). Figure 5.8 (a) illustrates how the QH of a 3DCP building is consistently lower than that of the TS825 scenario. Due to this, there are variances in how climate change will affect the annual need for heating under the two scenarios. The southeast-oriented walls should also get more solar heat, and when the 3DCP walls were examined, it was determined that the walls had the highest U-Values. When the two situations were compared, the 3DCP walls' heating demand (QH) was 2.3–0.98 and 0.63 kWh/m² higher than the 3DCP scenario.



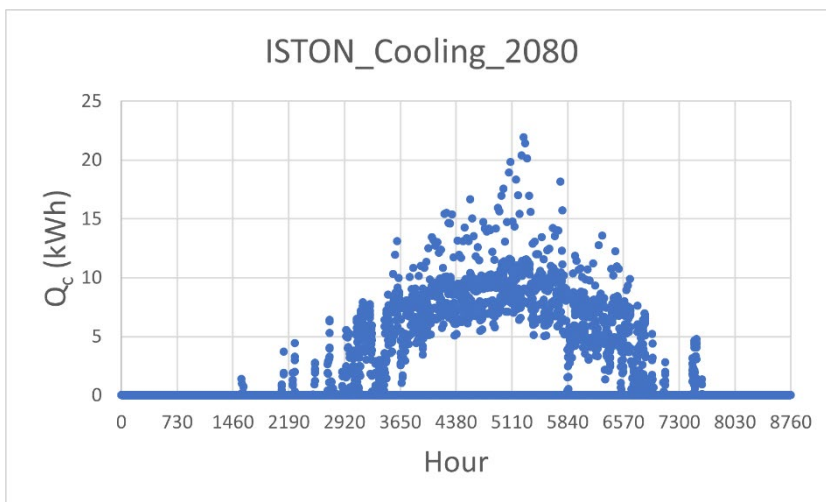
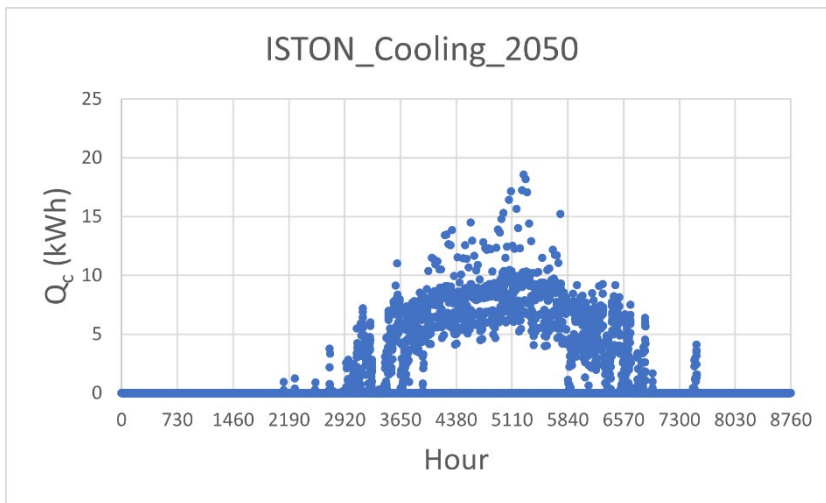
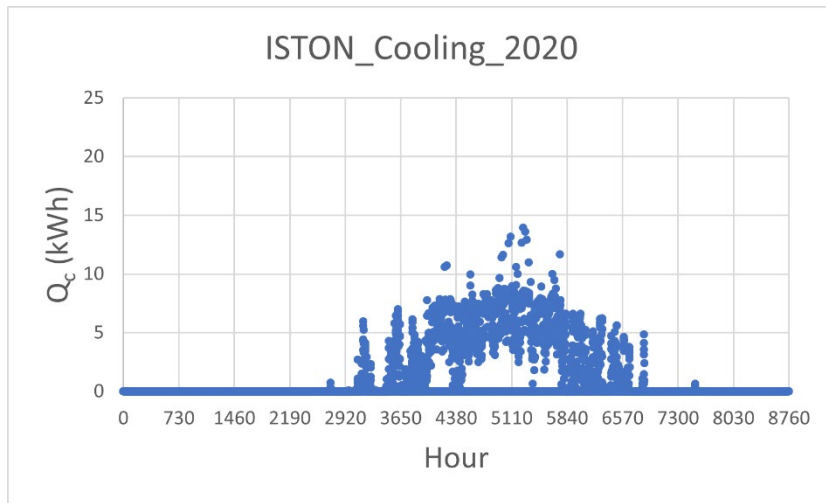
(a)



(b)

Figure 5.9. The office building's annual heating demand in baseline and projected future years for both 3DCP (a) and TS825 (b) scenarios

Cooling: Cooling requirement (QC) starts in May and ends in September. Figure 5.9 shows the results for each scenario under different climatic conditions. The highest demand was observed in TS825 2080 scenario, followed by ISTON 2080 scenario. Also, it can be seen that QC is always higher for TS825 scenario building.



(a)

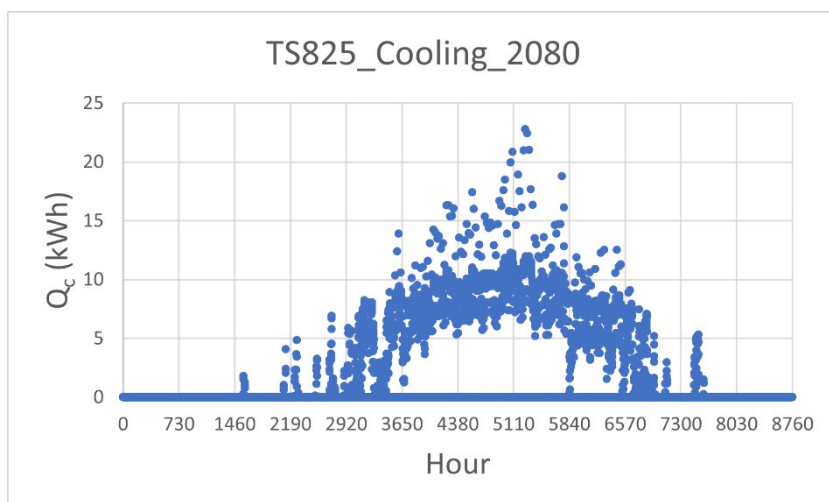
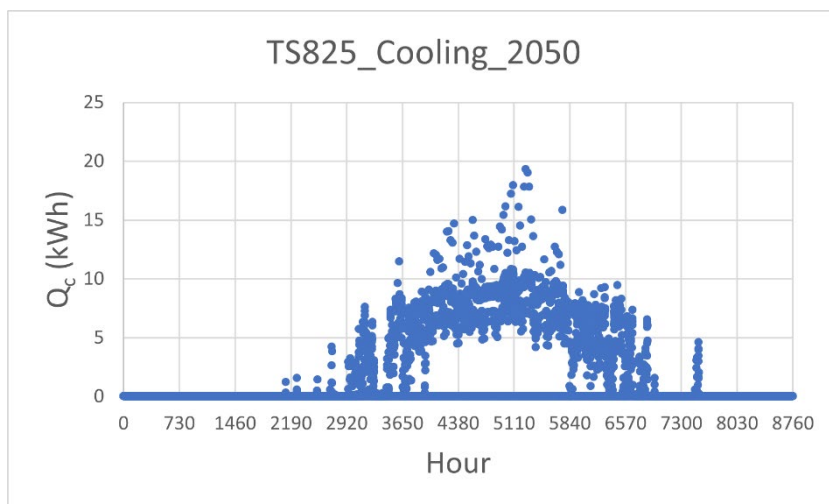
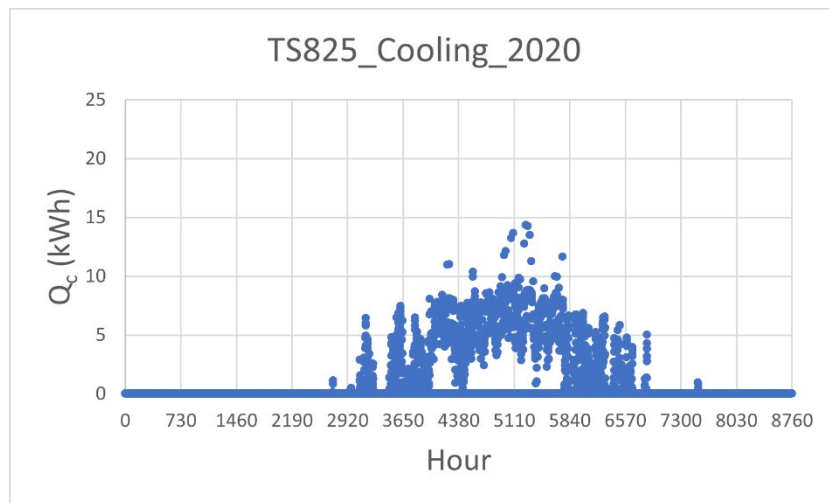
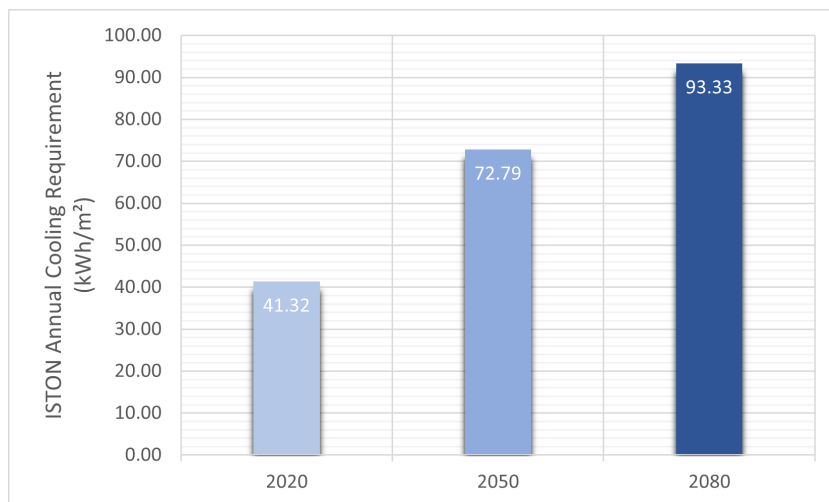


Figure 5.10. The cooling demand for (a) a 3DCP building and (b) a TS825 scenario

According to expectations, the QC also rises as the temperature rises in the future climate. For 3DCP buildings, the increase in cooling requirements (QC) is 31.47–52.01 kWh/m² (55.17–77.25%), and for the TS825 scenario, it is 31.93-51.91 kWh/m² (53.27–74.23%). Opposite to heating demand, the annual cooling demand of the TS825 scenario is higher for both current and predicted weather data than for the 3DCP building, as shown in Figure 5.11. The reason for that is the same as the heating demand; the U-value of the southeast-oriented walls is the lowest. Moreover, the conductive heat loss of all 3DCP walls is higher than in the TS825 scenario. Therefore, it needs more energy to cool the zone to keep it under the threshold.



(a)

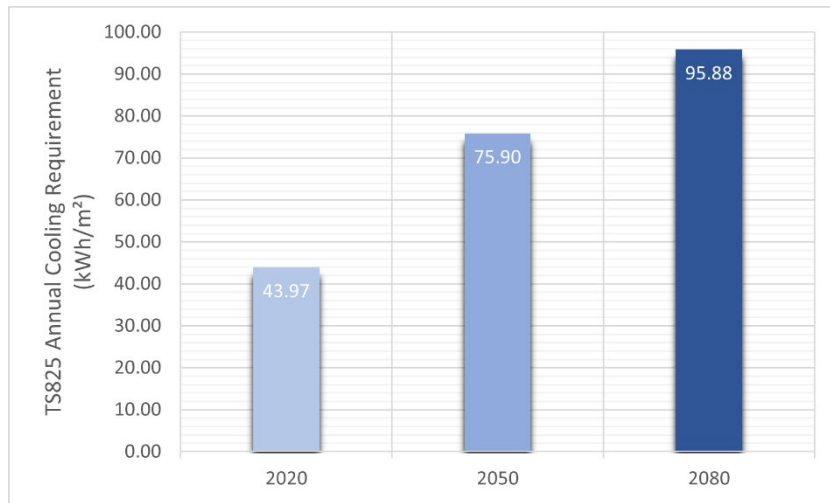
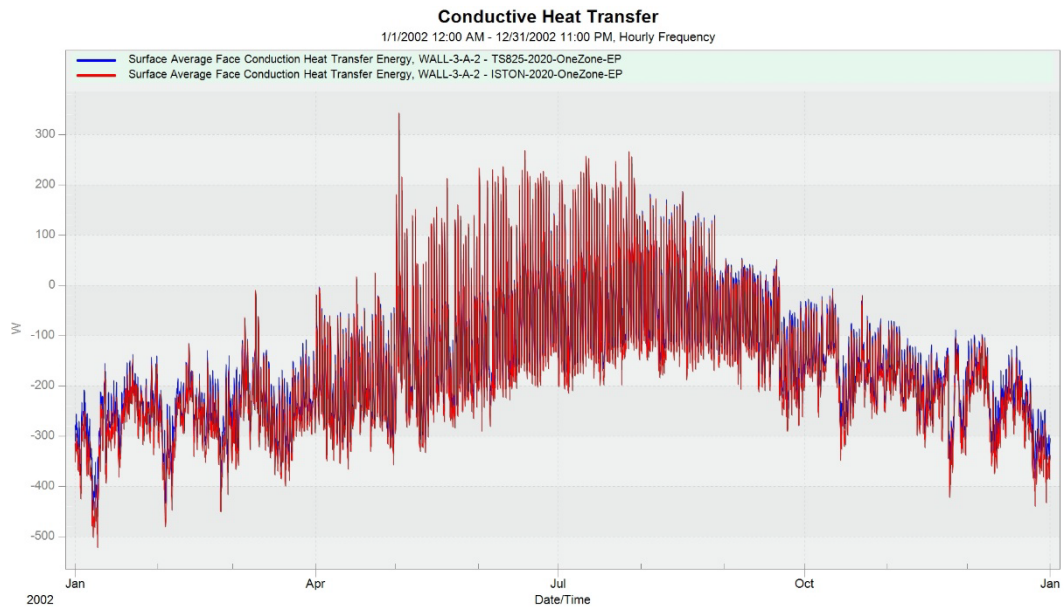
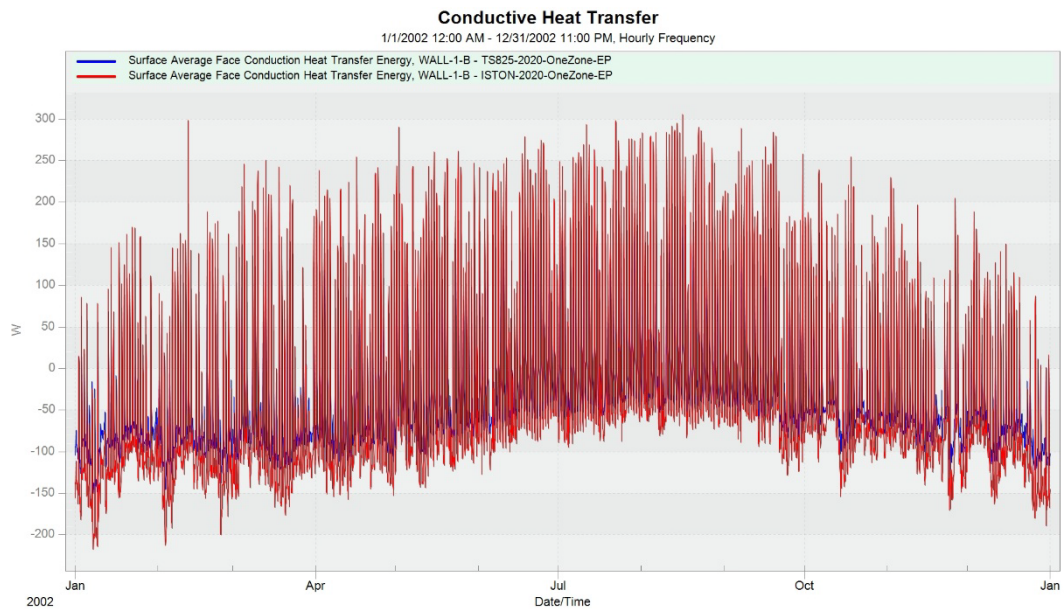


Figure 5.11. The office building's annual cooling demand in baseline and projected future years for both 3DCP (a) and TS825 (b) scenarios

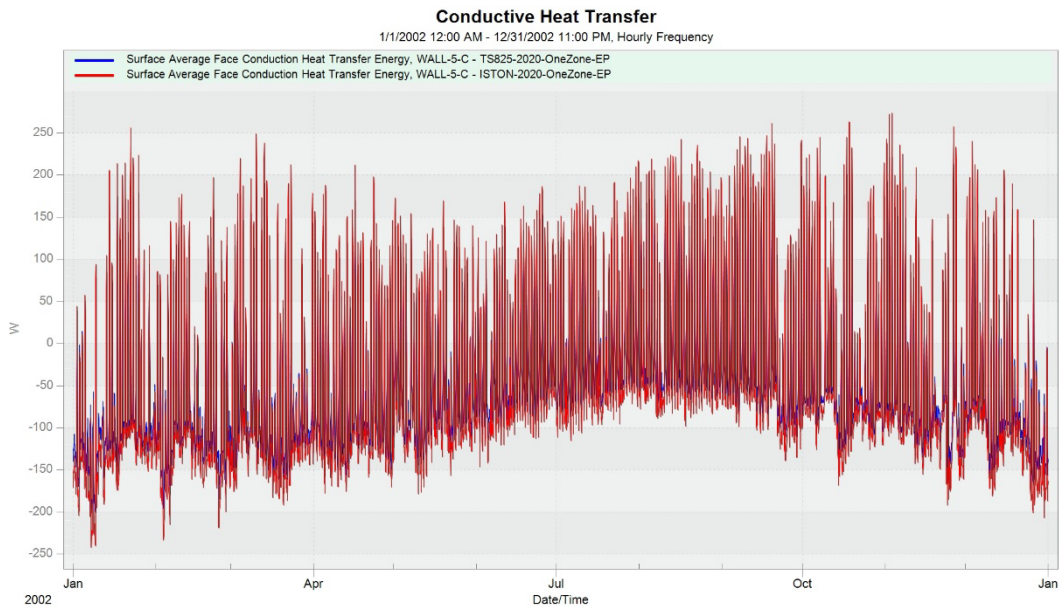
Conductive Heat Loss: If a solid has a temperature gradient, conduction as heat transfer occurs. When two adjacent molecules meet, conduction occurs, transferring energy from the more energetic to the less energetic molecules. Heat moves toward falling temperatures since molecular energy increases with temperature. Figure 5.12 shows the conductive heat loss results for the one wall from each facade for both ISTON and TS825 scenario under different climatic conditions. Detailed information about the conductive heat loss of each wall and graphs of the rest of the walls for the both scenarios can be seen in Appendix A.



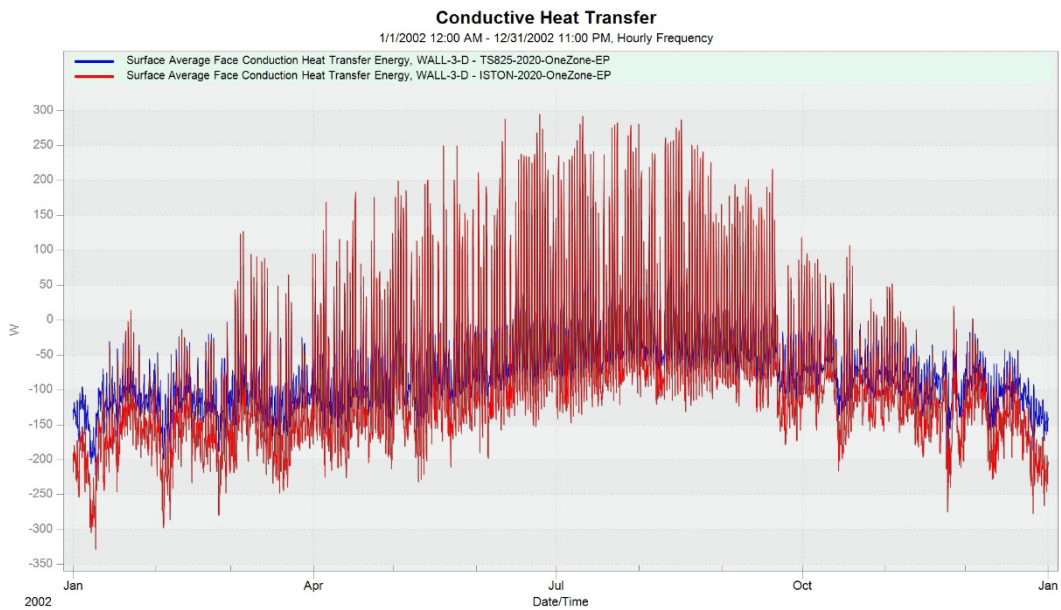
(a)



(b)



(c)



(d)

Figure 5.12. Conductive heat transfer graphs for both scenarios (a) wall 3a north-east façade, (b) wall 1 b south east façade, (c) wall 5c south-west façade, (d) wall 3D north-west façade

As seen in Table 5.3, the conductive heat loss of all the walls of the 3DCP building is higher than the TS825 scenario walls. The first reason is that all the 3DCP walls

have higher U-values than TS825 walls. Moreover, because of its construction method and differences in each wall's infill structures, each wall was expected to have different conductive heat loss percentages. The second reason is that the TS825 building has linear and the same material layers for each wall, so it will only depend on each wall's orientation and size and the number of windows. Moreover, while north-west oriented walls have the highest rate of conductive heat loss, it is followed by; north-east, south-east, and south-west oriented walls in order. The most heat energy lost by conduction was during spring, winter, and summer. Therefore, 3DCP walls' annual conductive heat loss energy is 15 W, which is higher than the TS825 scenario on average; it is expected that will have higher heating energy demand. Also, the climate change impact on the 3DCP and TS 825 scenario are very similar when we compare annual cooling energy demand for the years 2020; 3DCP building +42.83 kWh/m² annual energy consumption for 2050 and +64.14 kWh/m² for the year 2080 while it was +44.81 kWh/m² for 2050 and +65.30 kWh/m² for 2080.

Table 5.3. Conductive heat transfer table for each wall and both 3DCP and TS825 scenarios with 2020 weather data in total and average (W)

External Walls	All Year		Winter		Summer		Spring	
	Total (W)	Average (W)	Total (W)	Average (W)	Total (W)	Average (W)	Total (W)	Average (W)
3dpc_1_b	-347717	-40	36225	12	-63861	-91	-107258	-49
3dpc_2_b	-381536	-44	40515	14	-70209	-100	-117701	-53
3dpc_2_c	-363435	-41	-27237	-9	-49374	-72	-120522	-55
3dpc_3_a	-1519869	-174	-189421	-65	-190316	-272	-448906	-203
3dpc_3_b	-484399	-55	51029	17	-89079	-127	-149423	-68
3dpc_3_d	-846206	-97	-87903	-30	-112500	-160	-246790	-112
3dpc_4_c	-283498	-32	-21987	-8	-38280	-55	-94283	-43
3dpc_5_c	-459518	-52	-33936	-12	-62454	-91	-152761	-69
3dpc_5_d_1	-641215	-73	-64994	-22	-85530	-122	-187031	-85
3dpc_5_d_2	-629497	-72	-64487	-22	-83764	-119	-183468	-83
TS825_1_b	-249834	-29	29639	10	-45123	-65	-81861	-37
TS825_2_b	-268621	-31	32317	11	-48592	-70	-88043	-40
TS825_2_c	-310493	-35	-16065	-5	-42214	-62	-107688	-49
TS825_3_a	-1367150	-156	-189421	-65	-171834	-247	-418637	-190
TS825_3_b	-341327	-39	40797	14	-61710	-88	-111858	-51
TS825_3_d	-580104	-66	-50482	-17	-77264	-110	-176190	-80
TS825_4_c	-246821	-28	-13410	-5	-33363	-49	-85805	-39
TS825_5_c	-392582	-45	-19897	-7	-53397	-78	-136468	-62
TS825_5_d_1	-439186	-50	-37116	-13	-58688	-84	-133414	-60
TS825_5_d_2	-440155	-50	-37661	-13	-58676	-84	-133597	-61

CHAPTER 6

CONCLUSION

The primary goal of the thesis is to investigate the thermal and energy performance of the actual 3d concrete printed building, to understand how climate change would affect 3DCP buildings, and to compare it to a scenario for conventional structures. Thermal imaging and quantitative simulation-based building performance analysis form the foundation of this study's methodology. Investigating the effects of climate change on 3DCP buildings, the following conclusions have been drawn based on the findings of the entire research process and discussion:

- 3D concrete printing is a beneficial construction method with great potential, especially for the production process. Reducing construction time, creating a safer site environment by eliminating the human workforce from the construction process, and having the capability of creating amorph shapes make 3D concrete printing a unique construction method.
- Thermal imaging is a advantageous method for the U-value calculation of the 3DCP walls. While it is non-destructive and one of the most precise method, there are very important rules and assumptions for the calculations which should be conducted very carefully.
- Implementing thermal characterization and unique geometries with their infill structure of the 3DCP walls is a never done and complex process for the energy simulations. It is very important to have detailed 3D model of each wall for volume and dimension calculation of them.
- All the 3D printing parameters affect the thermal performance of the walls. Printing path, infill pattern, layer thickness, width, and void-solid ratio are the most important reasons for the walls' performance.

- More climate change effect studies are required to examine a broader range of building types, system configurations, and climate scenarios for more regions.

Building energy usage can be accurately predicted using data-driven models that depend on statistical analyses (Amber et al., 2017). The time and effort required for energy modeling and simulations are significantly reduced by data-driven models, while the efficiency of systematic assessments, which can positively impact the economy and the environment, is boosted (Tamer et al., 2022). Using pre-existing data, this processing the order supervised learning to identify relationships between input attributes and output targets. This research uses input features such as 3DCP wall form, infill structure, layer thickness, thermal characteristics, and weather variables to predict output targets like heating and cooling loads and conductive heat loss. On the other hand, as shown in this thesis, it is not always possible to obtain exact information about the structural details of 3DCP walls. The methods used in this thesis enable predicting the R-values of the 3DCP walls without conducting in-situ measurements of every wall of the building and reduce the dependence on the knowledge of the wall's infill structure.

Similar to conventional office buildings, 3DCP buildings must have adequate insulation to generate a suitable internal thermal climate, which is vital to the health of the occupants. In this research, a full-scale thermographic field inspection was done to evaluate the thermal performance of a real 3DCP building to reduce the current research gap. The results of a thermal imaging scan and building energy simulations indicate that the tested 3DCP building lacks adequate thermal insulation. The main wall body of the 3DCP building has R-values ranging from 0.82 to 1.15 $\text{m}^2\text{K}/\text{W}$ and U-values ranging from 0.86 to 1.21 $\text{W}/(\text{m}^2\text{K})$, which meet the criteria of today's standards (Turkish Standard, 2013). The substantially increased thermal transmittance (U-value) is mostly attributable to the material characteristics of 3D-printable concrete.

The evaluated 3DCP envelopes' thermal qualities must be improved to avoid the requirement for different insulation systems, and more research in this area is required. On the exterior surface of the tested house, temperature gradients along layer contours, as well as the vertical direction of the tested house, were expected to be found, but there were not any on the case building walls because all of these defects fixed with plaster after the printing process by hand. Each wall can have a U-value difference of up to 34%. This result suggests that 3D printing properties, such as layer counts, printing rest periods, and layer-by-layer appearance, can negatively affect 3DCP's thermal performance and result in flaws such as cracks. Therefore, it is crucial to consider heat considerations when designing and printing 3DCP. In general, there is a great need for in-depth study on 3DCP in the energy performance and climate change areas. There is still much room to investigate and improve the thermal and energy performance of 3DCP structures and elements since materials and geometrical factors influence the performance of the 3DCP structure. As a result, 3DCP technology will be able to play a more significant role in real-world applications and eventually help society and the environment.

6.1 Limitations and Further Studies

This thesis required acknowledgment of several limitations. The scope of the in-situ experiments conducted in ISTON has been restricted due to the challenges encountered in the thesis. Firstly, the case building is the first and only 3DCP structure in Turkey during this study that is accessible and available to conduct in-situ experiments. On the other hand, it was always a challenge to arrange a visit due to administrative issues of the ISTON and the location of the building, which is inside an active concrete factory.

Secondly, because 3D concrete printing is a very new field for Turkey, there have been many trial and error processes during the construction phase. For this kind of structure, simulations should have been conducted during the design phase to minimize errors afterward. Though, parameters such as infill structure, layer height,

and the form of the walls were designed according to the limitation of the robotic arm. As one of the main advantages of the 3DCP is eliminating framework from the construction phase and enabling the creation of different forms, all the walls of the case building were designed very basic. Thus, only primary prismatic-shaped walls were inspected during this research.

The predicted defects were fixed manually after the construction. This situation eliminates the thermal bridge and errors like cracks on the walls, which are also not included in the calculations. Also, some of the constructed walls were different from the architectural drawings. The drawings were fixed according to real-life measurements and modeled based on actual drawings. The layers with wider widths due to the printing process were ignored, and the average layer height was taken.

Lastly, during the both visits to the case building for the thermal imaging process, ISTON could only provide one oil filled heater which is not enough to heat even one room because the building is not actively in use. With extra two infrared heaters that were provided from other workshops the experiments were limited to two meeting rooms due to lack of heating source.

As mentioned above, the experiments could only be conducted on the similar type of walls with similar infill structures. To understand the effects of the structural design on the thermal performance of the walls, the proposed method can be used for the walls different forms and infill designs. A further study for the different 3DCP buildings from different climatic areas is therefore suggested.

REFERENCES

- Agkathidis, A., Berdos, Y., & Brown, A. (2019). Active membranes: 3D printing of elastic fibre patterns on pre-stretched textiles. *International Journal of Architectural Computing*, *17*(1), 74–87.
<https://doi.org/10.1177/1478077118800890>
- Alkhalidi, A., & Hatuqay, D. (2020). Energy efficient 3D printed buildings: Material and techniques selection worldwide study. *Journal of Building Engineering*, *30*, 101286. <https://doi.org/10.1016/j.jobe.2020.101286>
- Amber, K. P., Aslam, M. W., Mahmood, A., Kousar, A., Younis, M. Y., Akbar, B., Chaudhary, G. Q., & Hussain, S. K. (2017). Energy Consumption Forecasting for University Sector Buildings. *Energies*, *10*(10), 1579.
<https://doi.org/10.3390/en10101579>
- Andrew, R. M. (2018). Global CO2 emissions from cement production. *Earth System Science Data*, *10*(1), 195–217. <https://doi.org/10.5194/essd-10-195-2018>
- Andrić, I., Koc, M., & Al-Ghamdi, S. G. (2019). A review of climate change implications for built environment: Impacts, mitigation measures and associated challenges in developed and developing countries. *Journal of Cleaner Production*, *211*, 83–102.
<https://doi.org/10.1016/j.jclepro.2018.11.128>
- ASHRAE. (2013). Standard 90.1-2013. energy standard for buildings except low-rise residential buildings. *Am. Soc. Heating, Refrig. Air-Conditioning Eng. Inc*, 278.
- ASHRAE, A. G. (2002). Ashrae guideline 14: measurement of energy and demand savings. *American Society of Heating, Refrigerating and Air-Conditioning Engineers*, *35*, 41–63.

- Asprone, D., Menna, C., Bos, F. P., Salet, T. A. M., Mata-Falcón, J., & Kaufmann, W. (2018). Rethinking reinforcement for digital fabrication with concrete. *Cement and Concrete Research*, *112*, 111–121.
<https://doi.org/10.1016/j.cemconres.2018.05.020>
- Bai, G., Wang, L., Ma, G., Sanjayan, J., & Bai, M. (2021). 3D printing eco-friendly concrete containing under-utilised and waste solids as aggregates. *Cement and Concrete Composites*, *120*, 104037.
<https://doi.org/10.1016/j.cemconcomp.2021.104037>
- Barnes, B. T., Forsythe, W. E., & Adams, E. Q. (1947). The Total Emissivity of Various Materials at 100–500°C. *Journal of the Optical Society of America*, *37*(10), 804. <https://doi.org/10.1364/JOSA.37.000804>
- Berger, T., Amann, C., Formayer, H., Korjenic, A., Pospischal, B., Neururer, C., & Smutny, R. (2014). Impacts of climate change upon cooling and heating energy demand of office buildings in Vienna, Austria. *Energy and Buildings*, *80*, 517–530. <https://doi.org/10.1016/j.enbuild.2014.03.084>
- Bhattacharjee, S., Basavaraj, A. S., Rahul, A. V., Santhanam, M., Gettu, R., Panda, B., Schlangen, E., Chen, Y., Copuroglu, O., Ma, G., Wang, L., Basit Beigh, M. A., & Mechtcherine, V. (2021). Sustainable materials for 3D concrete printing. *Cement and Concrete Composites*, *122*, 104156.
<https://doi.org/10.1016/j.cemconcomp.2021.104156>
- Bos, F., Wolfs, R., Ahmed, Z., & Salet, T. (2016). Additive manufacturing of concrete in construction: potentials and challenges of 3D concrete printing. *Virtual and Physical Prototyping*, *11*(3), 209–225.
<https://doi.org/10.1080/17452759.2016.1209867>
- Buswell, R. A., da Silva, W. R. L., Bos, F. P., Schipper, H. R., Lowke, D., Hack, N., Kloft, H., Mechtcherine, V., Wangler, T., & Roussel, N. (2020). A process classification framework for defining and describing Digital Fabrication with Concrete. *Cement and Concrete Research*, *134*, 106068.

<https://doi.org/10.1016/j.cemconres.2020.106068>

Cesaretti, G., Dini, E., De Kestelier, X., Colla, V., & Pambaguian, L. (2014). Building components for an outpost on the Lunar soil by means of a novel 3D printing technology. *Acta Astronautica*, 93, 430–450.
<https://doi.org/10.1016/j.actaastro.2013.07.034>

CHANGE, I. P. O. N. C. (2007). *REPORT OF THE NINETEENTH SESSION OF THE INTERGOVERNMENTAL PANEL ON CLIMATE CHANGE (IPCC) Geneva, 17-20 (am only) April 2002.*

Chen, Y., He, S., Gan, Y., Çopuroğlu, O., Veer, F., & Schlangen, E. (2022). A review of printing strategies, sustainable cementitious materials and characterization methods in the context of extrusion-based 3D concrete printing. *Journal of Building Engineering*, 45, 103599.
<https://doi.org/https://doi.org/10.1016/j.jobe.2021.103599>

Cho, S., Kruger, J., van Rooyen, A., & van Zijl, G. (2021). Rheology and application of buoyant foam concrete for digital fabrication. *Composites Part B: Engineering*, 215, 108800.
<https://doi.org/10.1016/j.compositesb.2021.108800>

Craveiro, F., Bartolo, H. M., Gale, A., Duarte, J. P., & Bartolo, P. J. (2017). A design tool for resource-efficient fabrication of 3d-graded structural building components using additive manufacturing. *Automation in Construction*, 82, 75–83. <https://doi.org/10.1016/j.autcon.2017.05.006>

Craveiro, F., Duarte, J. P., Bartolo, H., & Bartolo, P. J. (2019). Additive manufacturing as an enabling technology for digital construction: A perspective on Construction 4.0. *Automation in Construction*, 103, 251–267.
<https://doi.org/10.1016/j.autcon.2019.03.011>

D-Shape. (2015). *Portfolio | D-shape*. <https://d-shape.com/portfolio-item/>

Dall’O’, G., Sarto, L., & Panza, A. (2013). Infrared Screening of Residential

- Buildings for Energy Audit Purposes: Results of a Field Test. *Energies*, 6(8), 3859–3878. <https://doi.org/10.3390/en6083859>
- De Schutter, G., & Feys, D. (2016). Pumping of Fresh Concrete: Insights and Challenges. *RILEM Technical Letters*, 1, 76. <https://doi.org/10.21809/rilemtechlett.2016.15>
- del Río Merino, M., Izquierdo Gracia, P., & Weis Azevedo, I. S. (2010). Sustainable construction: construction and demolition waste reconsidered. *Waste Management & Research*, 28(2), 118–129.
- Delgado Camacho, D., Clayton, P., O'Brien, W. J., Seepersad, C., Juenger, M., Ferron, R., & Salamone, S. (2018). Applications of additive manufacturing in the construction industry – A forward-looking review. *Automation in Construction*, 89, 110–119. <https://doi.org/10.1016/j.autcon.2017.12.031>
- Det Udomsap, A., & Hallinger, P. (2020). A bibliometric review of research on sustainable construction, 1994–2018. *Journal of Cleaner Production*, 254, 120073. <https://doi.org/10.1016/j.jclepro.2020.120073>
- Dörfler, K., Hack, N., Sandy, T., Giftthaler, M., Lussi, M., Walzer, A. N., Buchli, J., Gramazio, F., & Kohler, M. (2019). Mobile robotic fabrication beyond factory conditions: Case study Mesh Mould wall of the DFAB HOUSE. *Construction Robotics*, 3, 53–67.
- Emerging Objects*. (2013). <http://emergingobjects.com/>
- Energy, S. (2012). Climate change world weather file generator. *Renew Energy*.
- Fluke. (2013). *Ti480 Thermal Imagers. Users Manual. September 2013*, 50. https://dam-assets.fluke.com/s3fs-public/Ti200___umspa0400.pdf
- Fokaides, P. A., & Kalogirou, S. A. (2011). Application of infrared thermography for the determination of the overall heat transfer coefficient (U-Value) in building envelopes. *Applied Energy*, 88(12), 4358–4365. <https://doi.org/10.1016/j.apenergy.2011.05.014>

- Furet, B., Poullain, P., & Garnier, S. (2019). 3D printing for construction based on a complex wall of polymer-foam and concrete. *Additive Manufacturing*, 28, 58–64. <https://doi.org/10.1016/j.addma.2019.04.002>
- Gallego-Schmid, A., Chen, H.-M., Sharmina, M., & Mendoza, J. M. F. (2020). Links between circular economy and climate change mitigation in the built environment. *Journal of Cleaner Production*, 260, 121115. <https://doi.org/10.1016/j.jclepro.2020.121115>
- Ghaffar, S. H., Corker, J., & Fan, M. (2018). Additive manufacturing technology and its implementation in construction as an eco-innovative solution. *Automation in Construction*, 93, 1–11. <https://doi.org/10.1016/j.autcon.2018.05.005>
- Gorgolewski, M. (2007). Developing a simplified method of calculating U-values in light steel framing. *Building and Environment*, 42(1), 230–236. <https://doi.org/10.1016/j.buildenv.2006.07.001>
- Gosselin, C., Duballet, R., Roux, P., Gaudillière, N., Dirrenberger, J., & Morel, P. (2016). Large-scale 3D printing of ultra-high performance concrete – a new processing route for architects and builders. *Materials & Design*, 100, 102–109. <https://doi.org/10.1016/j.matdes.2016.03.097>
- Gregurić, L. (2021). *How Much Does a 3D Printed House Cost in 2021? | All3DP*. <https://all3dp.com/2/3d-printed-house-cost/>
- Halliday, S. (2018). *Sustainable Construction*. Routledge. <https://doi.org/10.1201/9781315514819>
- Ham, Y. (2015). *VISION-BASED BUILDING ENERGY DIAGNOSTICS AND RETROFIT ANALYSIS USING 3D THERMOGRAPHY AND BUILDING INFORMATION MODELING*. University of Illinois at Urbana-Champaign.
- Ham, Y., & Golparvar-Fard, M. (2013). An automated vision-based method for rapid 3D energy performance modeling of existing buildings using thermal

- and digital imagery. *Advanced Engineering Informatics*, 27(3), 395–409.
<https://doi.org/10.1016/j.aei.2013.03.005>
- Ham, Y., & Golparvar-Fard, M. (2014). 3D Visualization of thermal resistance and condensation problems using infrared thermography for building energy diagnostics. *Visualization in Engineering*, 2(1), 12.
<https://doi.org/10.1186/s40327-014-0012-0>
- He, Y., Zhang, Y., Zhang, C., & Zhou, H. (2020). Energy-saving potential of 3D printed concrete building with integrated living wall. *Energy and Buildings*, 222, 110110. <https://doi.org/10.1016/j.enbuild.2020.110110>
- ICON. (2018). *The Chicon House*. 2018.
<https://www.iconbuild.com/projects/chicon-house>
- Igaz, R., Krišťák, L., Ružiak, I., Gajtanska, M., & Kučerka, M. (2017). Thermophysical properties of OSB boards versus equilibrium moisture content. *BioResources*, 12(4), 8106–8118.
- Jha, K. N. (2012). *Formwork for concrete structures*. ew Delhi: Tata McGraw Hill Education Private Limited.
- Kaszynka, M., Olczyk, N., Techman, M., Skibicki, S., Zielinski, A., Filipowicz, K., Wroblewski, T., & Hoffmann, M. (2019). Thermal-Humidity Parameters of 3D Printed Wall. *IOP Conference Series: Materials Science and Engineering*, 471(8), 082018. <https://doi.org/10.1088/1757-899X/471/8/082018>
- Keerthan, P., & Mahendran, M. (2013). Thermal Performance of Composite Panels Under Fire Conditions Using Numerical Studies: Plasterboards, Rockwool, Glass Fibre and Cellulose Insulations. *Fire Technology*, 49(2), 329–356.
<https://doi.org/10.1007/s10694-012-0269-6>
- Khan, M. S., Sanchez, F., & Zhou, H. (2020). 3-D printing of concrete: Beyond horizons. *Cement and Concrete Research*, 133, 106070.
<https://doi.org/10.1016/j.cemconres.2020.106070>

- Khoshnevis, B. (2004). Automated construction by contour crafting - Related robotics and information technologies. *Automation in Construction*, 13(1), 5–19. <https://doi.org/10.1016/j.autcon.2003.08.012>
- Khoshnevis, B. (2010). *Research | Bkhoshnevis*.
<https://www.bkhoshnevis.com/research>
- Kontovourkis, O., & Tryfonos, G. (2020). Robotic 3D clay printing of prefabricated non-conventional wall components based on a parametric-integrated design. *Automation in Construction*, 110, 103005. <https://doi.org/10.1016/j.autcon.2019.103005>
- Li, V. C., Bos, F. P., Yu, K., McGee, W., Ng, T. Y., Figueiredo, S. C., Nefs, K., Mechtcherine, V., Nerella, V. N., Pan, J., van Zijl, G. P. A. G., & Kruger, P. J. (2020). On the emergence of 3D printable Engineered, Strain Hardening Cementitious Composites (ECC/SHCC). *Cement and Concrete Research*, 132, 106038. <https://doi.org/10.1016/j.cemconres.2020.106038>
- Liam Otten. (2018). *Changing how buildings are made*.
<https://source.wustl.edu/2018/08/changing-how-buildings-are-made/>
- Lim, S., Buswell, R. A. A., Le, T. T. T., Austin, S. A. A., Gibb, A. G. F. G. F., & Thorpe, T. (2012). Developments in construction-scale additive manufacturing processes. *Automation in Construction*, 21(1), 262–268. <https://doi.org/10.1016/j.autcon.2011.06.010>
- Lloret, E., Shahab, A. R., Linus, M., Flatt, R. J., Gramazio, F., Kohler, M., & Langenberg, S. (2015). Complex concrete structures: Merging existing casting techniques with digital fabrication. *Computer-Aided Design*, 60, 40–49. <https://doi.org/10.1016/j.cad.2014.02.011>
- Ma, G., Buswell, R., Leal da Silva, W. R., Wang, L., Xu, J., & Jones, S. Z. (2022). Technology readiness: A global snapshot of 3D concrete printing and the frontiers for development. *Cement and Concrete Research*, 156, 106774. <https://doi.org/10.1016/j.cemconres.2022.106774>

- Ma, G., Li, Z., Wang, L., & Bai, G. (2019). Micro-cable reinforced geopolymer composite for extrusion-based 3D printing. *Materials Letters*, 235, 144–147. <https://doi.org/10.1016/j.matlet.2018.09.159>
- Madding, R. (2008). Finding R-Values of Stud Frame Constructed Houses with IR Thermography. *Proceedings ITC*, 126(November), 2008–2013.
- Marais, H., Christen, H., Cho, S., De Villiers, W., & Van Zijl, G. (2021). Computational assessment of thermal performance of 3D printed concrete wall structures with cavities. *Journal of Building Engineering*, 41, 102431. <https://doi.org/10.1016/j.jobbe.2021.102431>
- Marchment, T., & Sanjayan, J. (2020). Mesh reinforcing method for 3D Concrete Printing. *Automation in Construction*, 109, 102992. <https://doi.org/10.1016/j.autcon.2019.102992>
- Marchon, D., Kawashima, S., Bessaies-Bey, H., Mantellato, S., & Ng, S. (2018). Hydration and rheology control of concrete for digital fabrication: Potential admixtures and cement chemistry. *Cement and Concrete Research*, 112, 96–110. <https://doi.org/10.1016/j.cemconres.2018.05.014>
- Marzouk, M., & Azab, S. (2014). Environmental and economic impact assessment of construction and demolition waste disposal using system dynamics. *Resources, Conservation and Recycling*, 82, 41–49. <https://doi.org/10.1016/j.resconrec.2013.10.015>
- Mechtcherine, V., Bos, F. P., Perrot, A., da Silva, W. R. L., Nerella, V. N., Fataei, S., Wolfs, R. J. M., Sonebi, M., & Roussel, N. (2020). Extrusion-based additive manufacturing with cement-based materials – Production steps, processes, and their underlying physics: A review. *Cement and Concrete Research*, 132, 106037. <https://doi.org/10.1016/j.cemconres.2020.106037>
- Moretti, M. (2023). *WASP in the Edge of 3D Printing* (pp. 57–65). https://doi.org/10.1007/978-3-031-09319-7_3

- Muthukrishnan, S., Ramakrishnan, S., & Sanjayan, J. (2021). Technologies for improving buildability in 3D concrete printing. *Cement and Concrete Composites*, *122*, 104144. <https://doi.org/10.1016/j.cemconcomp.2021.104144>
- Panda, B., Chandra Paul, S., & Jen Tan, M. (2017). Anisotropic mechanical performance of 3D printed fiber reinforced sustainable construction material. *Materials Letters*, *209*, 146–149. <https://doi.org/10.1016/j.matlet.2017.07.123>
- Parker, K., Garancher, J.-P., Shah, S., & Fernyhough, A. (2011). Expanded polylactic acid - an eco-friendly alternative to polystyrene foam. *Journal of Cellular Plastics*, *47*(3), 233–243. <https://doi.org/10.1177/0021955X11404833>
- Paul, S. C., Tay, Y. W. D., Panda, B., & Tan, M. J. (2018). Fresh and hardened properties of 3D printable cementitious materials for building and construction. *Archives of Civil and Mechanical Engineering*, *18*(1), 311–319. <https://doi.org/10.1016/j.acme.2017.02.008>
- Paul, S. C., van Zijl, G. P. A. G., Tan, M. J., & Gibson, I. (2018). A review of 3D concrete printing systems and materials properties: current status and future research prospects. *Rapid Prototyping Journal*, *24*(4), 784–798. <https://doi.org/10.1108/RPJ-09-2016-0154>
- Peel, M. C., Finlayson, B. L., & McMahon, T. A. (2007). Updated world map of the Köppen-Geiger climate classification. *Hydrology and Earth System Sciences*, *11*(5), 1633–1644. <https://doi.org/10.5194/hess-11-1633-2007>
- Perrot, A., Rangeard, D., Nerella, V. N., & Mechtcherine, V. (2019). Extrusion of cement-based materials - an overview. *RILEM Technical Letters*, *3*, 91–97. <https://doi.org/10.21809/rilemtechlett.2018.75>
- Pessoa, S., Guimarães, A. S., Lucas, S. S., & Simões, N. (2021). 3D printing in the construction industry - A systematic review of the thermal performance in buildings. *Renewable and Sustainable Energy Reviews*, *141*, 110794. <https://doi.org/10.1016/j.rser.2021.110794>

- Petrovic, V., Vicente Haro Gonzalez, J., Jordá Ferrando, O., Delgado Gordillo, J., Ramón Blasco Puchades, J., & Portolés Griñan, L. (2011). Additive layered manufacturing: sectors of industrial application shown through case studies. *International Journal of Production Research*, 49(4), 1061–1079. <https://doi.org/10.1080/00207540903479786>
- Radhi, H. (2009). Evaluating the potential impact of global warming on the UAE residential buildings – A contribution to reduce the CO2 emissions. *Building and Environment*, 44(12), 2451–2462. <https://doi.org/10.1016/j.buildenv.2009.04.006>
- Rael. (2018). *Printing Architecture: Innovative Recipes for 3D Printing*. Princeton Architectural Press.
- Roudsari, M. S., Pak, M., & Smith, A. (2013). Ladybug: a parametric environmental plugin for grasshopper to help designers create an environmentally-conscious design. *Proceedings of the 13th International IBPSA Conference Held in Lyon, France Aug*, 3128–3135.
- Ruiz-Valero, L., Faxas-Guzmán, J., Ferreira, J., González, V., Guerrero, N., & Ramirez, F. (2021). Thermal Performance of Facades Based on Experimental Monitoring of Outdoor Test Cells in Tropical Climate. *Civil Engineering Journal*, 7(12), 1982–1997. <https://doi.org/10.28991/cej-2021-03091773>
- Sailor, D. J. (2014). Risks of summertime extreme thermal conditions in buildings as a result of climate change and exacerbation of urban heat islands. *Building and Environment*, 78, 81–88. <https://doi.org/10.1016/j.buildenv.2014.04.012>
- Sanjayan, J. G., & Nematollahi, B. (2019). 3D Concrete Printing for Construction Applications. In *3D Concrete Printing Technology* (pp. 1–11). Elsevier. <https://doi.org/10.1016/B978-0-12-815481-6.00001-4>
- Scoolpt. (2015). *Dentist surgery*. <https://www.scoolpt.com/en/dentist-surgery/>
- Sepasgozar, S. M. E., Shi, A., Yang, L., Shirowzhan, S., & Edwards, D. J. (2020).

- Additive Manufacturing Applications for Industry 4.0: A Systematic Critical Review. *Buildings*, 10(12), 231. <https://doi.org/10.3390/buildings10120231>
- Shen, P., Braham, W., & Yi, Y. (2019). The feasibility and importance of considering climate change impacts in building retrofit analysis. *Applied Energy*, 233–234, 254–270. <https://doi.org/10.1016/j.apenergy.2018.10.041>
- Siddika, A., Mamun, M. A. Al, Ferdous, W., Saha, A. K., & Alyousef, R. (2020). 3D-printed concrete: applications, performance, and challenges. *Journal of Sustainable Cement-Based Materials*, 9(3), 127–164. <https://doi.org/10.1080/21650373.2019.1705199>
- Srinivasan, R. S., Braham, W. W., Campbell, D. E., & Curcija, C. D. (2012). Re(De)fining Net Zero Energy: Renewable Energy Balance in environmental building design. *Building and Environment*, 47, 300–315. <https://doi.org/10.1016/j.buildenv.2011.07.010>
- Subrin, K., Bressac, T., Garnier, S., Ambiehl, A., Paquet, E., & Furet, B. (2018). Improvement of the mobile robot location dedicated for habitable house construction by 3D printing. *IFAC-PapersOnLine*, 51(11), 716–721. <https://doi.org/10.1016/j.ifacol.2018.08.403>
- Sun, J., Xiao, J., Li, Z., & Feng, X. (2021). Experimental study on the thermal performance of a 3D printed concrete prototype building. *Energy and Buildings*, 241, 110965. <https://doi.org/10.1016/j.enbuild.2021.110965>
- Tamer, T., Gürsel Dino, I., & Meral Akgül, C. (2022). Data-driven, long-term prediction of building performance under climate change: Building energy demand and BIPV energy generation analysis across Turkey. *Renewable and Sustainable Energy Reviews*, 162, 112396. <https://doi.org/10.1016/j.rser.2022.112396>
- Tay, Y. W. D., Panda, B., Paul, S. C., Noor Mohamed, N. A., Tan, M. J., & Leong, K. F. (2017). 3D printing trends in building and construction industry: a review. *Virtual and Physical Prototyping*, 12(3), 261–276.

<https://doi.org/10.1080/17452759.2017.1326724>

- Tey, J. Y., Teh, D., Yeo, W. H., Shak, K. P. Y., Saw, L. H., & Lee, T. S. (2019). Development of 3D printer for functionally graded material using fused deposition modelling method. *IOP Conference Series: Earth and Environmental Science*, 268, 012019. <https://doi.org/10.1088/1755-1315/268/1/012019>
- Tibaut, A., Rebolj, D., & Nekrep Perc, M. (2016). Interoperability requirements for automated manufacturing systems in construction. *Journal of Intelligent Manufacturing*, 27(1), 251–262. <https://doi.org/10.1007/s10845-013-0862-7>
- Torelli, G., Fernández, M. G., & Lees, J. M. (2020). Functionally graded concrete: Design objectives, production techniques and analysis methods for layered and continuously graded elements. *Construction and Building Materials*, 242, 118040. <https://doi.org/10.1016/j.conbuildmat.2020.118040>
- Turkish Standard, T. S. (2013). *825 Thermal insulation requirements for buildings*. December.
- UNEP. (2021). *2021 Global Status Report for Buildings and Construction* | *Globalabc*. <https://globalabc.org/resources/publications/2021-global-status-report-buildings-and-construction>
- Verge. (2018). *This cheap 3D-printed home is a start for the 1 billion who lack shelter - The Verge*. 2018. <https://www.theverge.com/2018/3/12/17101856/3d-printed-housing-icon-shelter-housing-crisis>
- Wang, X., Chen, D., & Ren, Z. (2011). Global warming and its implication to emission reduction strategies for residential buildings. *Building and Environment*, 46(4), 871–883. <https://doi.org/10.1016/j.buildenv.2010.10.016>
- Wangler, T., Lloret, E., Reiter, L., Hack, N., Gramazio, F., Kohler, M., Bernhard, M., Dillenburger, B., Buchli, J., Roussel, N., & Flatt, R. (2016). Digital Concrete: Opportunities and Challenges. *RILEM Technical Letters*, 1(0 SE-

Articles). <https://doi.org/10.21809/rilemtechlett.2016.16>

Weng, Y., Li, M., Ruan, S., Wong, T. N., Tan, M. J., Ow Yeong, K. L., & Qian, S. (2020). Comparative economic, environmental and productivity assessment of a concrete bathroom unit fabricated through 3D printing and a precast approach. *Journal of Cleaner Production*, *261*, 121245.

<https://doi.org/10.1016/j.jclepro.2020.121245>

Wolfs, R. J. M., Bos, F. P., & Salet, T. A. M. (2019). Hardened properties of 3D printed concrete: The influence of process parameters on interlayer adhesion. *Cement and Concrete Research*, *119*, 132–140.

<https://doi.org/10.1016/j.cemconres.2019.02.017>

Wu, P., Wang, J., & Wang, X. (2016). A critical review of the use of 3-D printing in the construction industry. *Automation in Construction*, *68*, 21–31.

<https://doi.org/10.1016/j.autcon.2016.04.005>

Xiao, J., Ji, G., Zhang, Y., Ma, G., Mechtcherine, V., Pan, J., Wang, L., Ding, T., Duan, Z., & Du, S. (2021). Large-scale 3D printing concrete technology: Current status and future opportunities. *Cement and Concrete Composites*, *122*, 104115.

<https://doi.org/10.1016/j.cemconcomp.2021.104115>

Zhang, C., Nerella, V. N., Krishna, A., Wang, S., Zhang, Y., Mechtcherine, V., & Banthia, N. (2021). Mix design concepts for 3D printable concrete: A review. *Cement and Concrete Composites*, *122*, 104155.

<https://doi.org/10.1016/j.cemconcomp.2021.104155>

Zhang, Y., Zhang, Y., Liu, G., Yang, Y., Wu, M., & Pang, B. (2018). Fresh properties of a novel 3D printing concrete ink. *Construction and Building Materials*, *174*, 263–271.

<https://doi.org/10.1016/j.conbuildmat.2018.04.115>

Zhang, Y., Zhang, Y., She, W., Yang, L., Liu, G., & Yang, Y. (2019). Rheological and harden properties of the high-thixotropy 3D printing concrete.

Construction and Building Materials, *201*, 278–285.

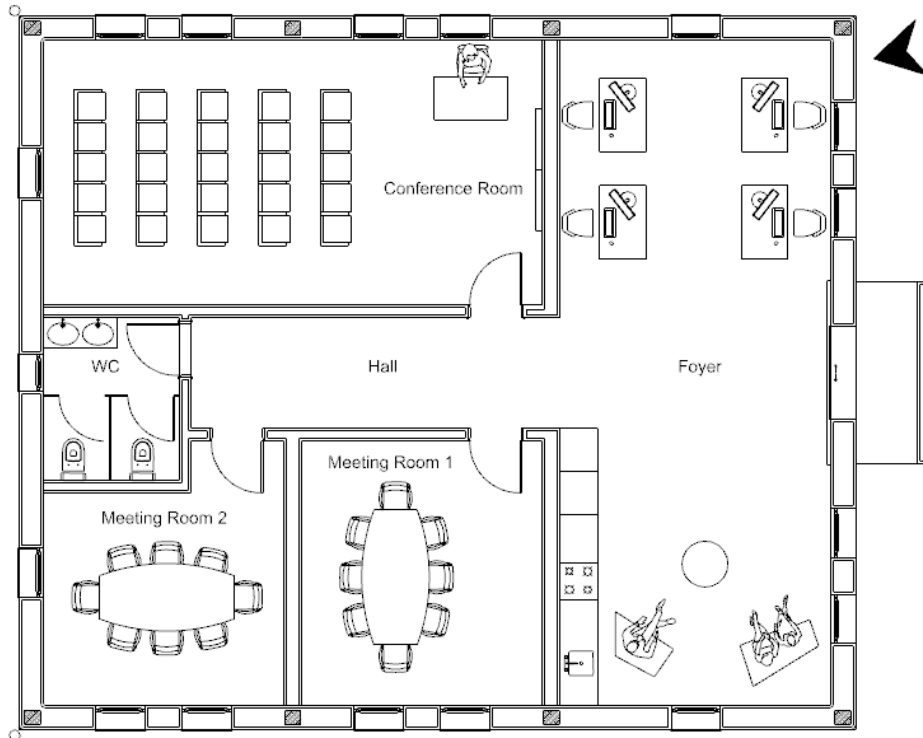
<https://doi.org/10.1016/j.conbuildmat.2018.12.061>

Zhu, B., Pan, J., Nematollahi, B., Zhou, Z., Zhang, Y., & Sanjayan, J. (2019).
Development of 3D printable engineered cementitious composites with ultra-
high tensile ductility for digital construction. *Materials & Design, 181*,
108088. <https://doi.org/10.1016/j.matdes.2019.108088>

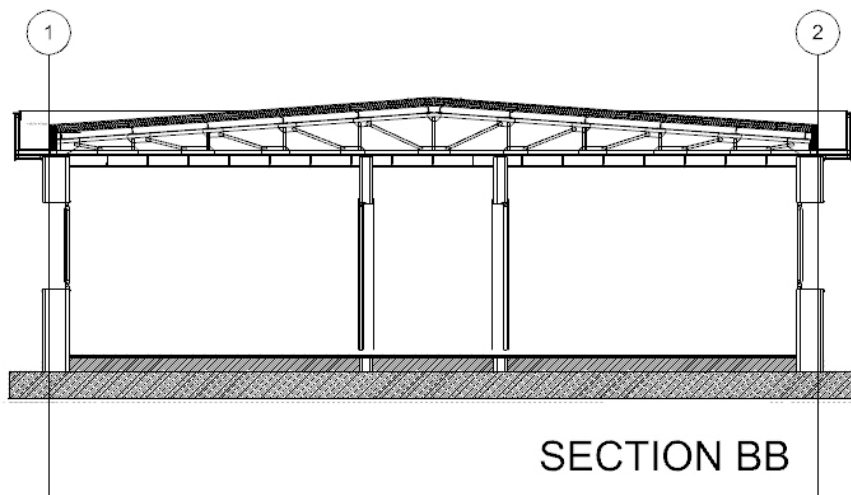
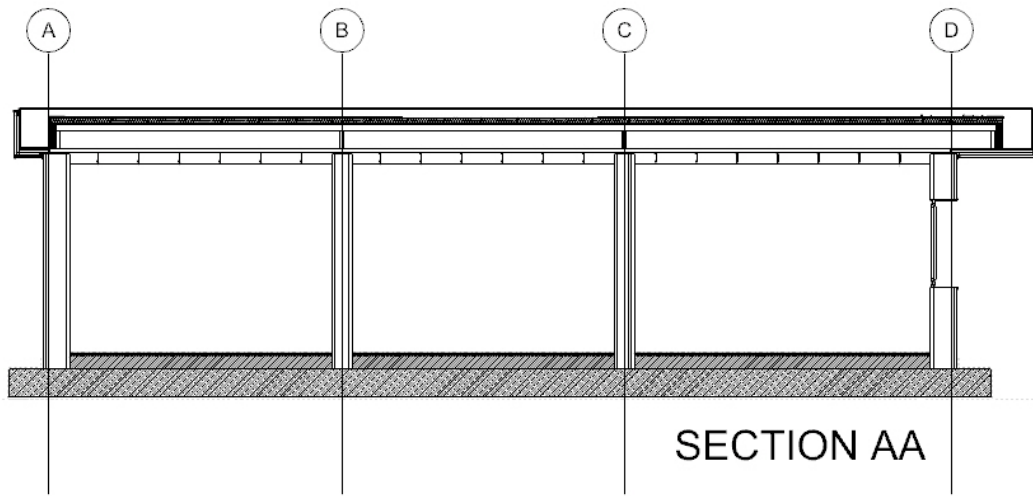
APPENDICES

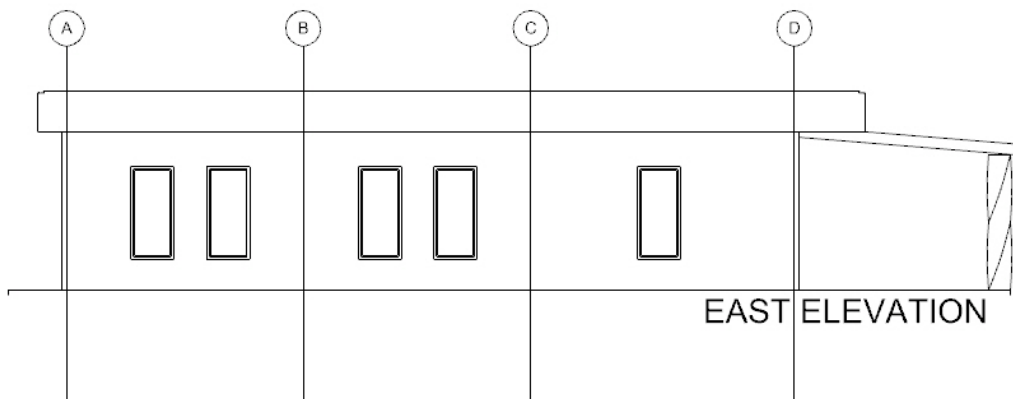
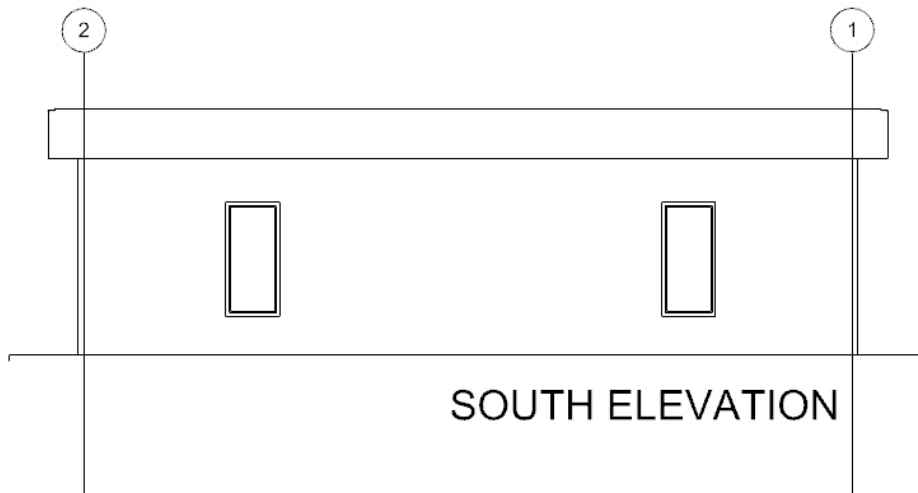
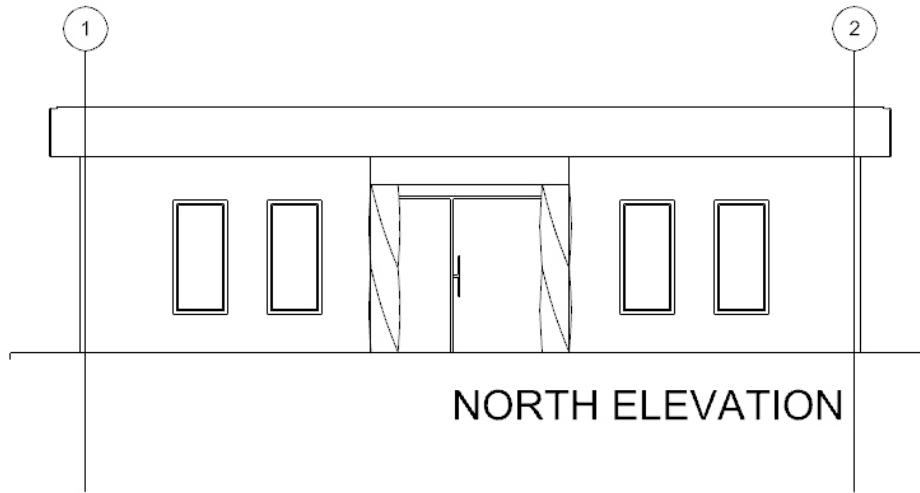
A. CASE BUILDING DETAILS

I. ARCHITECTURAL DRAWINGS

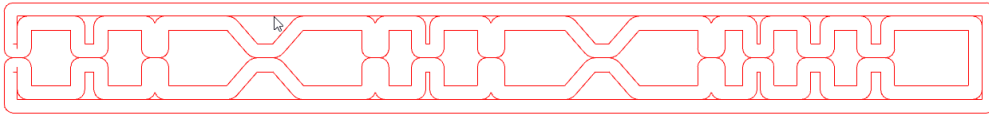


Floor Plan Drawing

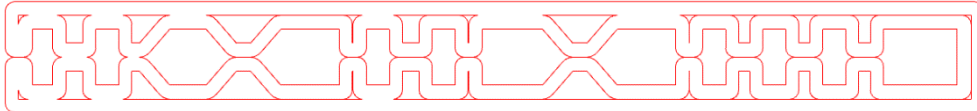




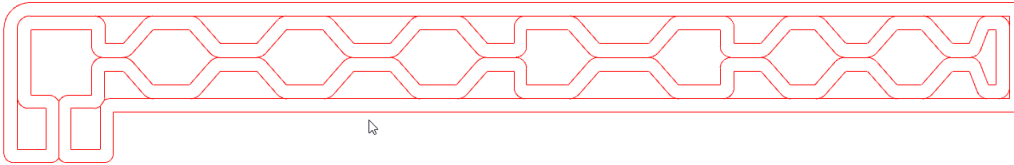
I. CASE STUDY EXTERNAL WALL INFILL STRUCTURES



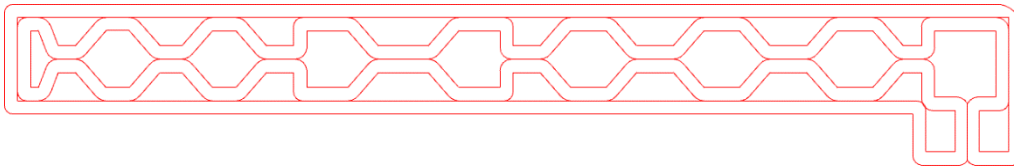
Wall 1_b



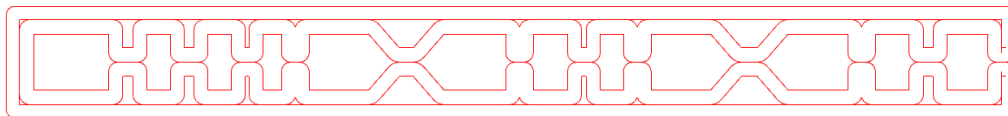
Wall 2_b



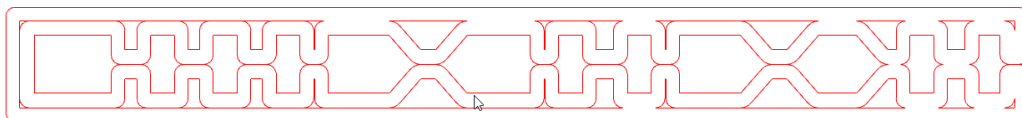
Wall 2_c



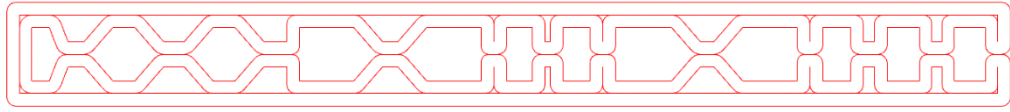
Wall 5_c



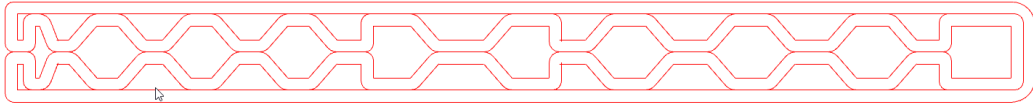
Wall 5d_1



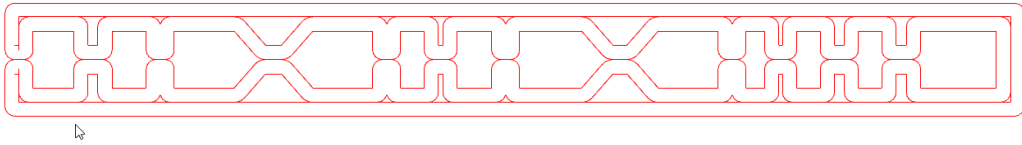
Wall 5d_2



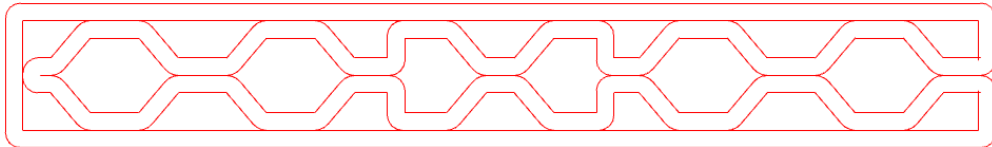
Wall 3_b



Wall_3a_1

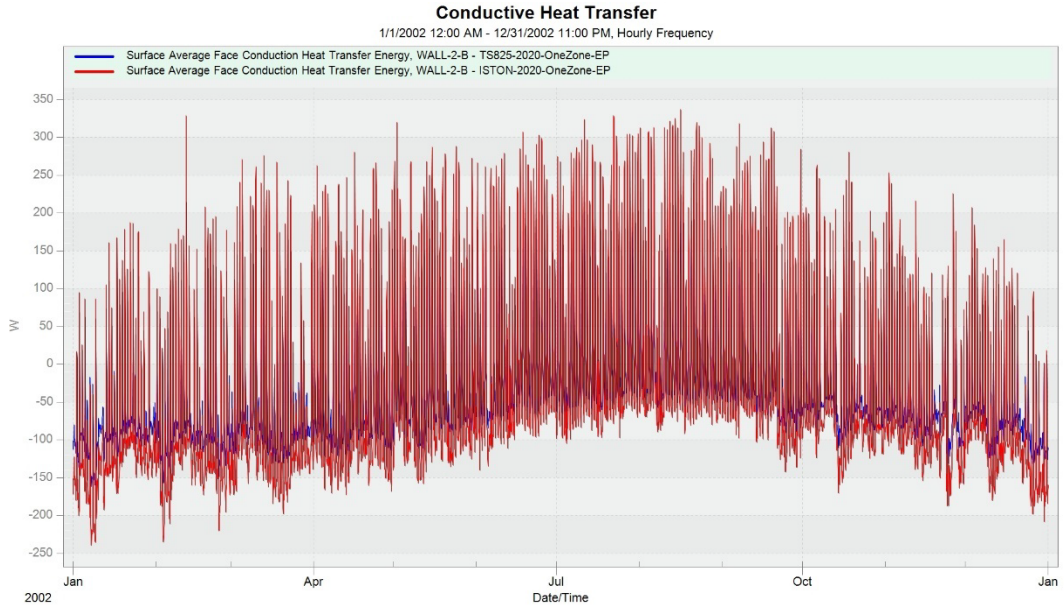


Wall_3a_2

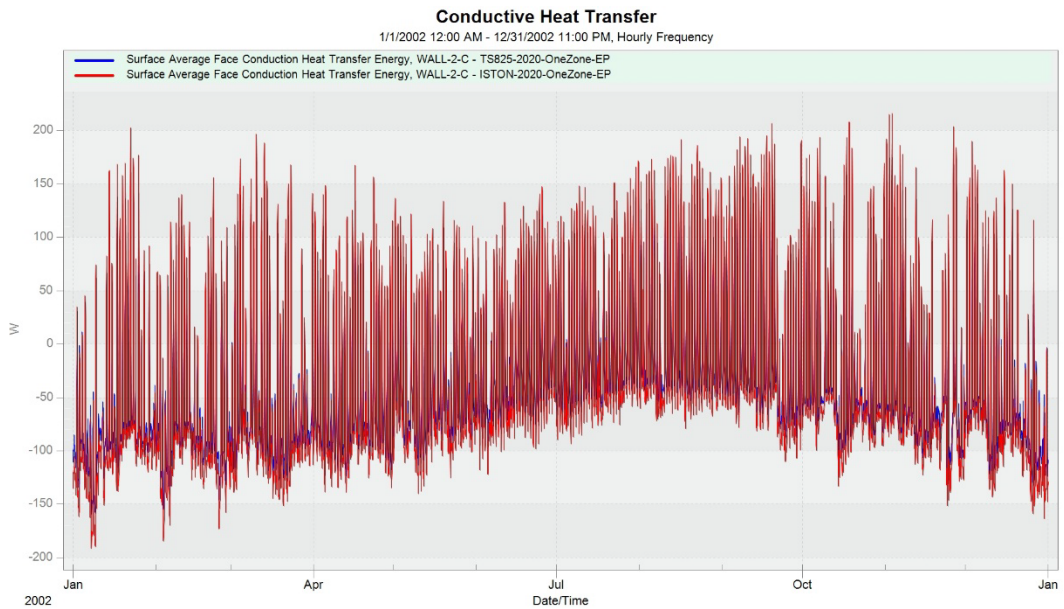


Wall_wc

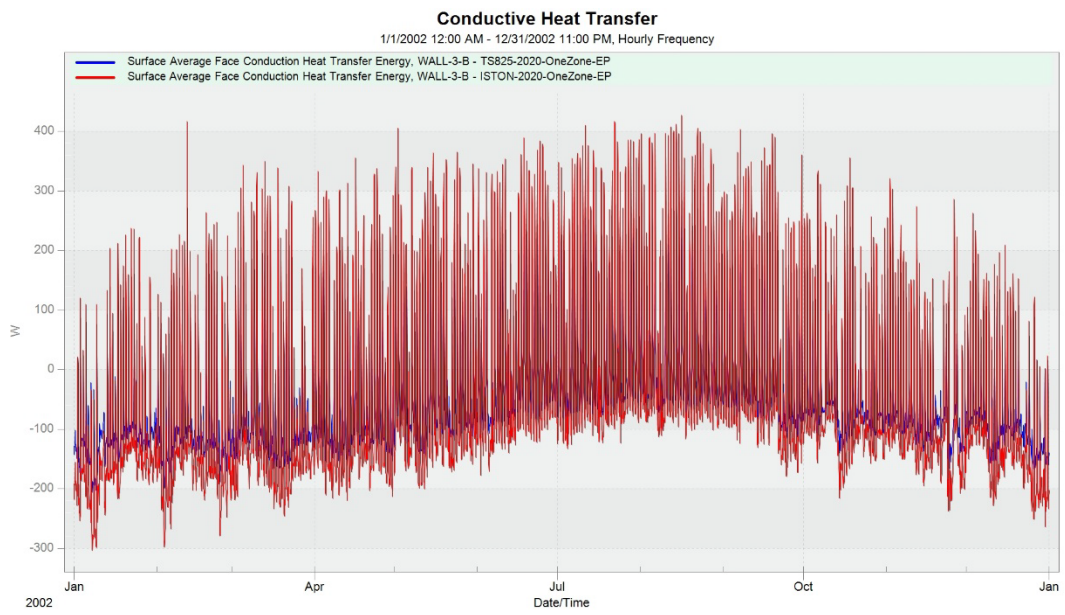
B. EXTERNAL WALLS CONDUCTIVE HEAT TRANSFER GRAPHS



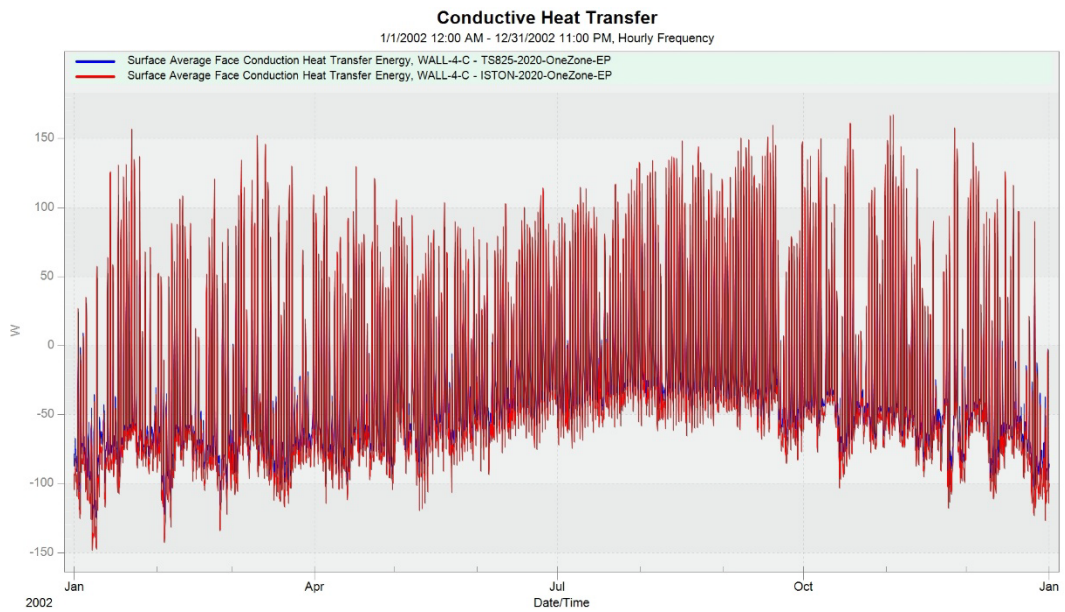
Wall 2_b (2020)



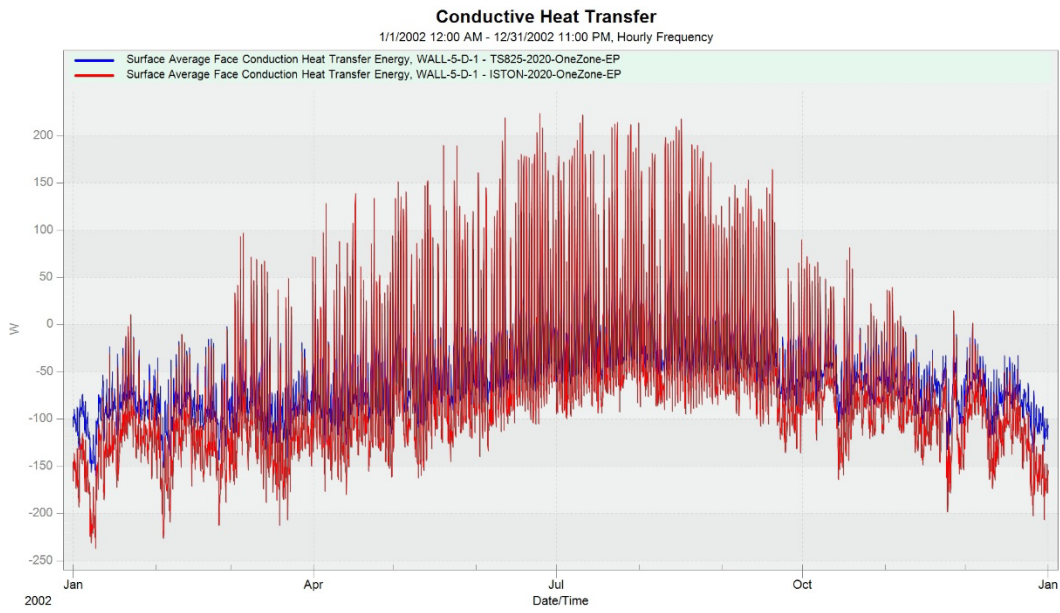
Wall 2_c (2020)



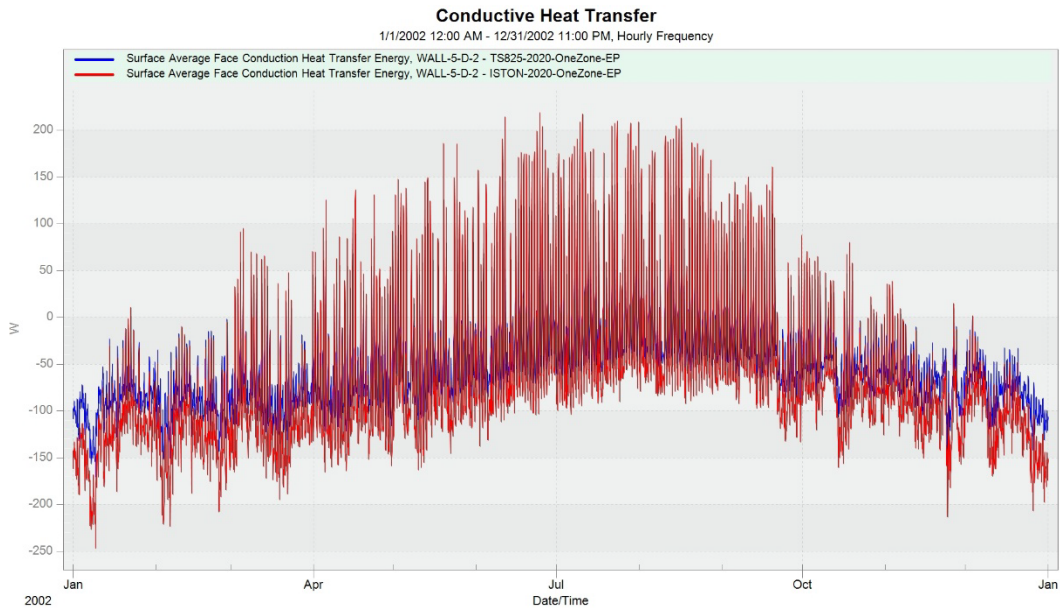
Wall 3_b (2020)



Wall 4_b (2020)



Wall 2_d_1 (2020)



Wall 2_d_2 (2020)